Physiological and biochemical constraints on photosynthesis of leguminous plants induced by elevated ozone in open-top chambers.

Cornelius Coenraad Wilhelm Scheepers

Dissertation submitted in fulfillment of the requirements for the degree *Master of Science in Plant Physiology* at the Potchefstroom campus of the North-West University

Supervisor:

Prof G.H.J. Krüger

November 2011

Monitoring the ozone concentration in the open-top chamber facility at the Potchefstroom campus.

***"To the philosopher, the physician, the meteorologist, and the chemist, there is perhaps no subject more attractive than that of ozone"* – Fox, 1873.**

Acknowledgements

Prof. Gert Krüger, my supervisor, for his expertise, advice and willingness to help me with my dissertation.

My trusted fellow student, Marie Minnaar for always being there to help and to support. She was truly an inspiration to me and without her assistance the work would have been much harder.

Riaan Strauss for his assistance with instrumentation as well as expertise in the lab.

Misha de Beer-Venter for her expertise in the lab. She pushed me to become the scientist I am today.

Prof. Leon van Rensburg for the advice and financial support.

Dr. Jaques Berner for his assistance in the lab.

My parents, Kosie and Annatjie Scheepers for their support, sacrifices, financial assistance and eagerness to provide me with this opportunity.

My wife, Illandi Scheepers, for her support and sacrifice. You are truly a remarkable person to whom I look up to.

A special thanks to my grandfather Kirrie Scheepers who has always been an inspiration.

My family and friends for their support.

Pieter Smit, for training me to be the scientist I am today. I am truly grateful for your friendship and willingness to guide me throughout my study years.

Prof. Reto Strasser (Bioenergetics Laboratory, University of Geneva, Switzerland) for all the discussions and data interpretations.

Dr. Louwrens Tiedt, for assistance with the preparations for SEM work.

Gilbert (Shorty) Batlhopeng, for maintaining the OTC site and for always lending a hand with experiments.

I hereby declare that this dissertation presented for the degree *Magister Scientiae* (M.Sc.), at the North-West University, Potchefstroom campus, is my independent work and has not previously been presented for a degree at any other university or faculty.

Summary

Physiological and biochemical constraints on photosynthesis of leguminous plants induced by elevated ozone in open-top chambers

Air pollution is one of the most critical and urgent problems globally and is also a growing concern in southern-Africa. Rapidly growing cities, increased traffic on roads, use of non-renewable fuels, reliance on outdated industrial processes and a lack of implementation of environmental regulations, are all major factors that contribute to the poor air quality in most developing countries such as South Africa (Agrawal, 2005). As a lot of air pollution is due to vehicles, no evident solution appears to be in sight. As a result of anthropogenic emissions of nitrogen oxides (NO_x) and volatile organic compounds (VOC), tropospheric ozone (O_3) has increased drastically during the last centuries. Although there are many oxidising pollutants in the atmosphere, O_3 is currently regarded as one of the most important air pollutants, since it causes more damage to vegetation world-wide than all the other air pollutants combined (Ashmore & Bell, 1991). In the Unites States of America, losses in the region of US$ 3 billion result each year from the impacts of O_3 pollution on crops (Holmes, 1994). Holland *et al*. (2002) estimated that the agricultural damage in Europe as early as 1990 due O_3 damage was in the order of £ 4.3 billion. The phytotoxicity of O_3 is due to its high oxidative capacity through the induction of reactive oxygen species (ROS) in exposed plant tissue, such as superoxide (O_2^-), hydrogen peroxide (H_2O_2), hydroxyl radical (•OH) and singlet oxygen ($^1O_2$) (Malhorta and Khan, 1984). Specifically in southern Africa, there is a growing concern that the concentrations of O_3 commonly found in the southern African troposphere may adversely affect natural vegetation, forests and crops (van Tienhoven and Scholes, 2003). While much research has been done in Asia, North America and Europe, little attention has been directed on Africa. Since agriculture plays a critical role in food security and economic growth in developing countries, it is of the utmost importance to understand and study the effect of air pollution on plants.

The aim of this study was to identify and quantify the physiological and biochemical constraints imposed by O_3 on two leguminous crops by analysing various parameters deduced from photosynthetic gas exchange and chlorophyll *a* fluorescence induction measured in parallel. In

our first experiment, *Phaseolus vulgaris* genotypes (S156 and R123) with known differences in sensitivity to O_3, were exposed to an elevated level of this pollutant at 80 nmol mol^{-1} in open-top chambers. The specific aim of this experiment was to identify the physiological and biochemical mechanism involved in the difference in resistant properties to O_3 of the two genotypes. In the second experiment *Pisum sativum* plants were subjected to a concentration of 80 nmol mol^{-1} O_3 and drought stress, singly or combined. The specific aims of this experiment were to evaluate whether a moderate drought stress in combination with O_3 would have any additional effects on the physiological and biochemical mechanisms of the test plants. With respect to the first experiment: The sensitive genotype (S156) of *Phaseolus vulgaris* developed visual symptoms after 12 days of fumigation, ultimately developing into bronze-coloured lesions, which gradually joined together after 35 days of O_3 exposure. A highly significant reduction of 58 % in the final pod weight occurred in the S156 genotype exposed to 80 nmol mol^{-1} O_3. The latter decrease was mainly due to the pronounced decreases in CO_2 assimilation as a result of a 61 % and 75 % decrease in the CO_2 saturated rate of photosynthesis (J_{max}) and carboxylation efficiency (CE), respectively. From the parameters obtained from the fluorescence data it could be concluded that the major effects responsible for the decrease in photosynthesis occurred in the reduction of end electron acceptors $[\delta_{Ro} / (1-\delta_{Ro})]$ and the efficiency of the conversion of trapped excitation energy to electron transport $[\psi_0 / (1-\psi_0)]$. The effect was also reflected by a decrease in the phenomological electron transport flux (ET/CS_0). This was also the main reason for the reduced J_{max} and CE in the S156 genotype.

With respect to the second experiment: It was illustrated that elevated O_3 levels of 80 nmol mol^{-1} reduced photosynthetic capacity of *Pisum sativum* without any accompanying visual injury throughout the experiment. CO_2 gas exchange analysis indicated that inhibition of the mesophyll reactions as well as stomatal limitation were responsible for inhibition of photosynthesis in *Pisum sativum*. Analysis of the data revealed severe inhibition of the carboxylation efficiency (CE; Rubisco activity) and maximum rate of CO_2 assimilation (J_{max}; regeneration capacity of RuBP), ultimately leading to a marked reduction in CO_2 assimilation (A_{370}). The in vitro analysis revealed a highly significant O_3 induced decrease in Rubisco activity in *Pisum sativum* test plants of up to 39 % corroborated the gas exchange data. As stomata regulate O_3 uptake, our hypothesis was that the drought stress decreased O_3 flux into the leaf due to stomatal closure. The stomatal conductance of the drought stressed treatments (DSCF and DSO_3) was on average

56 % of that of the control plants (WWCF). This large decrease in stomatal conductance also illustrated by the scanning electron micrographs, showing closure of the stomatal aperature in the drought treatments. Analysis of the chlorophyll *a* fluorescence transients revealed inhibition of electron transport on the acceptor side of PSII, resulting from the inability of the inactive donor side to donate electrons. That means that the donor side, especially the oxygen evolving complex (OEC), was damaged. The chlorophyll *a* fluorescence data further supported the gas exchange data by confirming that the inhibition of CO_2 assimilation was mainly due to impairment of the formation of end electron acceptors such as ATP and NADPH. The chlorophyll content decreased significantly in *Pisum sativum* plants exposed to O_3. This was also reflected by the moderate decrease of 5 % and 4 % in the density of reaction centers per cross-section (RC/CS) calculated from the fluorescence transients, in the well-watered and drought stressed treatments, respectively. It could be assumed that the decreased chlorophyll content contributed to the decreases in biomass and yield production. It was also shown that O_3 induced increases in the activity of the antioxidant enzyme, peroxidase (POD) after 20 days of fumigation in the O_3-treated test plants, which, after 30 days of fumigation, increased by a highly significant 40 % and 41 % in the WWO_3 and DSO_3 plants, respectively. The additional drought stress induced on the DSO_3 test plants showed no additional inhibitory effect on the test plants, indicating an ameliorating effect caused by the partial closing of the stomata. The latter finding proved the hypothesis set on the interaction between drought and O_3 on *P.sativum* to be true.

In conclusion: Using the resistant, R123 and sensitive, S156 bean genotypes as tool, valuable insight was gained into the inhibitory effect of O_3 on plants. Although the R123 genotype of *Phaseolus vulgaris* exhibited no stress symptoms with respect to fluorescence and gas exchange data, the seed yield was affected. Photosynthesis was largely inhibited in the S156 genotype, mainly due to inhibition of the photosynthetic electron transport, resulting in decreased reduction of end electron acceptors, ultimately causing a decrease in CO_2 assimilation. The above limitations ultimately lead to a large reduction in seed yield in S156. Our data show that the O_3 sensitivity of S156 is mainly due to a weakness of the photosynthetic apparatus and electron transport chain. Especially PSII function, including the OEC, proved to be very vulnerable. Exposing *P. sativum* to O_3 and drought stress simultaneously or singly lead to a drastic inhibitory effect on photosynthesis. Although it was shown that the decrease in stomatal conductance lead

to amelioration of the O_3-effect, the interaction was difficult to interpret as drought stress on its own has a constraints on photosynthesis.

Opsomming

Fisiologiese en biochemiese remming van fotosintese in peulplante deur verhoogde osoonvlakke in "open-top" groeikamers.

Lugbesoedeling is een van die mees kritiese en dringende probleme wêreldwyd en is ook 'n groeiende kommer in suidelike Afrika. Vinnig groeiende stede, toenemende verkeer op paaie, gebruik van nie-hernubare brandstof, steun op uitgediende industriële prosesse en gebrekkige implementering van omgewingsregulasies, is die hoof bydraende faktore tot swak lugkwaliteit in die meeste ontwikkelende lande soos Suid-Afrika. Aangesien 'n groot deel van lugbesoedeling te wyte is aan voertuie, is daar geen voor die hand liggende oplossing nie. Weens antropogeniese emissie van stikstofoksiede (NO_x) en vlugtige organiese verbindings (VOCs), het troposferiese osoon (O_3) drasties toegeneem oor die afgelope eeue. Hoewel daar baie oksiderende besoedelstowwe in die atmosfeer is, word O_3 tans beskou as een van die belangrikste lug besoedelstowwe, aangesien dit meer skade aan plantegroei veroorsaak as al die ander gasse saam. In die Verenigde State van Amerika kom verliese van 3 biljoen dollar elke jaar voor as gevolg van O_3 besoedeling op gewasse. Holland et al. (2002) het beraam dat die landbouskade in Europa as gevolg van O_3, reeds in 1990 in die orde van £4.3 biljoen was. Die fitotoksisiteit van O_3 is te wyte aan sy hoë oksidatiewe vermoë wat lei tot die induksie van reaktiewe suurstofspesies (ROS) in die blootgestelde plantweefsel, soos bv. superoksied (O_2^-) waterstofperoksied (H_2O_2), hidroksiedradikale ($\cdot OH$) en singletsuurstof ($^1O_2$). In suidelike Afrika in die besonder, bestaan 'n groeiende kommer dat die O_3 konsentrasies wat algemeen voorkom in die troposfeer, die natuurlike plantegroei, woude en gewasse nadelig mag beïnvloed. Ofskoon baie navorsing in Asië, Noordamerika en Europa gedoen is, is min aandag in Afrika hieraan gegee. Aangesien landbou 'n sleutelrol in voedselsekuriteit en ekonomiese groei in ontwikkelende lande speel, is dit noodsaaklik om die invloed van lugbesoedeling op plante te verstaan en te bestudeer.

Die hoofdoel van hierdie studie was om die fisiologiese en biochemiese beperking deur O_3 op twee peulplante te bestudeer deur verkillende parameters, afgelei van fotosintetiese gaswiseling en chlorofilfluoressensie metings in parallel gemeet, te analiseer. In die eerste eksperiment was *Phaseolus vulgaris* genotipes (S156 en R123) met bekende verkil in sensitiwiteit vir O_3, blootgestel aan 'n verhoogde O_3 vlak van 80 nmol mol^{-1} in 'open-top' groeikamers (OTCs). Die spesifieke doel van hierdie eksperiment was om die fisiologiese en biochemiese meganisme betrokke by die verskil in O_3-weerstand te bestudeer. In 'n tweede eksperiment is *Pisum sativum* plante blootgestel aan 80 nmol mol^{-1} O_3 én droogte, afsonderlik én gelyktydig toegedien. Die spesifieke doel van die eksperiment was om te bepaal wat die effek van matige droogte as ko-stres, op die fisiologiese en biochemiese respons van die proefplante op O_3 sou wees.

Wat die eerste eksperiment betref: Die sensitiewe *Phaseolus vulgaris* genotype (S156) het na 12 dae se fumigering sigbare simptome vertoon wat later in bronskleurige letsels ontwikkel het en geleidelik versmelt het na 35 dae se blootstelling. 'n Hoogs betekenisvolle verlaging van 58% in peulmassa het by die S156 genotipe, wat aan 80 nmol mol^{-1} O_3 blootgestel was, plaasgevind. Laasgenoemde afname was hoofsaaklik te wyte aan die skerp afname in CO_2 assimilering weens die 61% en 75% afname in die CO_2-versadigde fotosintesetemo (J_{max}) en die karboksileringsdoeltreffendheid (CE), onderskeidelik. Die parameters afgelei van die fluoressensiedata het getoon dat die hoofoorsaak van die O_3-geïnduseerde afname in fotosintese, die remming van die doeltreffendheid van die omsetting van eksiteringsenergie na elektrontransport en die reduksie van eindelektronontvangers was. Dit was die hoofoorsaak vir die afname in J_{max} en CE in die S156 genotipe. Hierdie afleiding is ook gestaaf deur deur die gepaardgaande afname in die fenomenologiese elektrontransportvloed (ET/CS_o).

Met betrekking tot die tweede eksperiment: Daar kon aangetoon word dat 'n O_3 vlak van 80 nmol mol^{-1}, fotosintese van *Pisum sativum* rem sonder enige gepaardgaande sigbare simptome vir die duur van die eksperiment. Analise van CO_2 gaswisseling het onthul dat remming van die mesofilreaksies én stomatale beperking, verantwoordelik was vir die inhibisie van fotosintese. Strawwe inhibisie van die karboksileringsfunksie (CE, Rubisco-aktiwiteit) en maksimum CO_2-assimileringstempo (J_{max}; regenerering van RuBP) het voorgekom en gelei tot die sterk afname in fotosintese (A_{370}). Die hoogs betekenisvolle 39% afname in *in vitro* Rubisco-aktwiteit veroorsaak deur O_3 in *Pisum sativum*, het hierdie bevinding ondersteun. Aangesien die stomata

O_3-opname beheer, was die hipotese dat droogte die O_3-vloed in die blaar in, sou verminder weens stomatale beperking. Die stomageleiding van die behandelings onder droogte (DSCF en DSO_3) was gemiddeld 56% laer as dié van die kontroleplante (WWCF). Hierdie groot afname in stomageleiding is ook deur die SEM-beelde wat die sluiting van die stomata in die droogtebehandelings aangetoon het, bevestig. Analise van die die chlorofilfluoressensie krommes in parallel gemeet, het inhibisie van elektrontransport aan die ontvangerkant van PSII, wat veroorsaak is deur die onvermoë van die onaktiewe skenkerkant om elektrone te skenk, ontbloot. Dit beteken dat die skenkerkant, veral die OEC, beskadig was. Die chlorofil-fluoressesiedata het die gaswisselingsdata verder ondersteun deur te bevestig dat inhibisie van CO_2-assimilering hoofsaaklik die gevolg was van versteuring van die vorming van eind-elektronontvangers soos Fd(gered.), NADPH en ATP. Die betekenisvolle afname in chlorofilinhoud van O_3-behandelde *P. sativum* plante is weerspieël deur die matige afname van 5% and 4% in digdheid van die PSII reaksiesentrums (RC/CS_o) soos bereken uit die fluoressensiekrommes van die benatte- (WWO_3) en droogtebehandelings (DSO_3), onderskeidelik. Dit is vanselfsprekend dat die afname in chlorofilinhoud bygedra het tot die afname in biomassa en opbrengs.

Daar is ook aangetoon dat ‘n toename in die aktiwiteit van die antioksidantensiem, peroksidase (POD) na 20 dae van O_3-behandeling in *P. sativum* voorgekom het en na 30 dae toegeneem het tot ‘n hoogsbetekenisvolle 40% en 41% in die WWO_3 en DSO_3 plante, onderskeidelik. Die bykomende droogtestres op die DSO_3 plante het egter geen addisionele remmende invloed op fotosintese gehad nie, wat toon dat droogte ‘n dempende invloed gehad het weens die gedeeltelike sluiting van die stomata. Met laasgenoemde bevinding is die hipotese gestel tov die interaksie tussen droogte en O_3 op *P. sativum*, as waar bewys.

Ten slotte: Deur gebruik van O_3 weerstandige (R123) en die sensitiewe (S156) boontjiegenotipes as werktuig, is waardevolle insig in die remmende invloed van O_3 op plante verkry. Ofskoon die die R123 genotipe van *P.vulgaris* geen stressimptome tov die chlorofilfluoressensie- en gaswisselingsdata getoon het nie was saadopbrengs tog beïnvloed. Fotosintese was grootliks gerem in die S156 genotipe, hoofsaaklik vanweë versteuring van fotosintetiese elektronoordrag wat gelei het tot vermindering in die reduksie van eindelektronontvangers en uiteindelik die afname in CO_2-assimilering. Hierdie beperkings het ‘n groot afname in die saadopbrengs van

S156 veroorsaak. Ons data toon dat die O_3-gevoeligheid van S156 hoofsaaklik toe te skryf is aan ‘n swakheid in die fotosintese-apparaat en elektrontransportketting. Veral PSII-funksie, insluitende die OEC, blyk kwesbaar te wees. Blootstelling van *P. sativum* aan O_3 én droogte gelyktydig en afsonderlik, het fotosintese erg gestrem. Hoewel die afname in stomageleiding die nadelige effek van O_3 gedemp het, was die interaksie moeilik om te interpreteer, aangesien droogte op sigself ‘n remmende invloed op fotosintese gehad het.

Table of content

Chapter 1 Literature review 21

1.1 Air Pollution 21
1.2 Ozone and its formation 23
1.2.1 The role of volatile organic compounds in the formation of O_3 28
1.3 Critical levels of O_3 29
1.4 Ozone's dispersal in the environment 30
1.5 Effects on plants 33
1.5.1 Photosynthesis and production 36
1.5.2 Defense: Anti-oxidant defense mechanisms 37
1.6 Ozone stress in combination with drought stress 39
1.7 Flux of pollutants 40
1.8 Aim of the study 41
1.9 Hypothesis 42

Chapter 2 Material and methods 43

2.1. Study area 43
2.2. Experimental design and ozone treatment 44
2.3. Plant cultivation and treatments 47
2.3.1. Cultivation of *Phaseolus vulgaris* – summer annual 2009 47
2.3.2. Cultivation of *Pisum sativum* – winter annual 2010 50
2.4. Non-destructive plant analysis 50
2.4.1. Chlorophyll content index (CCI) 50
2.4.2. Photosynthetic gas exchange 51
2.4.2.1. Overview 51
2.4.2.2. Measurement of photosynthetic gas exchange 56
2.4.3. Chlorophyll *a* fluorescence induction 58
2.4.4. Analysis of the chlorophyll *a* fluorescence transient by the JIP-test 60
2.5. Destructive plant analysis 63

2.5.1. Plant water status 63
2.5.1.1. Leaf water potential 64
2.5.1.2. Relative water content (RWC) 65
2.5.2. Biomass accumulation 65
2.5.3. Scanning electron-microscopy 65
2.5.4. Crop yield attribute 66
2.5.5. Rubisco (Ribulose-1,5-bisphosphate carboxylase/oxygenase) activity 65
2.5.6. Determination of peroxidase (POD) activity 66
2.5.7. Hydrogen peroxide (H_2O_2) levels 67
2.6 Statistical analysis 67

Chapter 3
Results and Discussion on: Effect of ozone on photosynthesis and seed yield of sensitive (S156) and resistant (R123) *Phaseolus vulgaris* L. genotypes in open-top chambers 68
3.1 Growth response 68
3.1.1 Plant development 68
3.1.2 Foliar injury 69
3.1.3 Crop yield 69
3.2 Physiological response parameters 71
3.2.1 Effect of O_3 on fast phase chlorophyll *a* fluorescence kinetics 71
3.2.2 Effect of O_3 on photosynthetic gas exchange 82
3.3 Effect of O_3 on chlorophyll content index (CCI) in *Phaseolus vulgaris* 85

Chapter 4
Results and Discussion on: Interaction of ozone fumigation and drought on photosystem II function and photosynthetic gas exchange in *Pisum sativum* in open-top chambers 86
4.1 Verification of the water regime of the different treatments, i.e. “well watered (WW) and drought stressed (DS)” 86
4.1.1 Relative water content (RWC) 86

4.1.2 Leaf water potential 87
4.2 Growth 88
4.2.1 Plant development 88
4.2.2 Effect of O_3 on stomata of *Pisum sativum* 89
4.2.3 Bio- and root mass accumulation 92
4.3 Physiological response 93
4.3.1 Effect of O_3 on fast phase chlorophyll *a* fluorescence kinetics 93
4.3.2 Effect of O_3 on photosynthetic gas exchange 103
4.4 Effect of O_3 on *in vitro* Rubisco activity in *Pisum sativum* 110
4.5 Effect of O_3 on chlorophyll content index (CCI) in *Pisum sativum* 111
4.6 Biochemical characteristics 112
4.6.1 H_2O_2 content in leaves of *Pisum sativum* 112
4.6.2 POD concentration in leaves of *Pisum sativum* 114

Chapter 5 Synthesis and Conclusion

5.1 Studying ozone impacts in OTCs 116
5.2 Growth and development 117
5.2.1 *Phaseolus vulgaris* 117
5.2.2 *Pisum sativum* 117
5.3 Biomass 117
5.4 Yield 118
5.5 Chlorophyll content 119
5.6 Photosynthesis 120
5.6.1 Photosynthesis of *Phaseolus vulgaris* 120
5.6.2 Photosynthesis of *Pisum sativum* 123
5.7 Antioxidative metabolism 127
5.8 Future perspectives 129

List of abbreviations

$\mathbf{A}_{360}$	CO_2 assimilation rate at ambient CO_2 concentration (360 μmol mol^{-1})
A_0	CO_2 assimilation rate at an intercellular CO_2 concentration of 370 μmol mol^{-1} i.e. a situation where stomatal limitation is eliminated artificially.
ABS/CS_M	Phenomological energy flux (per excited cross section of leaf) for light absorption
ABS/RC	The specific energy flux (per PSII reaction centre) for light absorption
C_a	Atmospheric CO_2 concentration
CCI	Chlorophyll content index
CE	Carboxylation efficiency
C_i	Intercellular CO_2 concentration
CS	Excited cross section of leaf
E_{370}	Transpiration rate at Ca = $mmol.m^{-2}.s^{-1}$
ET	Electron transport
ET_0/CS_M	Phenomenological energy flux (per excited cross section of leaf) for electron transport
ET_0/RC	Specific energy flux (per PSII reaction centre) for electron transport
F_V/F_M	Quantum yield of primary photochemistry
G_s	Stomatal conductance
J_{max}	Maximum CO_2 assimilation rate at saturating CO_2 concentration
ℓ	Relative stomatal limitation of photosynthesis
NADPH	β-Nicotinamide adenine dinucleotide

OEC	Oxygen Evolving Complex
PEA	Plant Efficiency Analyser
$PI_{ABS,tot}$	Photosynthetic performance index expressed on absorption basis
ppb	parts per billion
ppm	parts per million
PQ	Plastoquinone
PSI	Photosystem I
PSII	Photosystem II
RC	Photosystem II reaction centre
RC/ABS	Density of active PSII reaction centres on chlorophyll basis
Γ	CO_2 compensation concentration
RuBP	Ribulose-1,5-bisphosphate
Rubisco	Ribulose-1,5-bisphosphate carboxylase/oxygenase
TR	Trapping of excitation energy
TR_0/CS_M	The phenomenological energy flux (per excited cross section of leaf) for trapping
TR_0/RC	The specific energy flux (per PSII reaction centre) for trapping
VOCs	Volatile Organic Compounds
WUE	Water Use Efficiency

List of Figures

Figure 1.1:	Different layers present in the atmosphere	24
Figure 1.2:	Ozone isopleths diagram	25
Figure 1.3:	The Leighton relationship	27
Figure 1.4:	Visual illustration of O3 formation	28
Figure 1.5:	Surface O3 concentration	33
Figure 1.6:	Ozone injury on a bean leaf	35
Figure 1.7:	Schematic representation of main plant cell responses	38
Figure 1.8:	Main elements controlling ozone flux into plants	41
Figure 2.1:	OTC system of the North-West University	44
Figure 2.2:	Ventilation unit showing different components	46
Figure 2.3:	Control of ozone concentration in OTCs	47
Figure 2.4:	Pot-reservoir irrigation system	48
Figure 2.5:	Main components of pot-reservoir irrigation system	49
Figure 2.6:	Gas exchange by a leaf	52
Figure 2.7:	A:C_i response curve	55
Figure 2.8:	Measuring of photosynthetic gas exchange	57
Figure 2.9:	Typical chlorophyll *a* fluorescence transient	59
Figure 2.10:	Pressure chamber for measuring leaf water potential	64
Figure 3.1:	Growth effect of ozone on *Phaseolus vulgaris* growth	68
Figure 3.2:	Visual symptoms on leaves of *Phaseolus vulgaris*	69
Figure 3.3:	Raw chlorophyll *a* fluorescence transients of	

Phaseolus vulgaris before fumigation 72

Figure 3.4: Raw chlorophyll *a* fluorescence transients of *Phaseolus vulgaris* after 30 days of fumigation 72

Figure 3.5: Chlorophyll *a* fluorescence transients of *Phaseolus vulgaris* normalised between 50 µs and 2 ms 73

Figure 3.6: Chlorophyll *a* fluorescence transients of *Phaseolus vulgaris* normalised between 50 µs and 30 ms 74

Figure 3.7: Chlorophyll *a* fluorescence transients of *Phaseolus vulgaris* normalised between 50 µs and 30 ms plotted above 1 and 30 ms 75

Figure 3.8: Chlorophyll *a* fluorescence transients of *Phaseolus vulgaris* normalised between 30 ms and P_M, plotted in the 30 – 400 ms range. 76

Figure 3.9: Functional and structural parameters of PS II of *Phaseolus vulgaris* 76

Figure 3.10: Performance index ($PI_{ABS,tot}$) of *Phaseolus vulgaris* 78

Figure 3.11: Energy pipeline models of *Phaseolus vulgaris* 79

Figure 3.12: Relative variable chlorophyll *a* fluorescence of *Phaseolus vulgaris* after 25 days of O_3 fumigation 81

Figure 3.13: A:Ci response curve of *Phaseolus vulgaris* after 25 days of fumigation 83

Figure 3.14: Chlorophyll content in *Phaseolus vulgaris* after 30 days of fumigation 85

Figure 4.1: Relative water content of *Pisum sativum* plants 87

Figure 4.2: Leaf water potential of *Pisum sativum* plants 88

Figure 4.3: *Pisum sativum* growth inhibition 89

Figure 4.4: Influence of O_3 and drought stress on stomata of *Pisum sativum* 90

Figure 4.5: Scanning electronmicrographs of open stomata of *Pisum sativum* 91

Figure 4.6: Effect of O_3 and drought stress on biomass of *Pisum sativum* 92

Figure 4.7: Raw chlorophyll *a* fluorescence transients of *Pisum sativum* before fumigation 94

Figure 4.8: Raw chlorophyll *a* fluorescence transients of *Pisum sativum* after 30 days of fumigation 94

Figure 4.9: Chlorophyll *a* fluorescence transients of *Pisum sativum* normalised between 50 µs and 2 ms 95

Figure 4.10: Chlorophyll *a* fluorescence transients of *Pisum sativum* normalised between 50 µs and 30 ms 96

Figure 4.11: Chlorophyll *a* fluorescence transients of *Pisum sativum* normalised between 50 µs and 30 ms plotted above 1 and 30 ms 97

Figure 4.12: Chlorophyll a fluorescence transients of *Pisum sativum* normalised between 30 ms and P_M, plotted in the 30 – 400 ms range 97

Figure 4.13: Functional and structural parameters of PS II of *Pisum sativum* 99

Figure 4.14: Relative variable chlorophyll *a* fluorescence of *Pisum sativum* after 30 days of fumigation 101

Figure 4.15: Photosynthetic performance index ($PI_{ABS,tot}$) of *Pisum sativum* 102

Figure 4.16: A:Ci response curve of *Pisum sativum* after 15 days of fumigation 104

Figure 4.17: A:Ci response curve of Pisum sativum after 30 days of fumigation 107

Figure 4.18: Effect of O_3 and drought stress on assimilation rate, transpiration rate and stomatal conductance in *Pisum sativum* 109

Figure 4.19: Effect of O_3 and drought stress on Rubisco activity in *Pisum sativum* 111

Figure 4.20: Chlorophyll content in *Pisum sativum* 112

Figure 4.21: Effect of O_3 and drought stress on H_2O_2 concentration in *Pisum sativum* 113

Figure 4.22: Effect of O_3 and drought stress on POD activity in *Pisum sativum* 115

Figure 5.1: Scheme of inhibition sites in the chloroplast 128

List of Tables

Table 2.1:	Time schedule during growth of *Phaseolus vulgaris*	49
Table 2.2:	Time schedule during growth of *Pisum sativum*	50
Table 2.3:	JIP-test formulae	61
Table 3.1:	Yield parameters for *Phaseolus vulgaris*	70
Table 3.2:	Gas exchange parameters of *Phaseolus vulgaris* after 25 days of O_3 exposure	84
Table 4.1:	Gas exchange parameters of *Pisum sativum* after 15 days of O_3 exposure	105
Table 4.2:	Gas exchange parameters of *Pisum sativum* after 30 days of O_3 exposure and 15 days of drought treatment	108

Chapter 1

Literature review

1.1 Air Pollution

Air pollution is one of the most critical and urgent problems globally and is also a growing concern, primarily due to rapid economic growth, industrialisation and urbanisation associated with increases in energy demands. Rapidly growing cities, increased traffic on roads, use of non-renewable fuels, reliance on outdated industrial processes and lack of implementation of environmental regulations, are all major factors that contribute to the poor air quality of most countries (Agrawal, 2005). The occurrence of poor air quality and its effects are not necessarily a modern day phenomenon and problem. Some of the first documentations of air quality problems caused by mining activities go as far back as 900 BC. The problem really took effect during the Middle Ages in England, caused by the burning of coal instead of wood as main energy source, so much so that King Edward I stated: "whosoever shall be found guilty of burning coal shall suffer the loss of his head". These words must have fallen on deaf ears, because during the Industrial Revolution (18^{th} and 19^{th} centuries) the problem took a turn for the worst with dangerously high levels of air pollution causing a dramatic rise in the death rate (Cope, 2010). It is at this stage that the corrosive properties of this pollution and also its effect on vegetation became apparent.

Atmospheric pollution only emerged as a problem in southern Africa over the last few decades due to a drastic increase in commercial energy consumption, which has risen by 145 % since 1973 (McCormick, 1997). Large industries in South Africa, Zambia and Nigeria are responsible for the magnitude of source emissions (van Tienhoven, 2000). In South Africa, air pollution largely originates from thermal power stations (coal-fired power stations) and approximately 89 % of electricity in this region is generated from burning of coal (UNEP, 2000). Southern Africa also has one of the richest mineral deposits and the smelting of ores from these minerals give rise to major sources of different types of air pollution (Emberson, 2003). According to the United Nations Development Program (UNDP, 1998), global air pollution kills more than 2.7 million people annually, with the majority of these deaths (90 %) occurring

in developing countries. However, very little is known about actual pollutant concentrations in many suburban and rural areas where there may be significant indirect impacts on human health, through reduced crop yields, food quality and income. According to Convile (2002), the source origin of air pollutants can be divided into three categories. Firstly: combustion of fuel for energy, where pure hydrocarbon fuel is combusted in pure oxygen to produce carbon dioxide and water. No fuel currently burned on earth is completely pure, and small quantities of pollutants are present in natural gas. During the combustion stage the impurities are usually oxidised and emitted into the troposphere together with carbon dioxide and water. The impurities do not necessarily have to be in the fuel to aid in the dispersal of emissions, but can also be in the atmosphere. During combustion, abundant atmospheric nitrogen (N_2) sources are oxidised to a mixture of nitric oxide (NO) and nitrogen dioxide (NO_2), collectively known as NO_x. These oxides, together with sulphur dioxide (SO_2) are the most abundant pollutants produced after carbon dioxide (CO_2) (Convile, 2002). Secondly: pollutants originating as a result of chemical processes, which can be placed in another category. Thirdly: a wide range of air pollution sources do not fit into either of the two categories mentioned above and is placed in a separate category. These sources are more natural and range from volcanoes that emit SO_2 into the atmosphere, to lightning that is responsible for about 10^{10} kg NO_x gasses per year. Agricultural sources also fall into this category, where ammonia from both animal manure and the application of chemical fertilisers can be seen as a peculiar pollutant in that their polluting effects are the same as their intended use (Convile, 2002).

Because a lot of air pollution is due to vehicles, no evident solution appears to be in sight. Air pollutants currently considered to be of most concern to cause direct damage to vegetation in most countries, are SO_2, oxides of nitrogen (NO_2 and NO), photochemical oxidants (ozone), hydrogen fluorides (HF) and suspended particulate matter (SPM). Direct effects of air pollution can be further classified into either visible or invisible injury. Visible injury usually consists of discolourations of plant organs, e.g. leaf surface becoming discoloured due to internal cellular damage. Injuries not visible to the naked eye result from pollutant impacts on plant physiological or biochemical processes and can lead to loss of growth or yield and changes in the nutritional quality (e.g. protein contents) (Ashmore & Marshall, 1999).

Ultimately, modern research into the effects of air pollution on crops is aimed at generating data which can be employed in the formulation of pollutant control policies, whether at national or international levels (Bell & Treshow, 2002).

1.2. Ozone and its formation

Schönbein (1840) suggested the existence of an atmospheric substance having an electrical odour, and being freed in noticeable amounts during thunderstorms (lightning), and he proposed the name ozone (O_3) for this substance. Houzeau (1858) has chemically proven that O_3 exist at ground level. The latter finding sparked interest among scientists and during the late 1850s, at more than 300 stations, measurements commenced to determine the concentration of atmospheric O_3 (Fox, 1873).
Some 100 years elapsed since those first measurements of ground level O_3 were noted, before Richards *et al*. (1958) defined it as a phytotoxin and showed that O_3 caused foliar injury on grapes in California. This lead to a sequence of investigations and gave O_3 a great deal of attention regarding its status as a pollutant.

Ozone plays a dual role in our atmosphere, being both protective and or damaging to living organisms according to the atmospheric height where it accumulates (Peńarrubia & Moreno, 1999). Unlike other gaseous pollutants, O_3 forms naturally when sunlight interacts with oxygen molecules (photochemical reaction) in the stratosphere to form a three-atomic molecular combination of oxygen (O_2). This is known as the protective O_3 (good O_3) that protects the earth from damaging ultra-violet (UV) radiation emitted from the sun. Ninety percent of the total O_3 in the atmosphere sits in the stratosphere, between 10 and 50 km above the earth's surface (Peńarrubia & Moreno, 1999).

Closer to ground, however, in the troposphere, UV sunlight of sufficient short wavelength is not present to allow the photolysis of O_2 to occur. Thus, principally NO_2 is photolysed to generate O_3. Stratospheric O_3 can also be transferred into the troposphere, but predominantly O_3 formation is driven by two major classes of directly emitted precursors: NO_x and volatile organic compounds (VOCs) (Crutzen, 1975).

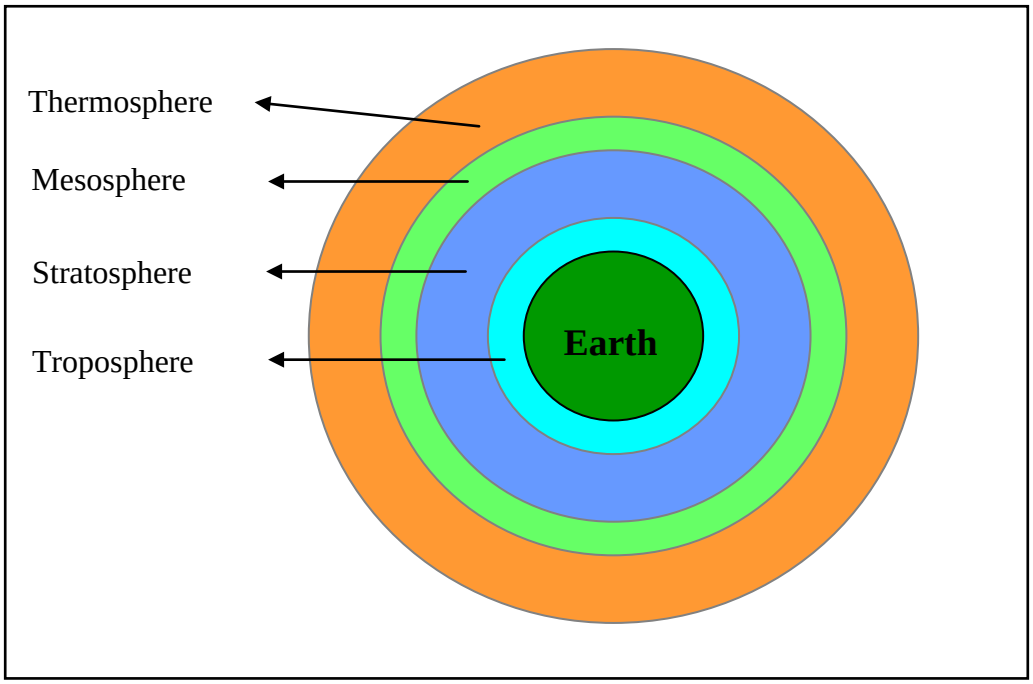

Figure 1.1: The different layers present in the atmosphere. The stratosphere and troposphere are the only two layers containing ozone.

Developing countries have all the right pre-cursors to result in O_3 concentrations above the natural background concentration of about 40 ppb. Motor vehicles, particular inefficient and poorly tuned engines which are characteristic for developing countries, can be seen as the major source of VOCs. Furthermore, the high temperatures together with high light intensity characteristic of many developing countries, such as South-Africa, favour the production of O_3 (Marshall, 2002). The relation between O_3, NO_x and VOC is driven by complex non-linear photochemistry, where sunlight acts as the energy source for the reaction, bringing forth UV radiation, which can be seen as a critical step in the formation of O_3 (Sillman, 1999).

The relation between O_3, NO_x and VOC can be illustrated using isopleth plots (**Figure 1.2**), showing peak O_3 concentrations during the afternoon as a function of NO_x and VOC mixing ratios. It is possible to identify two regimes with different O_3-NO_x-VOC sensitivity. Firstly, a NO_x-sensitive regime can be seen where there are relatively low NO_x and high VOC concentrations. Ozone increases with increasing NO_x and changes very little in response to increasing VOC. Secondly, a saturated or VOC-sensitive

regime can be seen, where O_3 decreases with the increase in NO_x concentration, and increases with increasing VOC concentration (Sillman & He, 2002).

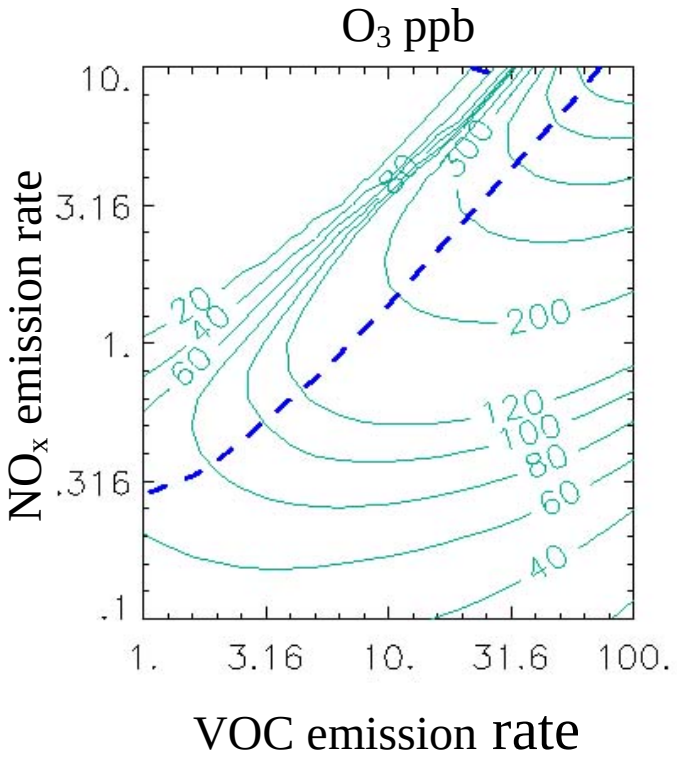

Figure 1.2: Ozone isopleths diagram showing hypothetical response of peak 1h average ozone concentrations within an air basin to changed levels of anthropogenic VOC and NO_x emissions. The short blue dashed line represents the transition from VOC-sensitive to NO_x-sensitive conditions (Sillman & He, 2002)

The latter accumulation of O_3 is a direct result of human action due to a rapid increase in urbanisation (Mage *et al.*, 1996). Because of the dependency of O_3 formation on sunlight (solar radiation), O_3 concentrations tend to vary considerably in time and space and show annual and diurnal patterns, with high concentrations during the afternoons. The latter characteristic makes the quantification of O_3 effects on vegetation enormously difficult as a result of this high unpredictability (Bender & Weigel, 2002).

Ozone levels are typically expressed in parts per billion (ppb), which represent the fraction of air molecules represented by O_3 molecules. The following O_3 concentrations can be seen as typical mixing ratios in different areas:

Natural background (pre-industrial)	10–20 ppb
Remote locations in the Northern Hemisphere	20-40 ppb (varying seasonally)
Rural areas during region-wide pollution events	80-100 ppb
Peak O_3 in urban areas during pollution events	120-200 ppb
Maximum urban O_3 (Los Angeles, Mexico City)	490 ppb
Stratospheric ozone layer	15 000 ppb

Nitrogen oxides are released into the troposphere from various sources that include both biogenic and anthropogenic sources (Lee *et al*., 1997). Of these, approximately 40 % originate as a result of the combustion of fossil fuels. The emissions are mainly in the form of NO, but a small fraction (generally 10 %) can be released as NO_2. Nitrogen oxide can also be formed when O_2 reacts with NO (PORG, 1997).

$$2NO + O_2 \rightarrow 2NO_2 \quad (1)$$

The rate of the reaction is strongly dependent on the concentration of NO. Thus at high concentrations of NO, the conversion of NO to NO_2 is rapid, but then decreases dramatically as NO is used up for the reaction. The conversion rate for NO is 5×10^{-6} s^{-1} at 1 ppmv NO, but under normal tropospheric conditions reaction (1) only accounts for a small amount of NO_2 that is emitted into the troposphere. The dominant pathway by which NO is converted to NO_2 is through the reaction with O_3 (Jenkin & Clemitshaw, 2000):

$$NO + O_3 \rightarrow NO_2 + O_2 \quad (2)$$

This reaction is however reversed in daylight, and NO_2 is converted back to NO as a result of photolysis, which also adversely leads to the formation of O_3,

$$NO_2 + h\nu\ (\lambda < 400\ nm) \rightarrow NO + O \quad (3)$$

whereas atomic O_2 reacts with molecular dioxygen to produce O_3:

$$O + O_2(+M) \rightarrow O_3(+M) \quad (4)$$

where M is a third chemical species, most likely N_2 or O_2, that dissipates the excess energy of the O_3 molecule that is produced. If there is no third chemical species present, the O_3 will not form at all or dissociate on formation. During the day however, in atmospheres with low carbons and CO, a dominant mode of action for NO is reaction with O_3. Under these conditions, as shown in **Figure 1.3**, a cyclic situation known as the Leighton relationship is created, with O_3 being continuously formed and consumed (Marsili-Libelli, 1996).

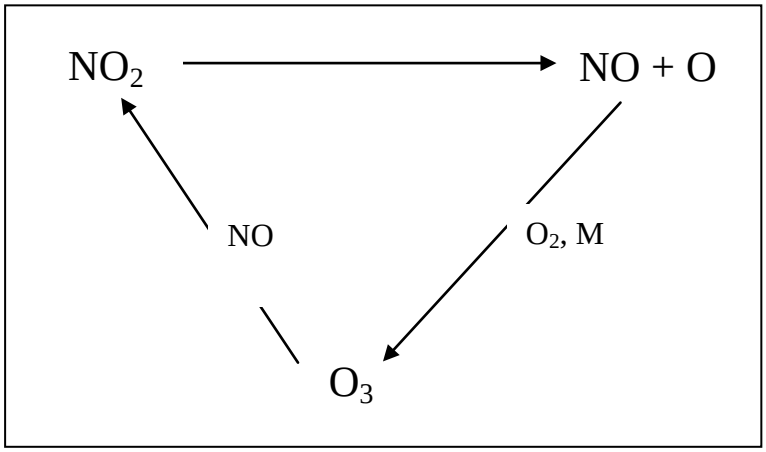

Figure 1.3: The Leighton relationship, which describes the cyclic reaction between NO, NO_2 and O_3 in the troposphere, with little or no hydrocarbons or CO.

In the absence of any other secondary reactions, steady concentrations of NO_2, NO and O_3 are eventually observed as time elapses. The relationship between these steady-state concentrations is given by:

$$\frac{[O_3][NO]}{[NO_2]} = \text{Constant}$$

Furthermore, NO, which is a product of the first step, is usually oxidised back to NO_2 through photochemically generated oxidants, thereby closing an O_3 producing-cycle (Peńarrubia & Moreno, 1999). The production of these photochemical oxidants usually occurs over several hours, which aids in the dispersal of the oxidative O_3 to other regions due to turbulence.

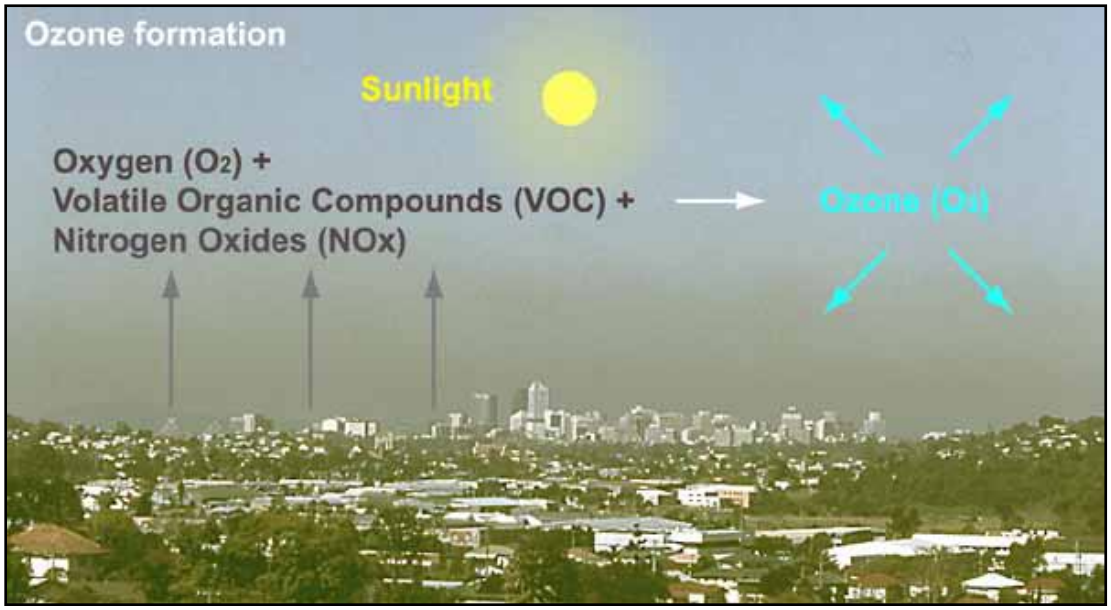

Figure 1.4: Visual illustration of O_3 formation in densely populated cities; note the fog that consists mostly of emissions by burning fossil fuels. Energy is mainly generated by burning fossil fuels, which indirectly results in the formation of O_3 (Queensland Government).

1.2.1 The role of volatile organic compounds in the formation of O_3

As mentioned previously, the formation of O_3 in the troposphere is promoted by the presence of VOCs, NO_x and sunlight. Sunlight starts the reaction by providing near UV radiation which promotes the dissociation of certain stable molecules. This dissociation leads to the formation of hydrogen-containing free radicals ($HO\bullet_x$). These free radicals catalyse the oxidation of VOCs in the presence of NO_x, leading to the formation of CO_2 and water vapour. Moderately oxidised organic species such as aldehydes, ketones and carbon monoxide (CO) are produced as intermediate oxidation products, with O_3 formed as a by-product. A vast variety of VOC classes can be emitted from various anthropogenic and biogenic sources and depending on location, they aid considerably in formation of photochemical O_3 (Sillman, 1999), especially in large cities (Kleinman *et al*., 2002.

The chemistry of the oxidation of VOCs can be shown schematically by the oxidation of a generic saturated hydrocarbon, RH (i.e., an alkane). The oxidation is initiated

when a hydroxyl radical (OH) reacts with the VOC, leading to various rapid reactions (Jenkin & Clemitshaw, 2000):

$OH\bullet + RH \rightarrow R + H_2O$ (5)

$R + O_2(+M) \rightarrow RO_2(+M)$ (6)

$RO_2 + NO \rightarrow RO + NO_2$ (7)

$RO \rightarrow$ carbonyl product(s) + HO_2, (8)

$HO_2 + NO \rightarrow OH + NO_2$ (9)

Since OH• is regenerated, this mechanism is a catalytic cycle with OH•, R (alkyl radical), RO_2, RO (alkoxy radical) and HO_2 acting as a chain propagating radicals. Reactions (7) and (9), involving the peroxy radicals, play a key role in O_3 formation by oxidising NO to NO_2. As discussed in Section 1.2, NO_2 is efficiently photodissociated by near UV radiation to generate O_3 by reactions (3) and (4) (Jenkin & Clemitshaw, 2000).

1.3 Critical levels of ozone

Critical levels refer to the direct effects of gaseous pollutants, such as O_3, and are defined as the concentrations of pollutants above which direct adverse effects on receptors, such as plants, ecosystems or materials, may occur according to current knowledge (UNECE, 1988 Workshop). The critical level concept is one devised for use in a policy context. In practice, policy evaluation is based on mapping to identify areas where the critical levels are exceeded and European-scale computer modelling to predict the effect of different emission control scenarios on the extent of these exceedances.

Critical levels for O_3 were first defined at a workshop at Bad Harzburg, Germany in 1988 (UNECE workshop) where the values were expressed as a seasonal mean concentration. At a workshop in Egham, UK in 1992, Ashmore & Wilson (1994) proposed to replace this basis of expression by a cumulative exposure over a threshold concentration for a given length of time. At a third workshop in Bern, Switzerland (Fuhrer & Achermann, 1994) this concept was adopted and the threshold

concentration was set at 40 ppb (billion = 10^9); the resulting index was termed the AOT40 (accumulated exposure over a threshold of 40 ppb). Finally, at a workshop in Kuopio, Finland in 1996, the use of the AOT40 index was agreed upon, and a revised set of critical level values based on this index were set for crops, forest trees and semi-natural vegetation (Kärenlampi & Sharby, 1996).

$$\text{AOT40} = \sum_{i=1}^{n} \left[C_{O3} - 40 \right] \quad \text{with } C_{O3} > 40 \text{ ppb}$$

The potential for O_3 to damage vegetation has been known for over 30 years, but it is only over the last decade that its impact has become of major concern in Europe. It is now clearly established that O_3, at ambient concentrations, can have a range of effects including visible leaf injury (Agrawal *et al*., 2003), growth and yield reductions (Fumagalli *et al*., 2003), and altered plant metabolism (Darrall, 1989). Because O_3 is a secondary pollutant with a regional distribution, these effects may occur over large areas of rural Europe. Research in recent years has advanced our understanding of the mechanisms underlying O_3 effects on agricultural crops and, to a lesser extent, on trees and native plants species. It is now possible to determine biologically meaningful, but simple, indices to characterise O_3 exposure and to identify the critical levels of exposure.

This looming threat of food security called for action in terms of air quality management. Before guidelines can be set in place, it is necessary to determine the effect of air pollution on matters of concern such as health, vegetation etc. within different regions. For the most part of Europe and North America these dose-response relationships have been produced and applied to improve air quality, however in developing countries, such as those in southern Africa, data are lacking.

1.4 Ozone's dispersal in the environment

Ozone is predominantly a gas at Normal Temperature and Pressure (NTP), which makes the dispersal from its origin a huge problem, since it can travel in air masses over long distances, causing higher concentrations to be reported in rural areas where the majority of a country's crops are produced (Agrawal *et al*., 2003). High

concentrations of O_3 are mostly correlated with hot sunny weather and occur over wide areas (Ashmore, 2005). The latter scenario makes southern Africa a favourable region for O_3 to form and accumulate, since the anticyclonic climatology suppresses vertical mixing (Jenkin & Clemitshaw, 2000).

In South Africa the tropospheric O_3 maximum possibly results from a combination of the tail end of pyrogenic emissions (vegetation fires) during August to October and the beginning of biogenic emissions during September to October (Scholes & Scholes, 1998). The addition of an increasing anthropogenic pollution load could result in damage thresholds being exceeded in the late winter and early spring, with consequent damage to vegetation. The South African Highveld sites are expected to fall within the 50 to 100 ppb range reported to cause damage to plants within zero to four hours exposure (Lacasse & Treshow, 1976).

Ground level O_3 is the most widespread and is a phytotoxic pollutant that frequently exceeds World Health Organisation (WHO) air quality guidelines for agricultural crops in many parts of the world (Fuhrer & Booker, 2003). Ground O_3 levels in many rural regions have increased significantly during the past 100 years due to rapid increases in urbanisation and industrialisation in many developing countries, including South Africa (Lefohn, 1992; Voltz & Key, 1988). Assessment of the response of crops under South African conditions are thus of paramount importance (Marshall *et al.*, 1998). Measurements over a time of 35 years have shown that the average ambient O_3 concentration have increased by 1-3 % per annum since the 1950's (Feister & Warmbt, 1985). Background surface concentrations of O_3 have risen from between 10 and 20 ppb[1] at the beginning of the twentieth century, to values between 20 and 40 ppb in recent times (Volz and Kley, 1988). It has been predicted that O_3 concentration will increase by 0.3-1.0 % per year for the next 50 years (Chameides *et al*., 1994).

Over the rural areas of southern Africa, surface O_3 concentrations also range between 20 and 40 ppb. In some monitoring stations around the heavily industrialised mining and energy generation regions of South Africa, hourly means of up to 110 ppb have

[1] ppb = parts per billion on a volume basis. It is equivalent to $nmol.mol^{-1}$. For ozone, 1 ppb is equal to about 0.5 $\mu g.m.^{-3}$

been measured (Rorich & Galpin, 1998). This increase in ambient O_3 levels spells disaster for developing countries. With an existing food shortage and the suppressing effect O_3 has on plants, crop yields are due to decline even further. This will not only lead to starvation and a severe economical impact, but also a decline in any further development for these struggling countries. While the impacts of air pollution, and particularly O_3, on agriculture in North America and Western Europe have received considerable attention, there has been little recognition of this issue in developing countries such as Asia, Africa, and Latin America. It is therefore extremely important to establish local field-based evidence to demonstrate the true cost of air pollution in these developing countries (Marshall, 2002).

In southern Africa there is a growing concern that the concentrations of O_3 commonly found in the local troposphere may adversely affect natural vegetation, forests and crops (van Tienhoven & Scholes, 2003). Agriculture in southern Africa is important for both export and survival purposes. Food production is essential for small-scale and subsistence farmers, since a large portion of people living in these parts rely solely on self grown agricultural products for survival (Rogerson, 2000). To get a clearer picture of the extent to which O_3 exposure influences the economy of countries, Holland *et al*. (2006), determined that Europe loses an estimated US$ 8 billion per year as a direct result of O_3 exposure. The analysis incorporated more than 20 crops that are currently cultivated throughout Europe.

Figure 1.5 provides an indication of surface O_3 concentrations from the World Meteorological Organization. From this figure, areas can be identified that exceed the average mean O_3 concentration AOT40. The model further indicates large areas on the sub-continent where surface O_3 concentrations exceed the critical level of 40 ppb for up to 10 h per day. The critical level is the concentration of pollutants in the atmosphere above which adverse effects occur on sensitive receptors such as plants, ecosystems or materials according to present knowledge.

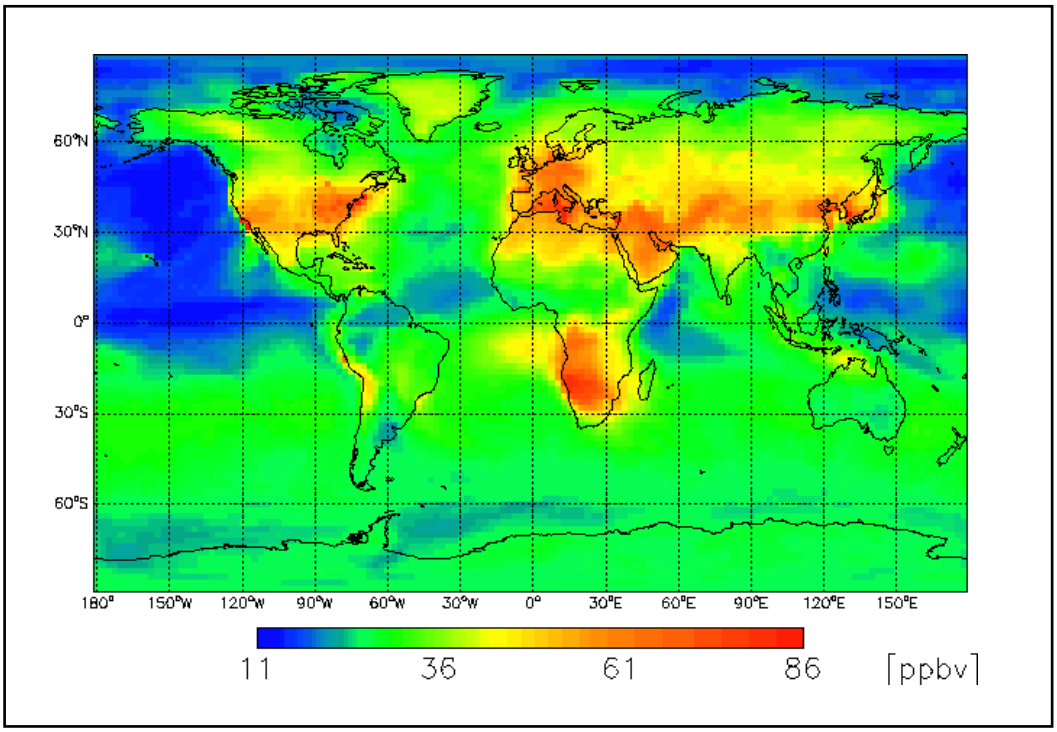

Figure 1.5: Monthly mean afternoon (1 to 4 PM) surface ozone concentration calculated for July 2001 using Harvard GEOS-CHEM model (World Meteorological Organization).

1.5. Effects on plants

In their effect on plants, air pollutants interact with other environmental abiotic and biotic stress factors in a complex way. Ozone has been shown to affect plant growth at all biological levels, ranging from sub-cellular effects to effects on whole ecosystems. Ozone is one of the most powerful oxidants known, with a slightly lower oxidation potential than fluorine. The solubility of O_3 in pure water is 0.29 m^{-3} at 25° C. Despite its oxidation potential of +2.07 eV in pure water with a pH equivalent to that of the apoplast (5.0-6.5), its half life exceeds 1 hour at 25° C (Moldau, 1998).

Unlike SO_2 and NO_x, the process by which O_3 causes injury to vegetation is not complicated by its role as a source of an essential nutrient (Emberson *et al.*, 2003). Although O_3 is highly reactive, primary damage is restricted to the leaves, and then also primarily the mesophyll (Black *et al.*, 2000). Since O_3 entry through the leaf

cuticle is negligible, the flux of O_3 is largely determined by the rate of stomatal gas exchanges, which in turn also depends on the number and dimension of stomata and the degree of their opening (Paoletti & Grulke, 2005). Moist surfaces within the leaves (e.g. extracellular fluid of mesophyll), all low in O_3, provides a favourable concentration gradient for O_3 to dissolve and diffuse similar to that of CO_2. The total amount of O_3 uptake depends on several factors, i.e.; the degree of solubility, rate of decomposition, and the pH of various media influences. However, O_3 is approximately one-third as soluble as CO_2, which makes O_3 much less stable in aqueous mediums in the leaves (Wellburn, 1994). This stability of O_3 in solution greatly depends on the pH in the leaf, and it increases significantly under acidic conditions (Thorp, 1955).

When O_3 has entered to the sub-stomatal cavity, it reacts with water and other constituents of the aqueous matrix that is associated with the cell wall to form derivatives or free radicals. These free radicals or reactive oxygen species (ROS) are short lived, highly reactive molecular fragments that contain one or more unpaired electrons which are formed by the splitting of a molecular bond. These reactive radicals oxidise sensitive components of the plasmalemma and cytosol that play an important part in the maintenance of the plant as a whole (Kley *et al.,* 1999). Ozone also reacts with the hydroxyl ions of water to form the extremely reactive hydroperoxide ($\bullet O_2H$) and superoxide ($\bullet O_2^-$) radicals:

$$HO^- + O_3 \rightarrow \bullet O_2H + \bullet O_2^-$$

Hydroperoxide radicals can combine, forming hydrogen peroxide:

$$\bullet O_2H + \bullet O_2H \rightarrow H_2O_2 + O_2$$

Because O_3 is such a strong oxidant, prolonged exposure to high concentrations will damage the plasmalemma to the extent that the cell will be unable to maintain its ion balance, ultimately leading to cell death. The latter situation will cause symptoms such as chlorosis and necrosis, due to the loss of cell function. It is however, almost impossible to distinguish whether the above symptoms in the field are caused by O_3 or

normal senescence, and an in-depth study should be carried out to distinguish between the latter.

In South Africa, O_3 monitoring in various Highveld sites has reported maximum hourly mean concentrations in the range of 76 to 110 ppb (Rorich & Galpin, 1998). This falls within the 50 to 100 ppb (98-196 $\mu g.m^{-3}$) range reported to cause damage within 2-4 hours exposure (Lacasse and Treshow, 1976). It is however important to note that the threshold dose of O_3 that causes injury, varies tremendously between species and even cultivars of the same species (Scholes *et al*., 1996). The plant responses to air pollutants in hot, dry climates may be further influenced by water and temperature stresses, and can even protect plants from air pollutants. Plants respond to water stress by closing their stomata in order to reduce the loss of water by transpiration. Subsequently the uptake of air pollutants decreases and damage to plants is reduced (Schenone, 1993).

O_3 exposure leads to some very explicit symptoms, eg i) flecks, which are tiny irregular spots less than 1 mm in diameter, and ii) stipples, which are small darkly pigmented areas approximately 2-4 mm in diameter (**Figure 1.6**). These symptoms can also be called bronzing and redding, because of the brownish colour the spots represent on the damaged leaves of the plant. The severity of visual and non-visual injuries is dependent on several factors including duration and concentration of O_3 exposure, weather conditions and the genetics of the specific plant (Anon, 2009).

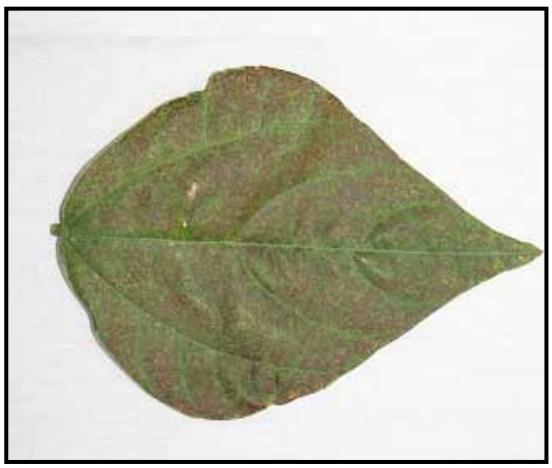

Figure 1.6: Ozone injury on a bean leaf (*Phaseolus vulgaris*), note the brownish flecks and stipples between the leaf veins.

Ozone symptoms usually occur between the veins on the adaxial (upper) leaf surface of older and middle aged leaves. Older leaves are damaged due to a longer exposure period. Ozone can reduce agricultural yield and subsequently cause economic limitations, as previously mentioned, by a variety of mechanisms. Two of these mechanisms that are mostly responsible for economic losses are:

(i) Visible injury on specific species with a market value based on their appearance, which can lead to an immediate loss in economic value. Not only does this affect the immediate visual characteristic, but can also lead to a bad taste and lower nutritional value.

(ii) Ozone can also reduce the marketable yield of a range of crop species, in the absence of previously discussed visible injury, primarily through its effects in reducing photosynthetic rates and accelerating leaf senescence (Ashmore, 2005).

Losses in agricultural crops are currently significant in the United States of America (Adams *et al.*, 1988; Holmes, 1994) and in Europe (Holland *et al*., 2002), estimated to $ 3 billion and £ 4.3 billion, respectively, in recent years. Damages due to O_3 range from visible ones such as leaf spotting to yield or quality reductions (Ollerenshaw *et al*., 1999; Fumagalli *et al*., 2001; Fuhrer & Booker, 2003).

Only little attention has been directed to the role of O_3 in agriculture in Africa. To date, O_3 injury assessment of plants on southern Africa has been undertaken on an extremely limited scale, using green beans (*Phaseolus* sp.) (Botha *et al*., 1990) and maize (van Huyssteen, 2003; van Tienhoven *et al*., 2004).

1.5.1 Photosynthesis and production

The oxidative stress imposed by O_3 at the biochemical level is reflected at higher levels of organisation by a decline in the photosynthetic capacity, increased respiration, changes in patterns of carbon distributions, accelerated leaf senescence and foliar injury induced by a loss of chlorophyll, increase in fluorescence and change in energy levels (Wellburn, 1994). Cells of plant tissue will become injured and may even die when the uptake of O_3 through the stomata exceeds the detoxification rate and capability of repair systems (Tingey & Anderson, 1991).

Intercellular effects include inhibition of chloroplast function and pigment loss. Reductions in net photosynthetic rate due to O_3 exposure have been related to decreased levels and activity of Rubisco and impaired electron transport (Pell *et al*., 1997). Ozone induces a reduction in net photosynthesis e.g., as measured by photosynthetic gas-exchange). Besides this decline in the photosynthetic capacity of individual leaves, a decrease in stomatal conductance and an increase in rates of maintenance respiration may further contribute to a reduction in net photosynthesis (Darrall, 1989). While elevated background levels of O_3 are often insufficient to produce visible injury, lower photosynthesis is often reported (McKee *et al*., 1997). Morgan *et al.* (2003) showed impairment of photosynthetic carbon acquisition in leguminous plants at chronic O_3 exposure of 70 ppb through meta-analyses based on 53 peer review studies. In addition, O_3 decreases the total amount of CO_2 assimilated, can reduce leaf duration (i.e., accelerated leaf senescence) and alter the pattern by which the reduced amount of assimilate is distributed throughout the plant. Ozone also reduces resource distribution to the roots and reproductive organs to favour shoot growth instead (Miller, 1998).

1.5.2 Defense: Anti-oxidant defense mechanisms

According to Laisk *et al.* (1989), the concentration of O_3 is virtually undetectable in the apoplast because immediately after its entry into the sub-stomatal chamber, it spontaneously decomposes or reacts with numerous compounds, forming ROS such as free radicals (OH•, $O_2^{-\bullet}$) and peroxides (H_2O_2 and R_2O_2) (Kanofsky & Sima, 1991; Chameides, 1989), which can damage the components of plasmamembranes, such as proteins and lipids. Reactive oxygen species can be produced either during normal physiological processes, particularly during the light-dependent photosynthetic reactions in plants (Foyer *et al*., 1994), or during stress responses to various stresses such as exposure to O_3 (Polle & Rennenberg, 1993). Plants can deal with O_3 in one, or both, of two ways. Firstly, stomatal control of O_3 uptake can be seen as the ability of a plant to avoid stress by closing its stomata, hence stress avoidance. Stomatal closure in response to O_3 can be regarded as a protective mechanism, which limits the dose/concentration delivered to the intercellular space. Differences in stomatal

frequency or response have been related to differences in plant sensitivity to O_3 (Degl'Innocenti *et al.*, 2003). Secondly, scavenging enzymes inside the cell protect the plant against the ROS that forms (**Figure 1.7**).

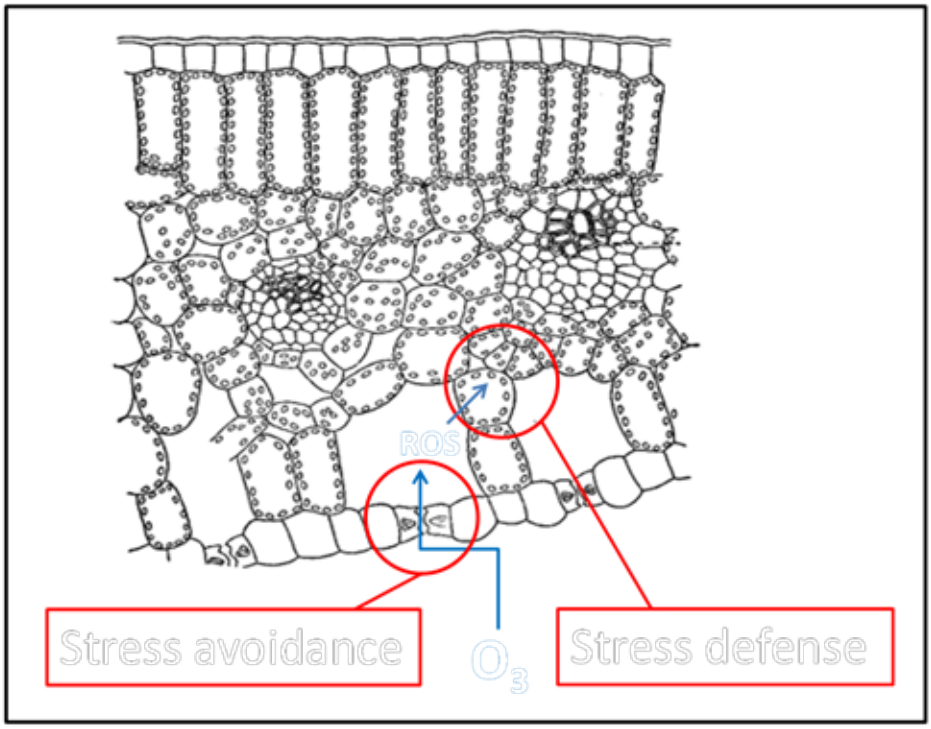

Figure 1.7: Schematic representation of the two main plant cell responses; (i) stress avoidance by stomatal closure and (ii) stress defense by scavenging enzymes (Castagna & Ranieri, 2009).

Antioxidant enzymes, such as superoxide dismutase (SOD), catalase (CAT), peroxidase (POX), as well as the enzymes of the ascorbate-glutathione cycle (Halliwell-Asada cycle): ascorbate peroxidase (APX), glutathione reductase (GR), monodehydro-ascorbate reductase (MDHAR) and dehydro-ascorbate reductase (DHAR) provide endogenous defense against the accumulation of harmful ROS concentrations (Lee *et al.*, 1984). In the process of detoxification of H_2O_2 of particularly importance is the large family of peroxidases (POD, which includes both the specific ascorbate peroxidase enzyme (APX) and the so-called unspecific peroxidases (POD). Peroxidase activity increases in plants in response to a great variety of stresses, including viral, microbial, or fungal infections, salt stress, wounding, or air pollution (Gaspar *et al.*, 1982). Several pollutants such as O_3 (Curtis *et al.*, 1976), SO_2 (Horsman & Wellburn, 1977), or NO_2 (Horsman & Wellburn, 1975)

are known to induce an enhancement of the total POD activity of plants. The POD increase following an exposure to O_3 is different in different species and is a function of the resistance of the plant to O_3 (Curtis *et al*., 1976).

1.6 O_3 stress in combination with drought stress

The response of plants to air pollutants should be investigated in a "multi-stress" context to understand how air pollutants affect plants and to predict how air pollution impacts will be modified by elements of climate change (Winner, 1994). Water stress is often associated with regions receiving insufficient rainfall; however, even under adequate rainfall or irrigation, plants may experience transient stress during the noon hours of hot days. O_3 injury largely depends on the amount of O_3 taken up into the leaves through the stomata, which is directly dependant on the stomatal conductance (Guiderian *et al*., 1985; Heath, 1994a or b?) and also on the plant's capability to detoxify oxygen radicals. Changes in environmental conditions such as light, temperature, humidity and soil drought influence stomatal opening and therefore also affect O_3 uptake. Open-top chamber experiments (Freer-Smith *et al*., 1989; Dobson *et al*., 1990; Fincher & Alscher, 1992) as well as field studies (Havranek & Wieser, 1993) indicated that drought stress protected plants from O_3 injury mainly through its influence on stomatal aperture. However, there is also evidence that drought stress leads to an increase in the production of free radicals in leaves (Badiani *et al*., 1990; Buckland *et al*., 1991; Quartacci & Navari-Izzo, 1992), which may contribute to leaf injury. Willmer and Pantoja (1992) found that when water stress is continued and drought conditions persist, the stomata progressively lose their ability to close and finally remain permanently open. On the other hand evidence exists that the effect of O_3 on stomatal conductance may not be as straightforward as the above studies imply. Firstly, evidence from various studies indicate that O_3 has a direct effect on guard cells which leads to stomatal closure in the absence of effects on photosynthesis, mainly through the changes in intra- and extracellular calcium concentration (Mansfield, 1998; McAinsh *et al*., 2002). Secondly, rather than reducing stomatal conductance, elevated O_3 opens stomata in some cases, and/or prevents them from closing in response to drought or other closing signals (Barnes *et al*., 1990; Grulke *et*

al., 2007). Vahisalu *et al*. (2008) also showed that when severe water stress was imposed on individual leaves previously exposed to O_3 by excision from the plant, the leaves exhibited enhanced water loss compared with O_3-untreated leaves. In other research, Bernacchi *et al*. (2006) found that O_3 apparently has no effect on stomata at all.

1.7 Flux of pollutants

As in the case of other gaseous air pollutants, O_3 uptake by leaves is crucial for the effect of the gas on structural and functional components of plants. In other words, plants respond to the absorbed dose rather than to the external concentration in ambient air. Pollutant flux, i.e. the rate at which the pollutant is absorbed (PAD) by plant surfaces, is determined by three transport components (**Figure 1.8**)

- Atmospheric transport by turbulent diffusion
- Molecular diffusion across the leaf boundary layer
- Diffusion through the stomatal pore, i.e. stomatal uptake

Thus the pollutant flux (F_s) is a function of (*i*) air conductivity or atmospheric resistance (r_{am}), (*ii*) diffusive resistance at the leaf-air boundary layer (r_{bg}), and (*iii*) stomatal resistance (r_{st}), and F_s can be expressed as:

$$F_s = - r_t^{-1} (t) \{[X]z_1 (t) - \{[X]z_2 (t)\}$$

where r_t is the total transport resistance, $r_t = r_{am} + r_{bg} + r_{st}$, and $[X]_{z1}$ and $[X]_{z2}$ are time-dependant concentrations of the pollutant gas at the height z_1 or z_2, respectively. By convention, the minus sign is needed to indicate that the flux is from the atmosphere towards the ground. The three main transfer resistances, operating in series, are influenced by atmospheric conditions, plant surface characteristics, soil moisture, and by the physiological status of the plant (Nussbaum *et al*., 2003). Under most circumstances, PAD will largely depend on stomatal uptake (Massmann and Grantz, 1995). In open-top chambers, r_{am} and r_{bg} are virtually zero, and O_3 uptake follows canopy conductance to water vapor very closely (Fuhrer *et al*., 1997). Thus, the assessment of the risk for O_3 damage should be based on measured canopy-level O_3

concentrations and should account for the modifying influences of environmental factors on specific stomatal conductance (g_s) (Grünhage and Jäger, 1994; Musselman & Massmann, 1999).

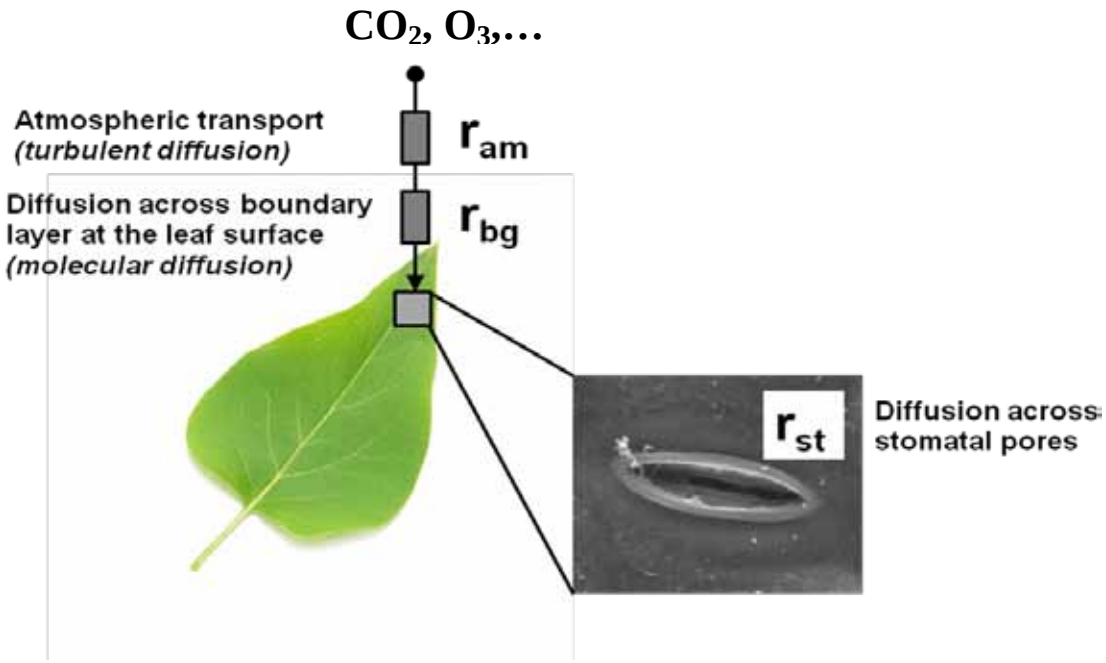

Figure 1.8: Conceptual diagram showing the main elements controlling ozone flux to plants.

1.8 Aim of the study

The aim of this study was to identify and quantify the growth, physiological and biochemical constraints imposed by O_3 on two leguminous crops namely, *Phaseolus vulgaris* and *Pisum sativum* by exposing them to this oxidative pollutant in an open-top chamber system. An integrative approach was followed, studying the effects of O_3 on reductionistic as well as whole plant level, measuring different processes in parallel. As photosynthesis coordinates all aspects of plant physiology and metabolism, we focused on O_3 effects on photosynthesis. Two *Phaseolus vulgaris* genotypes with different sensitivity to O_3 were used to study the effect of O_3 on photosynthesis, which will give a more descriptive insight as to why the resistant genotype is more tolerant to elevated O_3. *Pisum sativum* plants have been subjected to

a combination of stresses, namely that of O_3 with the combination with moderate drought stress. The purpose of the latter investigation was to determine whether or not drought stress will ameliorate the effect O_3 has on the photosynthesis of crop plants.

The investigation was aimed at elucidating the effect of O_3 by:

- determining the effect of O_3 on growth, biomass accumulation and yield
- determining the effect of O_3 on photosynthetic gas exchange by looking in depth at the Rubisco activity (*in vivo*), regeneration capacity of Ribulose-bisphosphate (RuBP) and stomatal conductance
- analysing fast phase chlorophyll a fluorescence kinetics, to determine the effect of elevated O_3 exposure on primary photochemistry and electron transport
- giving insight into the possible sites of inhibition
- determining the effect of O_3 on chlorophyll content
- determining the *in vitro* Rubisco activity to complement the gas exchange data
- assessing the effect of O_3 on the activity of the antioxidative defence system of the test plants; H_2O_2 levels and POD activity were measured.

1.9 Hypotheses

(i) The CO_2 assimilation capacity is inhibited by the decreased production of reducing equivalents by the photosynthetic electron transport chain.

(ii) The CO_2 assimilation capacity is inhibited through reduced activity of RuBP.

(iii) Drought ameliorates the inhibitory effects of O_3 on plants through decreased stomatal conductance. With a combination of elevated O_3 and moderate drought stress the effect that O_3 has on plants should decrease, provided that the stomata conductance under drought stress decreases to inhibit the air pollutant to enter the stomatal cavity.

Chapter 2

Material and Methods

2.1 Study area

The study was conducted at the Potchefstroom campus of the North-West University in an open-top chamber (OTC) system (**Figure 2.1**). The elevation of the study site is 1348 m above sea level and the coordinates are 26°40′50″S, 27°05′48″E. OTCs have been in use for the last 20 years and were first employed in the United States to investigate the relationship of crop growth and yield to gaseous air pollutants *in situ* (Heagle *et al*., 1973). OTCs are a widely accepted design to enclose vegetation, allowing air quality to be modified whilst maintaining natural climatic conditions close to ambient conditions in the field. Various designs have been described in the past (Heagle *et al*., 1973; Mandl *et al*., 1973; Heagle *et al*., 1989; Dunin & Greenwood, 1986). OTCs are essentially cylindrical plastic enclosures, with or without a rain cap at the top to prevent rain from entering the controlled system.

Each of the OTCs used in this study (Heyneke *et al*., 2011) consists of a cylindrical aluminium framework with a height of 2.2 m and diameter of 1.7 m (specially built by Hydro Arch, Secunda, RSA), covered with transparent sheeting. The individual chambers have a capacity of 5 m^3. The opening between the top of the chamber and the rain cap allows air to pass freely through the chamber (**Figure 2.1**). Air is provided by large axial, high capacity output fans with variable speed that is fitted inside an enclosed fan box positioned next to the chamber. One ventilation unit provides ventilation for two OTCs. The air is sucked from the atmosphere (ambient air) and blown through a stainless steel duct which divides horizontally into two PVC tubes which enters at the base of the chamber via a Perspex tube that serves as a manifold onto which two toroids could be positioned. For the control chambers the incoming air was filtered through a fine-grained charcoal-Purafil blend (Purafil ®, Georgia, USA) filter which removes gaseous pollutants such as SO_2, NO_2 and especially O_3 from the air. The air is then evenly distributed throughout the chamber through two perforated toroids consisting of lay-flat tubing, 1 meter and 1.2 meters respectively from the base of the chamber, surrounding the inside of the chamber wall. Uniform ventilation over the plant canopy was ensured by positioning the holes of the upper toroid to project from the base of the chamber diagonally inwards and the holes of the

bottom toroid projecting horizontally into the canopy. Treatment control is therefore ensured by a constant positive air pressure from the base inside the chamber (Buckenham *et al*., 1981).

Figure 2.1: OTC-system of the North-West University, Potchefstroom, RSA. The site contains 12 OTCs for continues exposure of plants to a controlled (desired) ozone concentration.

2.2 Experimental design and ozone treatment

An electrical O_3 generator (OLGEAR UV-20 HO) was fitted in the enclosed fan box to provide a constant O_3 supply (3000mg/H) into the air stream feeding two OTCs (**Figure 2.2**). The generator module is based on UV ray O_3 generating technologies, using four high output OEM UV lamps. The lamps have an output of 185nm, which allows for almost double the normal O_3 output that regular modules generate. Ambient air is pushed through a UV cartridge by a regular air pump. In the UV cartridge the UV ray (185nm) causes the available molecular O_2 energy to split, forming single oxygen atoms (O_1). These atoms then recombine with other molecular O_2 forming O_3 (OLGEAR). The O_3 generated, is fed through teflon tubing, into the stainless steel

duct leading to two OTCs, allowing the O_3 to mix into the air stream ventilating the OTCs. The O_3 enriched air enters the chamber near the bottom of the OTCs through the 2 perforated toroids of lay flat tubing (discussed in 2.1) and flows out at the open top of the chamber.

The O_3 concentration in the chamber was controlled by means of an overflow valve, which could be adjusted to control the O_3 concentration within 10% of the target concentration in the chambers. During the course of the fumigation the desired average of 80 ppb O_3 was maintained in the chambers ± 9 hours per day for 40 days. This way of long-term exposure to O_3 (at concentrations <100 ppb) has generally been termed 'chronic' exposure in the literature (Kangasjärvi *et al*., 2005). In contrast to 'chronic' O_3 exposure, 'acute' exposure typically is the exposure of plants to high levels of O_3 (>100 ppb) for short periods of time.

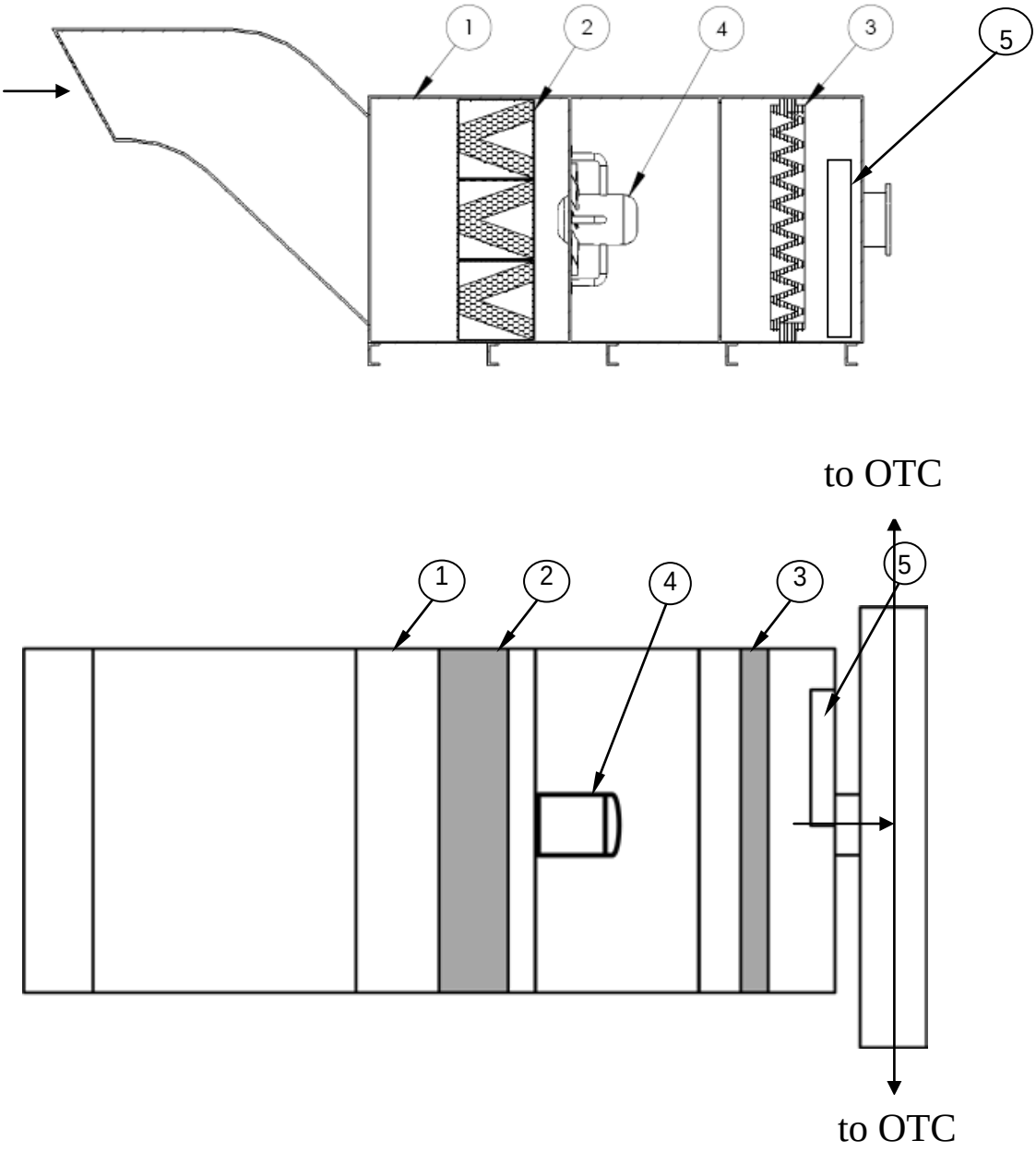

Figure 2.2: Schematic representation of a typical ventilation unit showing the components located inside the weatherproof fan box: (1) Rough filter retaining coarse-grained impurities, (2) 6 exchangeable cartridges filled with fine-grained charcoal-Purafil blend, (3) zigzagged cloth-like filter, retaining finer particles coming from the charcoal/Purafil blend media, (4) 3Kw Volt axial fan and (5) ozone generator fitted in after the final dust filter.

The O_3 concentration in the OTCs was measured with an O_3 monitor (Model 205, 2B Technologies, Inc.) placed in the OTCs. The instrument is designed to enable accurate measurements of atmospheric O_3 over a wide dynamic range extending from a limit of detection of 1.5 ppb by volume (ppbv) to an upper limit of 100 parts-per-million (ppmv) based on the well established technique of absorption of UV light at 254 nm, as O_3 molecules has an absorption maximum at 254 nm. Fortunately, few molecules found on earth at significant concentrations absorb light at this wavelength and therefore the latter characteristic enables the O_3 monitor to be quite accurate (Anon, 2005). O_3 levels of the treatment and control OTCs were monitored (**Figure 2.3**).

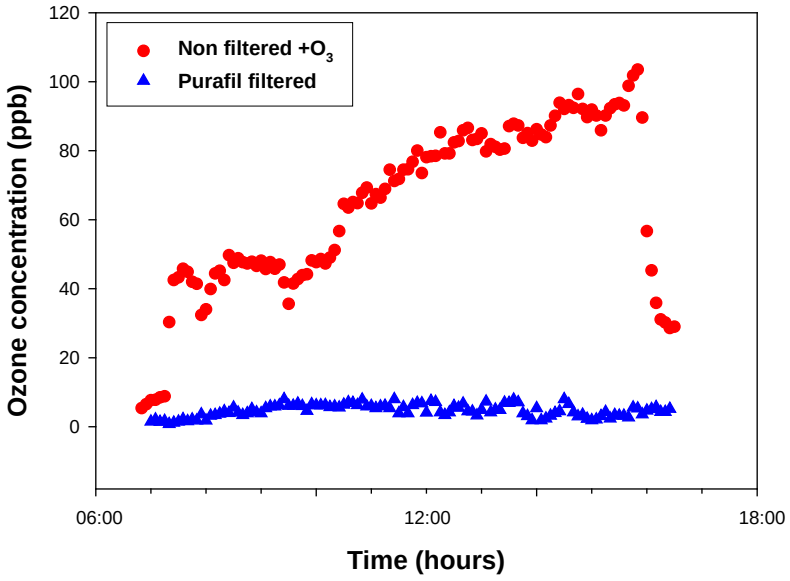

Figure 2.3: Daily ozone concentration in OTCs during an experiment at Potchefstroom. The red dots represent the concentration of O_3 in the non-filtered chambers, and the blue triangles represent the purafil filtered O_3 concentration in the control chambers.

2.3 Plant cultivation and treatments

2.3.1 *Phaseolus vulgaris* – summer annual 2009

Seeds of snap bean (*Phaseolus vulgaris* L.) genotypes, lines 'S156' (O_3-Sensitive) and 'R123' (O_3-tolerant) were obtained from Prof. Kent Burkley, USDA-ARS Plant Science Unit field site

near Raleigh, North Carolina, USA via Dr Felicity Hayes (CEH, Bangor, UK). The bean lines were developed from a genetic cross reported by Dick Reinert (Reinert and Eason, 2000). Seeds were planted in 16 dm^3 plastic pots on 29 September 2009. The pots, filled with a mixture of sand, soil and vermiculite (1:2:1), were positioned over plastic buckets with an overflow hole to prevent the base of the pot coming in contact with the water in the bucket (**Figure 2.4**). The buckets served as a water reservoir. The buckets inside the open-top-chambers were connected to a water tap through a network of PVC tubing, which allowed easy refilling of the reservoirs. The pots were watered by hand daily until the plants reached the desired age for the treatments to commence. Thereafter water uptake by the soil medium in the pots took place through special glass fibre wicks (Thoenes Dichtungstechnik GmbH, Germany) placed at different levels in the soil of the pots with one end protruding through the holes in the bottom of the pot and hanging in the water of the reservoir. The wicks were cut to proper lengths and layered in a clockwise direction at different, evenly spaced depths within each pot to ensure uniform wetting of the soil (**Figure 2.4**).

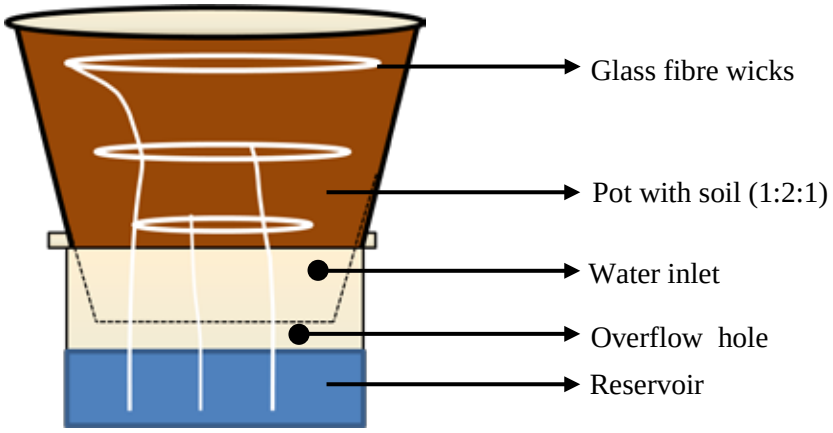

Figure 2.4 Schematic illustration of the pot-reservoir irrigation system used in the experiments. By reducing the number of glass fibre wicks used, drought stress could be induced in experimental plants. Three glass fibre wicks were used per pot for the control (well watered), while only one was used per pot to mimic drought stress.

Figure 2.5 Photograph showing some of the main components of the pot-reservoir irrigation system. Left: glass fibre wicks used to irrigate the soil medium by simple capillary action. Right: pot and reservoir (bucket).

Table 2.1 Time schedule of the events during the growing season of Mung bean (*Phaseolus vulgaris*) – summer annual 2009.

Event	Date
Sowing	29 September 2009
Emergence	6 October 2009 (1•)
Ozone fumigation started	30 October 2009 (25•)
Final harvest	10 December 2009 (71•)

- **Days after emergence (d.a.e)**

2.3.2 Cultivation of *Pisum sativum* – winter annual 2010

Commercial seeds of garden peas (*Pisum sativum* cv Greenfeast) supplied by Mayford seeds (Pty) Ltd., were planted in 16 dm^3 plastic pots on 25 March 2010. The same protocol was used for this experiment as described in 2.3.1. The only addition to the experiment was a application of a second stress factor namely drought. Half of the potted plants were supplied with only one glass fibre wick, placed near the middle of the pot, to induce water stress conditions, i.e. sustaining the water regime at 20 % of field capacity. Three glass fibre wicks were used in the control pots, maintaining the water regime at 80 % of field capacity.

Table 2.2 Timeline of the events during the growing season of peas (*Pisum sativum*) – winter annual 2010.

Event	**Date**
Sowing	**25 March 2010**
Emergence	**1 April 2010 (1•)**
Thinning out **Ozone fumigation started** **Drought stress treatment started**	**22 April 2010 (21•)** **23 April 2010 (22•)** **11 Mei 2010 (40•)**
Final harvest	**17 June 2010 (•)**

- **Days after emergence (d.a.e)**

2.4 Non destructive plant analysis

2.4.1 Chlorophyll content index (CCI)

The chlorophyll content index (CCI) of leaves of *Glycine max* was measured before the start of the O_3 treatment and then weekly thereafter with a hand-held chlorophyll content meter (CCM-200, Opti-Sciensces, Inc, USA). This instrument uses differential transmission at two wavelengths, namely 940 and 665 nm, to determine the absorbance of chlorophyll pigments.

LED's generate the energy (beams). This is a non-invasive technique. The energy is sampled pre- and post-transmission to determine the ratio of the red absorbance beam to the standardised infrared reference beam. The latter then represents the CCI.

2.4.2 Photosynthetic gas exchange

2.4.2.1 Overview

The energy captured during photosynthetic electron transport is used in several ways; the most common is the reduction of CO_2 to sugars. Two ATP and two NADPH molecules are used to reduce one CO_2 molecule to the level of sugar (CH_2O). An additional ATP is used to activate the substrate in order to prepare it for carboxylation (Farquhar & Sharkey, 1982). The reactions are linked together in a cycle called the Calvin-Benson cycle, or photosynthetic carbon reduction cycle (PCRC). Terrestrial vegetation responds to a variety of environmental stresses including air pollution. Two of the most sensitive physiological processes are CO_2 assimilation (A) and stomatal conductance (g_s). Measurment of CO_2 assimilation is thus an effective non-destructive, non-invasive method for studying short-term effects on carbon gain of individual organs, allowing quantitative assessments of the effect of environmental variables on different steps in the diffusion pathway (Long & Hällgren, 1993). This information provides additional information to effects on long-term carbon gain, which is analysed as the final biomass and yield.

Information concerning the relative importance of stomatal and non-stomatal (mesophyll) components in controlling the rate of CO_2 assimilation can be obtained from the response of CO_2 assimilation to intercellular CO_2 concentration (Farquhar & Sharkey, 1982). The approach of measuring photosynthetic gas exchange in plants is in essence based on Fick's first law of diffusion, which states that the net flux of a gas in a one-dimensional diffusional pathway is proportional to the ratio of the concentration difference to the diffusion resistance across that pathway to the concentration or vapour pressure gradient, and that it is inversely proportional to the length of the diffusion path (Long & Hällgren, 1993). Thus, in photosynthetic CO_2 assimilation and transpiration:

$$A = (c_a - c_i)/\sum r$$

$$E = (w_i - w_a)/\sum r''$$

where $c_a - c_i$ is the CO_2 gradient from ambient air (C_a) to the intercellular (C_i) space and $w_i - w_a$ is the water vapour gradient between intercellular space (W_i) and the outside air (W_a). The $\sum r$ and $\sum r''$ are the total resistances to transfer of CO_2 and water vapour, respectively, across these gradients. The diffusion pathway into the leaf may be divided into several stages, each analogous to a resistor in an electrical circuit (Long & Hällgren, 1993), before it can be used by the PCRC.

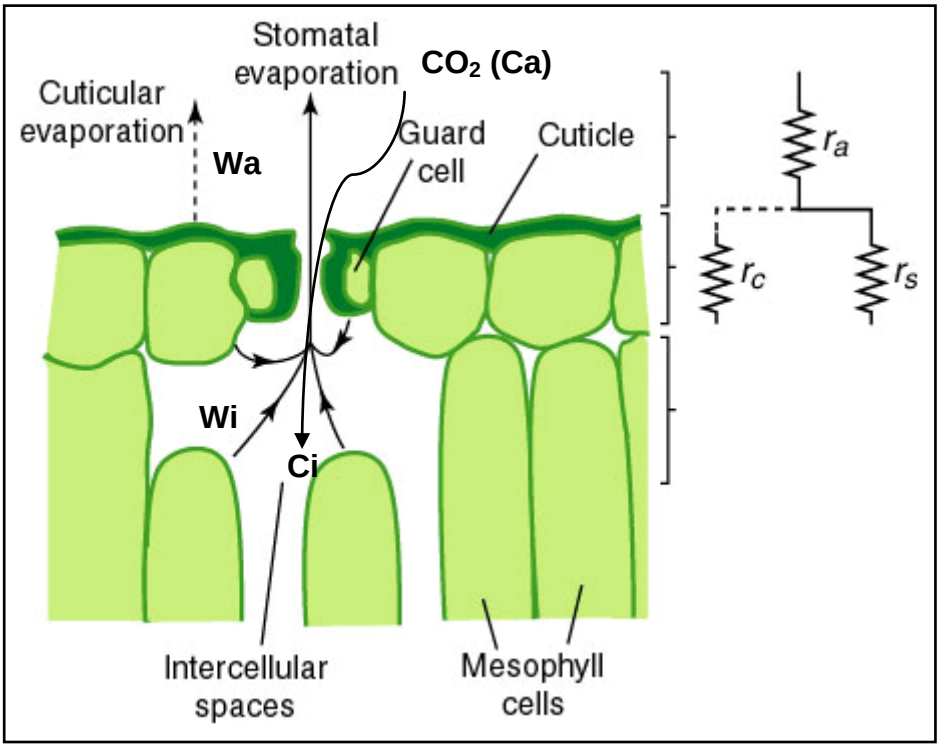

Figure 2.6: Pathways for water loss from one surface of a leaf, showing the boundary layer (r_s), cuticular (r_c) and stomatal (r_s) resistances. CO_2 entering the leaf also face the same resistances before it can be used by the PCRC (Adapted from Jones, 1983).

When an intact plant leaf is exposed to a constant photosynthetic active radiation (PAR) of 1200 μmol $m^{-2}s^{-1}$, a response curve is created when the partial pressure of CO_2 is manipulated in a step wise process, from a pressure of 0 µmol.mol^{-1} to about 1500 µmol.mol^{-1}. At the CO_2 partial

pressure (mole fraction) where c*i* = c*a*, an artificial situation is created where no stomatal limitation exists. The photosynthetic CO_2 assimilation rate under this condition is then used as reference point (operational point) to calculate the percentage stomatal limitation (Farquhar & Sharkey, 1982; Von Caemmerer & Farquhar, 1981). The rate at which carbon is assimilated (A) is plotted against the intercellular CO_2 concentration to obtain the CO_2 response curve (A:C_i curve) (**Figure 2.7)**. Rather than expressing the relation of photosynthesis to the atmospheric CO_2 pressure, the effect of stomatal conductance is removed by calculating the internal CO_2 (C_i) (Lawlor, 1993). The conductance of the leaf surface and the rate of photosynthesis determine the concentration of CO_2 in the intercellular spaces c_i.

Calculation of c_i is from:

$$c_i = c_a - \frac{A}{(g_s + g_c + g_a)}$$

where $g_s + g_c + g_a$ are the stomatal, cuticular and boundary layer conductances to CO_2. The CO_2 assimilation rate is expressed as the amount of CO_2 assimilated per unit leaf area and time (μmol CO_2 m^{-2} s^{-1}). The CO_2 response curve is then used to investigate the response of the photosynthetic apparatus of the leaf to the intercellular CO_2 concentration (A:C*i* response), thus measuring the function of the mesophyll components of photosynthesis (i.e. the dark and light reactions) (Pammenter, 1989). The CO_2 response curve has an initial linear portion, where CO_2 assimilation is limited by intercellular CO_2 and saturated with RuBP. The slope is known as the carboxylation efficiency (CE) or demand function and has been related to the activity of RuBP carboxylase. The demand function, $A = CE(c_i - \Gamma)$ expresses the rate of CO_2 assimilation in terms of the effectiveness and the capacity of the system to assimilate CO_2 (Farquhar & Sharkey, 1982). The symbol Γ represents the CO_2 compensation concentration which can be defined as the CO_2 concentration at which net efflux of CO_2 from the plant is zero, i.e. CO_2 fixed by photosynthesis and CO_2 produced by photo-respiration plus mitochondrial respiration (**Figure 2.7**) balance each other. After the initial linear portion, the curve levels off and assimilation is now limited by the rate at which RuBP is regenerated by the PCRC. The supply function, $A = g_s(c_a - c_i)$, of an A:C_i response expresses the rate of CO_2 assimilation in terms of the difference in concentration between c_a and c_i, which represents the driving force for the inward movement of

CO_2 and the prevailing stomatal conductance (g_s) (Farquhar & Sharkey, 1982). As the atmospheric concentration of CO_2 is considered to be about 360 μmol.mol^{-1}, the actual assimilation rate is denoted as A_{360} and given by the simultaneous solution of the demand and the supply function, depicted graphically by the intersection of the corresponding two lines (**Figure 2.7**). That means, the point of intersection of the supply and demand functions gives the rate of assimilation and the intercellular CO_2 concentration that prevails under those ambient conditions that give rise to that particular stomatal conductance and activity of the mesophyll processes. This point is known as the operational point (Lange *et al*., 1987).

The operational point can provide information on which of the component processes are limiting CO_2 assimilation. If the supply function intercepts the A:c_i curve on the initial linear portion, small changes in stomatal conductance (g_s) will cause noticeable changes in A under ambient conditions, and assimilation can be considered to be predominantly limited by the stomata. If the point of intersection is on the flat portion of the A:c_i curve, small changes in g_s will have little effect on A, and CO_2 assimilation will be limited by the rate of the mesophyll processes, rather than by stomatal conductance.

Farquhar & Sharkey (1982) employed a simple method to determine the degree of stomatal limitation of photosynthesis, namely the calculation of the percentage stomatal limitation:

$$\ell = (A_0 - A_{360})/A_0 \text{ X } 100$$

where A_{360} is the CO_2 assimilation rate that actually occurs at ambient CO_2 concentrations (c_a = 360 μmol.mol^{-1}) and A_0 the rate which would occur if resistance to CO_2 diffusion were zero (no stomatal limitation = ci≥ 360 μmol.mol^{-1}). Stomatal limitation (ℓ) represents the proportionate decrease in CO_2 assimilation rate that may attribute to stomatal restrictions. The apparent CE of photosynthesis can be deduced from the initial linear response of the A:c_i response curve which is an *in vivo* estimation of Rubisco activity (Bolhàr-Nordenkampf & Öquist, 1993). The maximal CO_2 assimilation rate at saturation (J_{max}) can be regarded as a reliable indicator of the maximal electron transport rate and RuBP regeneration capacity of the leaf.

The rate of CO_2 assimilation is given by the rate at which the gas diffuses down a concentration gradient into the intercellular air spaces of the leaf. This process is described by the following equation:

$$A = g_s (c_a - c_i)$$

where A is the rate of net CO_2 assimilation, g_s is the conductance to CO_2 transfer, c_a the concentration of CO_2 in the ambient air, and c_i the intercellular CO_2 concentration. If g_c and c_a are known, this function can be evaluated for varying values of c_i and plotted on the CO_2 assimilation curve to give the 'supply function'.

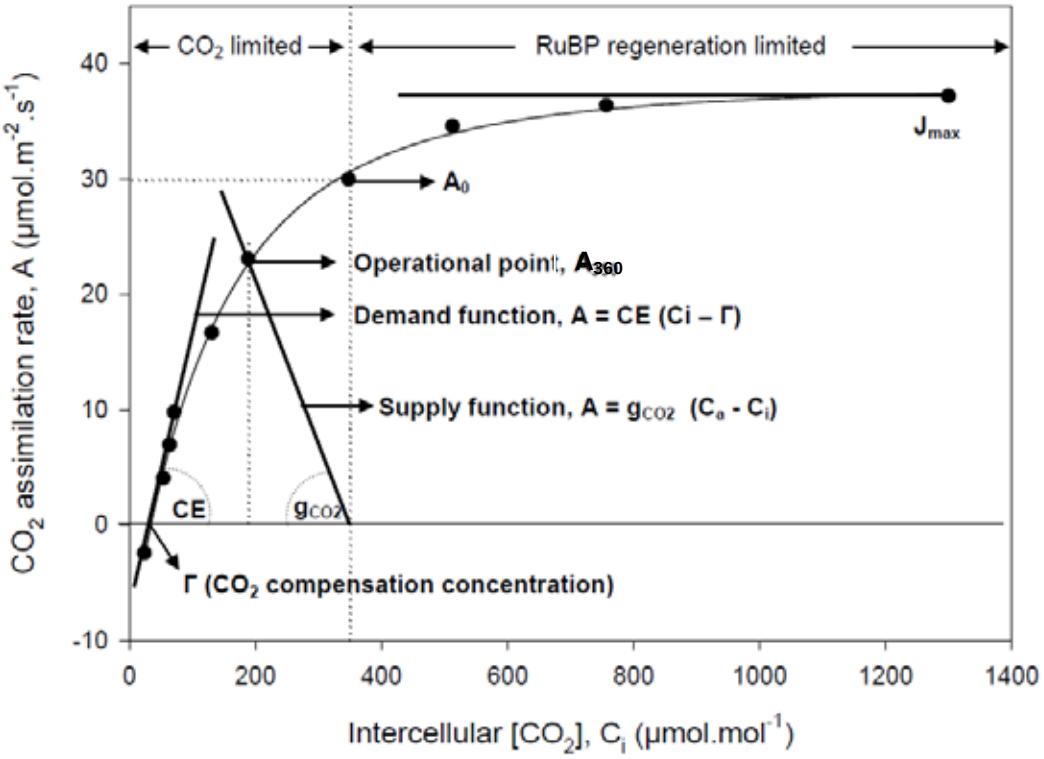

Figure 2.7: Response of CO_2 assimilation rate (A) vs. intercellular CO_2 concentration (C_i). A_{360} is the assimilation rate under atmospheric conditions, i.e. the point of simultaneous solution of the demand and supply functions. The carboxylation efficiency (CE) is represented by the initial slope of the demand function, the CO_2 compensation concentration (Γ) is the intercellular CO_2 level where the net usage of CO_2 equals zero, the maximum rate of assimilation (J_{max}) represents the rate of CO_2 assimilation at saturated levels of CO_2. A_0 is the rate of assimilation at the point where stomatal limitation is artificially eliminated by raising the ambient CO_2 concentration (C_a) to attain a resulting internal CO_2 concentration (C_i) of 360 µmol.mol^{-1} (Lange et al., 1987). The solid points symbolise data generated with an infrared gas analysing system.

2.4.2.2 Measuring of photosynthetic gas exchange

Photosynthetic gas exchange was measured with an infrared gas analysis system (CIRAS-2, PP-Systems, Hertz, UK). Measurements were conducted on four randomly selected plants in each chamber of each treatment. A 2.5 cm^2 section of the third fully expanded leaf was clamped into a broad leaf photosynthetic leaf chamber (PLC) with light and temperature control (**Figure 2.8**). The light intensity was kept at 1200 µmol photons m^{-2} s^{-1} to ensure full activation of Rubisco (Taylor and Terry, 1984), while the leaf temperature was kept constant at 26 °C, by the Peltier cooling unit of the PLC during measurements. To ensure steady-state activation of Rubisco, the leaf in the cuvette was first acclimated at a CO_2 concentration of 360 µmol.mol^{-1} at a saturating photosynthetic photon flux (1200 µmol m^{-2} s^{-1}) for 5 minutes. After gas exchange reached a steady state, the intercellular CO_2 concentration (C_i) was manipulated by varying ambient CO_2 concentration (C_a). The linear slope of the response curve was constructed by lowering the C_a in the cuvette from 360 µmol.mol^{-1} in five steps to 200, 100, 50 and 25 µmol.mol^{-1}. C_a was again stabilised at 360 µmol.mol^{-1} to ensure open stomata and to verify the stability of the photosynthetic apparatus. Lastly, C_a was stepped up from 360 µmol.mol^{-1} in four steps to 500, 700, 1000 and 1500 µmol.mol^{-1} in order to generate A:C_i response curve (Singsaas *et al*., 2001).

Figure 2.8 Measuring photosynthetic gas exchange in *Pisum sativum* for generating A:C_i curves using an automatic PLC coupled to an IRGA. A 2.5 cm^3 section of a leaf was clamped into the cuvette and temperature and light conditions could be kept near constant while CO_2 levels was adjusted as required.

2.4.3 Chlorophyll *a* fluorescence induction

Light energy (sunlight) is absorbed by chlorophyll molecules and converted to produce sugar, which cellular respiration converts into ATP, the "fuel" used by all living things. Absorption of light by a pigment molecule is a very rapid, photophysical, electronic event, occurring within a femtosecond (fs = 10^{-15}) (Hopkins & Hüner, 2004). An exited molecule has a very short lifetime, normally in the order of a nanosecond. The exited molecule however has an even shorter stable state (less that 10^{-8}) and during this short period, a charge separation within the reaction centre takes place, comprising the primary photochemical step of photosynthesis. If this important separation does not take place, the absorbed light energy is released as heat and/or fluorescence light (between 600 – 800 nm), when the exited electron of the chlorophyll molecule returns to its ground state (Bolhàr-Nordenkampf & Öquist, 1993). It is this fluorescence that Kautsky &

Hirsch (1934) first reported when dark adapted leaves were exposed to light. They assumed that the kinetics of fluorescence emission during induction reflected the initial phases of the induction of photosynthesis. The latter assumption was proven by later researchers, and the fluorescence transient, or Kautsky transient was born, and used today as a sensitive, *in vivo* probe of photosynthetic function (Kautsky *et al*., 1960).

The fluorescence transient (induction curve) shows an initial fast O-P ($F_0 - F_P$) rise only lasting for approximately 1 s, whereafter a subsequent decrease (P-S) can be observed (**Figure 2.9**) (Strasser *et al*, 2004). It was shown that the fluorescence rise kinetics is polyphasic, exhibiting clearly, when plotted on logarithmic time scale, the steps J (at 2 ms) and I (30 ms) between the initial F_0 and maximum (F_P or F_M) fluorescence level (hence denoted as O-J-I-P transient).

The O-P part of the curve is generally accepted to reflect the closure of reaction centers (RCs), which is equivalent to the accumulation of reduced Q_A. Under normal dark conditions it is assumed that the Q_A pool is completely reduced (oxidised), i.e. all RCs are open. Thus, the fluorescence transient actually reflects the filling up of the electron acceptor side of Photosystem II (PS II) (Q_A, Q_B and PQ pool) with electrons from the donor side of PS II (Papageorgiou, 1975; Lavorel and Etienne, 1977; Strasser & Govindjee, 1992; Strasser *et al.*, 2004). This open state of RCs gives rise to F_O at the onset of illumination, which quickly changes to the first intermediate step J within ca. 2 ms. This first part of the transient curve (O-J) is called "single turnover region" (Strasser *et al*., 2004). It expresses the photochemical events and represents a single event of reduction of Q_A. The latter phase is followed by a further rise to the second intermediate step I within ca. 30 ms and to the final peak P (maximum fluorescence intensity) in ca. 200 ms. The J-I-P region ("multiple turnover phase") of the fluorescence transient reflects the velocity of ferredoxin reduction beyond Photosystem I (PS I) (Schansker *et al*., 2003). The I-P phase is related to electron transfer through PSI (Schansker *et al*., 2005). The maximum fluorescence intensity F_P is the state which is achieved when all of RCs are closed. Since the OJIP fluorescence transients reflects the kinetics and heterogeneity involved in filling up of the PQ pool with electrons, it can be used as a very sensitive tool for studying the function and structure of the photosynthetic apparatus *in vivo* (Strasser and Strasser, 1995).

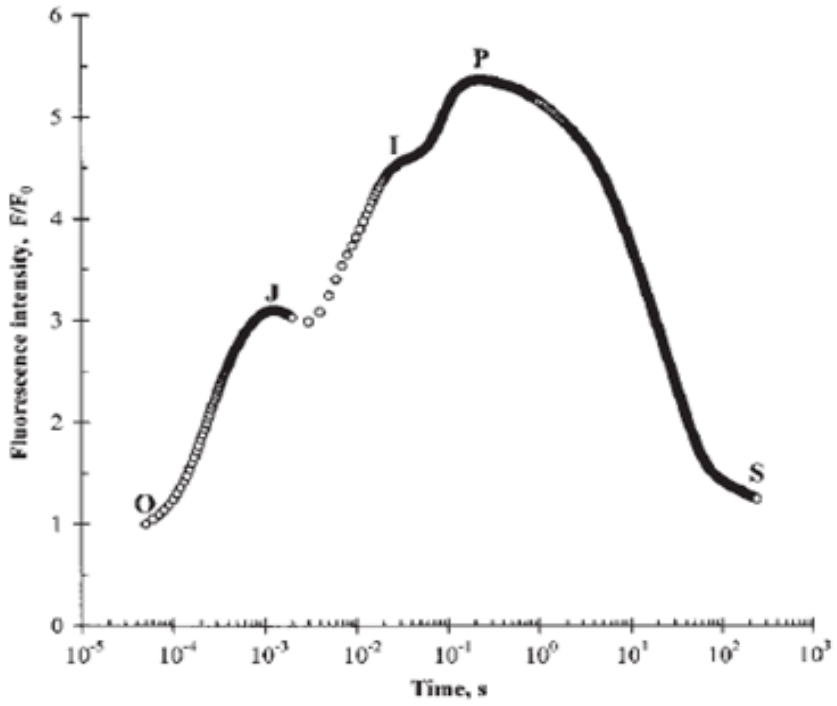

Figure 2.9: A typical chlorophyll *a* fluorescence transient exhibited upon illumination of a dark-adapted pea leaf by saturating red light, plotted on a logarithmic time scale from 50µs (Fo) to 5 min (Fs) The labels refer to the fluorescence data used by the JIP-test for the calculation of various parameters quantifying Photosystem II (PS II) structure and function. F_O is the initial fluorescence (at 50µs); F_J the fluorescence intensity at 2 ms; F_I the fluorescence intensity at 30 ms; F_P (also known as F_M) the maximal fluorescence intensity and S, which is a steady state (Strasser *et al.*, 2004).

2.4.4 Analysis of the chlorophyll *a* fluorescence transient by the JIP-test

The shape of the O-J-I-P transient has been found to be very sensitive to stress caused by changes in different environmental conditions. These conditions range from a variety of environmental aspects such as light intensity, temperature, drought, atmospheric CO_2 or O_3 elevation (Srivastava & Strasser, 1997; Tsimilli-Michael et al., 1999; Krüger et al., 1997). Strasser *et al*., (2004) introduced a quantitative analysis of the O-J-I-P transient, called the 'JIP-test' which can be used to quantify several structural and functional parameters of PS II.

The JIP-test applies to the fast phase fluorescence transient induced within 1 second by actinic light, strong enough to induce maximal values of the fluorescent yields at the J- and, I- step, as well as the peak P-step (F_m). In the instrument the light is supplied by three LEDs and is focused on the sample surface (4mm diameter). In our experiments the Handy Plant Efficiency Analyser (Handy-PEA, Hansatech Instruments Ltd., Kingslynn, UK) were used to record the data. The transients were translated to the energy fluxes of absorption (ABS), trapping (TR) and electron transport (ET) through PS II and other fluorescence parameters (**Table 2.3**) by the JIP test, using the Biolyzer computer program.

The JIP-test represents a translation of the original fluorescence transients to biophysical parameters that quantify the stepwise flow of energy through PS II at the reaction centre (RC) as well as at the exited cross-section (CS) level (Strasser & Strasser, 1995; Force *et al*, 2003; Strasser *et al.*, 2004). The parameters, which all refer to time zero (onset of fluorescence induction), are: (1) the specific energy fluxes (per reaction centre) for absorption (ABS/RC), trapping (TR_o/RC), where TR is the excitation energy flux trapped by a RC and utilised for the reduction of Q_A to Q_A^-), dissipation at the level of the antenna chlorophylls (DI_o/RC) and electron transport (ET_o/RC), where ET is the flux of electrons from Q_A into the electron transport chain; (2) the flux ratios or yields, i.e. the maximum quantum yield of primary photochemistry ($\varphi_{Po} = TR_o/ABS = F_V/F_M$), the efficiency by which a trapped exciton, having triggered the reduction of Q_A to Q_A^- can move an electron further than Q_A into the electron transport chain ($\Psi_0 = ET_0/TR_0$), the quantum yield of electron transport ($\varphi_{Eo} = ET_o/ABS = \varphi_{Po} \bullet \psi_o$, and the quantum yield of the formation of reduction equivalents ($\varphi_{Ro} = \varphi_{Eo} \bullet \delta$) (Strasser & Tsimilli-Michael, 2001); (iii) the phenomenological energy fluxes (per excited cross section of leaf, CS) for absorption (ABS/CS), trapping (TR_o/CS), dissipation (mostly heat) (DI_o/CS) and electron transport (ET_o/CS). The fraction of active PS II RCs per excited cross section (RC/CS) is also calculated. The formulae in **Table 2.3** illustrate how each of the above-mentioned parameters can be calculated from the original fluorescence measurements.

The initial stage of photosynthetic activity of an RC complex is regulated by four functional steps namely absorption of light energy (ABS), trapping of excitation energy (TR), conversion of excitation energy to electron transport (ET) and reduction of end acceptors (RE). Tsimilli-Michael & Strasser (2008), and Yordanov *et al*. (2008), introduced a multi-parametric expression

of these four independent steps contributing to photosynthesis, the so called performance index ($PI_{ABS,total}$) :

$$PI_{ABS,total} = \frac{\gamma_{RC}}{1-\gamma_{RC}} \bullet \frac{\varphi_{Po}}{1-\varphi_{Po}} \bullet \frac{\psi_{Eo}}{1-\psi_{Eo}} \bullet \frac{\delta_{Ro}}{1-\delta_{Ro}}$$

where $\gamma_{RC}/(1 - \gamma RC) = (RC/ABS)$ is the fraction of reaction centre chlorophyll (Chl_{RC}) per chlorophyll of the antennae ($Chl_{Antenna}$). This expression can be deconvoluted into two JIP-test parameters and estimated from the original fluorescence signals as $RC/ABS = RC/TR_0 \bullet TR_0/ABS = [(F_{2ms} - F_{50\mu s})/4(F_{300\mu s} - F_{50\mu s})] \bullet F_V/F_M$. The factor 4 is used to express the initial fluorescence rise per 1 ms. The expression RC/ABS shows the contribution to the $PI_{ABS,total}$ due to the RC-density on a chlorophyll basis. The contribution of the light reactions for primary photochemistry is estimated according to the JIP-test as $(\varphi_{Po}/(1 - \varphi_{Po})) = TR_0/DI_0 = k_P/k_N = F_V/F_0$. The contribution of electron transport past Q_A is derived as $(\psi_0/(1 - \psi_0)) = ET_0/(TR_0 - ET_0) = F_M - F_{2ms})/(F_{2ms} - F_{50\mu s})$. The contribution of the reduction of end equivalents is derived as $(\delta_0/(1 - \delta_0)) = RE/ABS = (1 - F_{30\mu s})/(1-F_{2ms})$.

Table 2.3. Summary of the JIP-test formulae using data extracted from the fast fluorescence transient O-J-I-P (modified from Strasser & Tsimilli-Michael, 2001).

Data extracted from the recorded fluorescence transient OJIP	
F_t	fluorescence at time t after onset of actinic illumination
F_0	$F_{50\mu s}$, fluorescence intensity at 50μs
$F_{100\mu s}$	fluorescence intensity at 100μs
$F_{300\mu s}$	fluorescence intensity at 300μs
$F_J \equiv F_{2ms}$	fluorescence intensity at the J-step (at 2ms) of OJIP
$F_I \equiv F_{30ms}$	fluorescence intensity at the I-step (at 30ms) of OJIP
F_M	maximal recorded fluorescence intensity, at the peak of P OJIP
t_{FM}	time (in ms) to reach the maximal fluorescence intensity F_M
V_J	relative variable fluorescence at the J-step = $(F_{2m}s - F_o)/(F_M - F_o)$
$(dV/dt)_o = M_o$	fractional rate of PS II reaction centre closure = $4.(F_{300} - F_o)/(F_M - F_o)$

Quantum Efficiencies or Flux Ratios or Yields	
$\varphi_{Po} = TR_0/ABS = [1 – (F_0/F_M)] = F_V/F_M$	maximum quantum yield for primary photochemistry
$\Psi_{Eo} = ET_0/TR_0 = (1\text{-}V_J)$	efficiency/probability that an electron moves further than Q_A^-
$\varphi_{Eo} = ET_0/ABS = [1 – (F_o/F_M)].(1\text{-}V_J)$	quantum yield for electron transport (ET)
$\varphi_{Ro} = RE_0/ABS_0 = (1\text{-}V_I)/(1\text{-}V_J)$	efficiency/probability with which an electron from the intersystem electron carrirs is transferred to reduce end electron acceptors at the PS I acceptor side (RE)
$\Psi_o = ET_0/TR_0 = (1\text{-}V_J)$	
Specific Fluxes or Specific Activities	
$ABS/RC = M_o . (1/V_J . (1/ \varphi_{Po})$	absorption flux (of antenna Chls) per RC
$TR_o/RC = M_o . (1/V_J)$	trapped energy flux (leading to Q_A reduction) per RC
$ET_o/RC = M_o . (1/V_J) . \Psi_0$	electron transport flux (further than Q_A^-) per RC
$RE_0/RC = M_0 (1/V_J)(1\text{-}V_J)$	electron flux reducing end electron acceptors at the PS I acceptor side, per RC
Phenomenological Fluxes or Phenomenological Activities	
$ABS/CS= F_o$ or ABS/CS_M	absorption flux per CS
$TR_o/CS = \varphi_{Po} . (ABS/CS)$	trapped energy flux per CS (at t = 0)
$ET_o/CS = \varphi_{Po} . \Psi_{0\,.\,.} (ABS/CS)$	electron transport flux per CS (at t = 0)
$DI_o/CS = (ABS/CS)$	Dissipated energy flux per CS (at t = 0)

Density of Reaction Centres	
RC/CS	$= \varphi_{Po} . (V_J/M_o . ABS/CS$
Performance Indices	
PI_{ABS}	$= (RC/ABS) . [\varphi_{Po} / (1- \varphi_{Po})] . [\Psi_o / (1- \Psi_o)]$
PI_{TOT}	$= (RC/ABS) . [\varphi_{Po} / (1- \varphi_{Po})] . [\Psi_o / (1- \Psi_o)] . [\varphi_{Ro}/(1- \varphi_{Ro})]$

Subscript “0” (or “o” when written after another subscript) indicates that the parameter refers to the onset of illumination, when all RCs are assumed to be open.

An extended analysis of the fluorescence transients can also be obtained by calculation of the difference in relative variable fluorescence kinetics, i.e. the so calledΔV curves . The original transients are firstly normalised between F_0 and F_m, whereafter the normalised values of the different treatments are subtracted. The difference between the treated and the control samples can be calculated and plotted, or $\Delta V = (V_{treatment} – V_{control})$. The difference can either be seen as a positive (trajectory above the reference line) or negative band (trajectory below the reference

line). ΔK, ΔJ and ΔI-band appear around 0.3 ms, 2ms and 30 ms, respectively. ΔK-bands are associated with uncoupling of the OEC (oxygen evolving complex), ΔJ-bands are associated with accumulation of Q_A^-, i.e. inhibition of the reoxidation of Q_A^- (Strasser *et al.*, 2004) while ΔI-bands indicate inhibition of the final reduction of end acceptors (Yordanov *et al*., 2008).

2.5 Destructive plant analysis

2.5.1 Plant water status

Plant water status of *Pisum sativum* plants was measured in order to quantify the availability of water status of the test plants. Plant water status strongly influences plant growth and biomass production through its effect on leaf and root expansion and on photosynthesis. In general, biomass production is directly proportional to the supply and use of water. Therefore the measurement of plant water status is an important part of understanding biomass production (Long, 1982). Measuring leaf water potential (Ψ_{xylem}) and relative water content (RWC) are two techniques used to assess plant water relations. These two techniques were employed to provide insight towards the drought stress (DS) used as co-stress besides O_3 in the winter annual *Pisum sativum*.

2.5.1.1 Leaf water potential

Leaf water potential was measured using a Scholander pressure chamber. This technique is based on the assumption that tension in the xylem stream is equilibrated with the water potential of the leaf cells. The water potential of the xylem stream is dependent only on the negative pressure (tension) in vessel elements. To determine the magnitude of xylem tension, a leaf of *Pisum sativum* was excised from the plant and placed into the pressure chamber **(Figure 2.10)**. The pressure was then increased slowly until the xylem water returned to the cut surface. The degree of pressure that it takes to cause water to appear at the cut end of the petiole tells you how much water tension the leaf was exposed to: a high positive pressure value corresponds to a high value of tension (negative pressure) and a high degree of water stress.

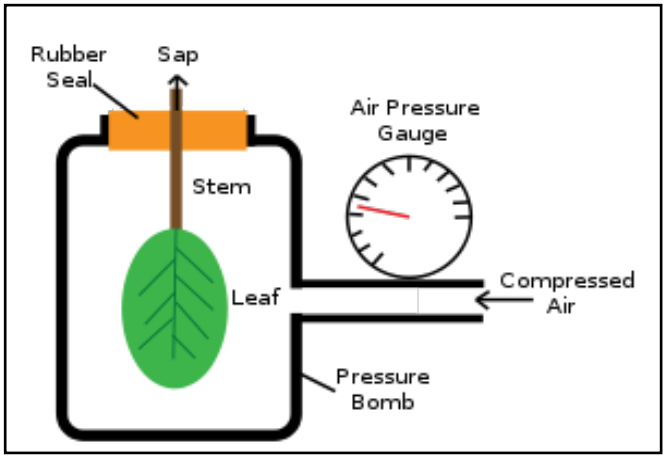

Figure 2.10: Schematic diagram of a pressure chamber, for measuring the xylem pressure (P^{xylem}), average over the material placed into the chamber. The air pressure (P^{air}) in the chamber is gradually increased until it just causes the exudation of xylem sap at the cut end. At this stage, the resulting pressure of the sap, which equals $P^{xylem} + P^{air}$, is zero, and so P^{xylem} equals $- P^{air}$, which is read on the pressure gauge. If the xylem osmotic pressure can be ignored, P^{xylem} would be approximately equal to ψ^{xylem}, which can be the same as the water potential of the other tissue in the camber (if water equilibrium has been achieved) (Scholander *et al.*, 1964).

2.5.1.2 Relative water content

The relative water content of the leaves of *Pisum sativum* were measured by sampling a circular piece of leaf with a cork borer. The weight of the leaf was measured instantly to determine the fresh weight (FW). The leaf was then placed in a bowl of water for an hour to allow the piece of leaf tissue to reach its maximum hydration potential or turgid weight (TW). The leaf tissue was then allowed to dry, until the mass was constant to obtain the dry weight (DW). The relative water content could then be calculated using the following equation:

$$\text{Relative water content} = \text{RWC} = \frac{\text{FW} - \text{DW}}{\text{TW} - \text{DW}}$$

A RWC of 1 would represent tissue at their maximum hydration. The amount of water deficit (WD) or the amount of water less than full hydration can be calculated as 1 – RWC. The closer the RWC is to 1 (WD close to zero), the more favorable the hydration of the tissue (Nilsen &

Orcutt, 1996). RWC is closely related to leaf water potential, but large differences in osmotic adjustment among species will cause a deviation between the two measurements (Lafitte, 2002).

2.5.2 Biomass accumulation

Biomass was determined only for *Pisum sativum* plants. The plants were harvested seventy one days after emergence. The plants were placed inside paper bags and dried in an oven at 60°C for 48h or until constant mass.

2.5.3 Scanning electron-microscopy

Leaf and anthocarp material collected in 70 % ethanol was dehydrated in 90 % ethanol for ten minutes followed by two changes in 100 % ethanol for ten minutes each. This was followed by critical point drying. The material was then mounted on specimen stubs and sputter-coated with gold/palladium and micrographs were taken with a FEI Quanta 200 ESEM Scanning Electron Microscope (SEM).

2.5.4 Crop yield attributes

Yield attributes were determined for both of *Phaseolus vulgaris* and *Pisum sativum* plants. The pods were carefully removed from each plant and placed in a separate paper bag. The pods were then dried in a oven at 60 °C for 48 h or until constant mass. The total pod weight, number of seed, total gram seed per plant, grams per 100 seeds, gram per seed, and total seeds per pod were determined.

2.5.5 Rubisco (Ribulose-1,5-bisphosphate carboxylase/oxygenase) activity

The method of Keys & Parry (1990) was used to determine initial and total Rubisco activity. Leaf discs of *Pisum sativum* were sampled after 30 days of exposure to O_3. Sampling occurred around midday to ensure optimal Rubisco activity. After the sampling the leaf discs were immersed in liquid nitrogen (-196 °C) to allow the leaf samples to be transported from the study site to the laboratory. The collected leaf discs were then stored at -84 °C until it was used to assay the Rubisco activity.

The leaf discs were ground in liquid nitrogen and extracted with 1 ml extraction buffer containing 100 mM Bicine-NaOH (pH 8.0), 20 mM $MgCl_2.6H_2O$, 50 mM mercaptoethanol and

0.1 M PSMF. Approximately 30 mg of acid-washed insoluble polyvinylpolypyrrolidone (PVPP) was also added to the mortar during extraction. The extract was transferred to a pre-cooled micro centrifuge tube and centrifuged at 10 000 x g at 4°C for 1 min. 25 µl of the supernatant was immediately used to measure initial Rubisco activity. The latter was measured in a total volume of 500 µl containing 100 mM Bicine-NaOH (pH 8.2), 20 mM $MgCl_2$, 10 mM $NaH^{14}CO_3$ (0.5 µCi μmol^{-1}), 400 µM ribulose-1,5-bisphosphate (RuBP) and 25 ml leaf extract. The enzyme reaction was terminated after 1 min with 200 µl formic acid (10 mM). This was done to obtain the initial activity of the enzyme at the exact time of sampling.

Total Rubisco activity was determined after 25 µl of the extract (described above) had been incubated in 415 µl extraction buffer (without mercaptoethanol) for 3 minutes in the absence of RuBP in order to fully activate the enzyme. The reaction was then started by adding RuBP and stopped after 1 min with 200 µl of 10 mM fomic acid.

All the acidified samples were dried in an oven at 60 °C. A 4 ml solution, containing 3.5 ml scintillation cocktail (Packard Ultima Gold) and 0.5 ml water was added to each vial. The incorporation of ^{14}C into 3-phosphoglycerate was determined with a liquid scintillation analyser (Beckman LS 6000TA). The soluble protein content was then determined with the remaining supernatant according to the method of Bradford (1976).

2.5.6 Determination of Peroxidase (POD) activity

Peroxidase (POD) activity was determined according the method of Bergmeyer (1974) by which the rate of decomposition of hydrogen peroxide by peroxidase, with guaiacol as hydrogen donor, is determined by measuring the rate of colour development spectrophotometrically at 470 nm and 25 ºC:

$$4 \text{ guaiacol} + 4H_2O_2 \rightarrow \text{tetraguaiacol} + 8H_2O$$

Frozen leaf tissue was ground in liquid nitrogen and proteins were subsequently extracted in 3 ml extraction buffer [100 mM Na-acetate (pH 5.5), 10 mM mercaptoethanol, 2 mM EDTA, 2 mM phenylmethylsulfonyl fluoride (PMSF)]. The homogenate was centrifuged (12 000g, 20 min) at -2 ºC. The peroxidase assay mixture consisted of 40 mM potassium buffer (pH 7), 0.36 mM

guaiacol and 0.16 mM H_2O_2 inside a 1 mL quartz cuvette. The change in absorbance was measured at 470 nm for 180 °C at 30 °C (Hitachi U-2000 double-beam spectrophotometer) (Zieslin & Ben-Zaker; 1991).

2.5.7 Hydrogen peroxide (H_2O_2) levels

Endogenous hydrogen peroxide (H_2O_2) was measured by a modification of the method of Brennan & Frenkel (1977). Hydroperoxide forms a specific complex when it reacts with titanium (Ti^{4+}), and can then be measured by colorimetry (MacNevin & Uron, 1953). Plant material was sampled at two time intervals 20 and 30 days after O_3 exposure commenced. The leaf samples were immediately placed in liquid nitrogen (-196 °C) to allow the leaf samples to be exported from the study site to the laboratory. The samples were then stored at -84 °C until it was used to assay.

Peroxides were extracted by grounding the leaves with liquid nitrogen to a fine powder. 0.6 µl ice cold acetone was then added to approximately 0.3 g of plant tissue. The extract and washings were centrifuged (1250*g*) and then 0.15 ml $TiCl_4$ in HCl (20 % titanic tetrachloride in concentrated HCl, v/v) was added to the supernatant. The solution was shaken, whereafter 1.05 ml of one-fifth strength NH_4OH was added dropwise with thorough mixing to precipitate the peroxide-titanium complex (MacNevin & Uron, 1953). The mixtures were then centrifuged (5000 *g*) and the precipitates washed repeatedly with 1 ml volumes of acetone until the supernatant was colourless. The precipitates were solubilised in 6 ml 2N H_2SO_4, and filtered prior to the measurement of H_2O_2 at 415 nm against a blank which had been carried through the same procedures. Standards in the range of 0.1 to 0.5 mmol H_2O_2 ml^{-1} were also reacted with TiCl and carried through the procedure.

2.6 Statistical analysis

Statistical analysis was conducted with the software package Statistica for Windows version 6 (StatSoft, Inc, USA). In data sets with parametric distribution, significant differences between treatment means were determined using Student‟s t-test.

Chapter 3

Results and discussion on: Effect of ozone on photosynthesis and seed yield of sensitive (S156) and resistant (R123) *Phaseolus vulgaris* L. genotypes

3.1 Growth response

3.1.1 Plant development

After 35 days of O_3 fumigation a marked O_3-induced decrease in growth was evident in the S156 *Phaseolus vulgaris* genotype (treatment AO_3S) when compared to the carbon filtered test plants (treatment CFS) (**Figure 3.1**). Although the R123 genotype was fumigated with the same O_3 concentration (treatment AO_3S), no inhibition of growth was evident compared to its control (AO_3R).

Figure 3.1: Ozone resistant (R123) and sensitive (S156) *Phaseolus vulgaris* genotypes 35 days after exposure to carbon filtered (CF) air and 80 nmolmol^{-1} ozone AO_3 respectively.

3.1.2 Foliar injury

Symptoms characteristic of O_3 stress were visible on the S156 genotype's (AO_3S) leaves 12 days after fumigation at 80 ppb O_3 levels started. Symptoms first appeared as grey/green flecking between the veins, developing into bronze-coloured lesions, which gradually grew together to cover large parts of the leaf surface 35 days after O_3 fumigation started (**Figure 3.2**). Burkley *et al*. (2005) observed similar symptoms in the same genotype. On the other hand the R123 genotype (AO_3R) treated with the same O_3 concentration, showed much less symptoms, which were restricted to older leaves only.

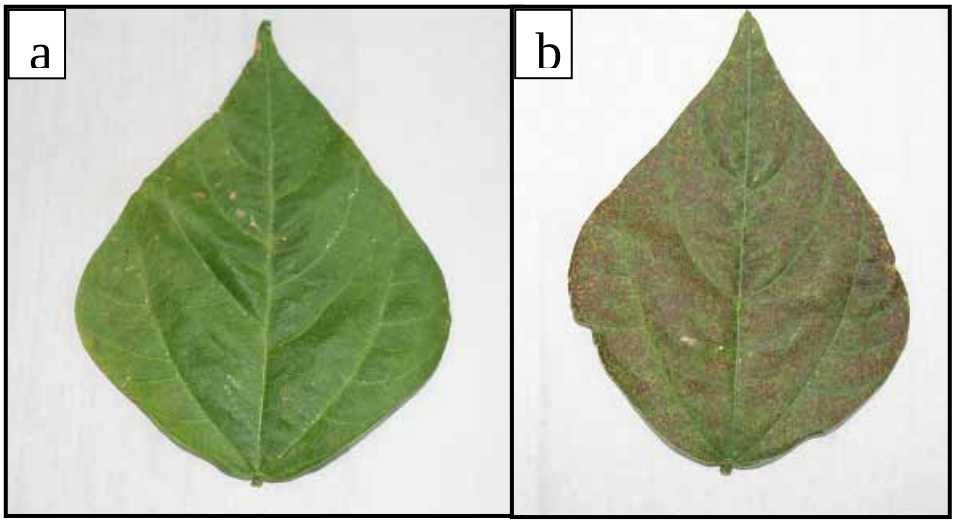

Figure 3.2: Visual symptoms on leaves of *Phaseolus vulgaris* 35 days after exposure to 80 nmol mol^{-1} O_3 in OTC chambers (a) resistant genotype R123 plants (b) sensitive genotypes S156 plants.

3.1.3 Crop yield

Crop yield attributes were assessed as dry weight at the end of the experiment. Various yield components of the sensitive (S156) and resistant (R123) genotypes exposed to elevated O_3 concentrations of 80 nmol.mol^{-1} were markedly suppressed when compared to the control resistant plants (CFR) (**Table 3.1**). The S156 plants displayed a severe reduction in most of the

attributes. The total pods per plant, number of seeds per pod, total seeds per plant and total gram of seed per plant were reduced by 30 %, 32 %, 53 % and 59 % respectively. All mentioned differences were statistically significant, with p values of less than 0.001. Yield in terms of grams per 100 seed of AO_3S was 8 % less than that of the CFR test plants. AO_3R test plants were less affected in all yield parameters measured. Total pods per plant decreased by 16 %. The number of seeds per plant, total seeds per plant and total gram of seed decreased by 21 %, 34 % and 31 %, respectively, though grams per 100 seeds increased by 5 %. When the response of AO_3S was compared to that of AO_3R with respect to the yield parameters, the total pods, number of seeds per plant, total seeds per plant, total grams of seed and grams per 100 seeds, showed decreases of 16 %, 15 %, 28 %, 40 % and 12 %, respectively. The 40 % reduction in total grams of seed differed significantly from the total of the AO_3R genotype.

Table. 3.1: Mean yield parameters (± standard errors) for *Phaseolus vulgaris* measured after seed maturity. Parameters include, total pods per plant, number of seeds per pod, total seeds per plant, total gram of seed per plant and grams per 100 seeds, with * and ** indicating significant differences at p<0.05 and p<0.01 respectively, compared to control plants (CFR).

Treatments	Total pods	Number of seeds per pod	Total seeds per plant	Total gram of seed	Grams per 100 seeds
CFR	36.12 (1.43)	3.78 (0.10)	136.87 (7.07)	34.37 (2.13)	25.25 (1.36)
AO_3R	30.12 (1.12)	2.97 (0.13**)	90.00 (6.04**)	23.42 (1.47**)	26.09 (0.35)
AO_3S	25.25 (0.97**)	2.55 (0.08**)	64.50 (3.20**)	14.19 (0.93**)	23.06 (0.66)
CFS	38.25 (2.32)	3.25 (0.06*)	130.66 (6.60)	31.65 (1.88)	24.65 (0.51)

3.2 Physiological response

3.2.1 Effect of O_3 on fast phase chlorophyll a fluorescence kinetics

Average chlorophyll *a* fluorescence transients of dark adapted leaves of *P. vulgaris* are presented on a logarithmic time scale in **Figure 3.3** and **Figure 3.4**. These transients show the typical O-J-I-P fluorescence rise, starting from an initial level of F_0, up to a maximum F_M (peak P), which can be considered representative of the maximum fluorescence yield, since the actinic light source of the fluorimeter (600 $W.m^{-2}$, peak at 650 nm) is high enough to ensure the closure of all the reaction centres. Important to note, is the fact that F_0 of the chlorophyll *a* fluorescence transients of the test plants were remarkably similar before fumigation commenced, indicating that the plants were physiologically homogenous (**Figure 3.3**). The similar and low F_0 value furthermore indicates that the plants were fully dark adapted, i.e. all the reaction centres were fully open (oxidised). After 25 days of fumigation with 80 $nmol.mol^{-1}$ O_3, a major treatment effect was visible in the AO_3S plants when their average fluorescence transients were compared to the transients of the CFR treatment (**Figure 3.4**). Changes occurred in the single turn-over region (0 – 2 ms) and in the multiple turnover region (2 ms – F_M). To further evaluate the fluorescence transients they were normalised between F_0 (50 μs) and F_J (2 ms). From this presentation (**Figure 3.5**) it appears that the major effect of O_3 occurred in the multiple turn-over events of PS II function of the S156 plants, i.e. in the transition J (2 ms) to P (700 ms). The transition from O to J represents the single turnover range of the transient (i.e. Q_A only reduced once) which reflects mainly photochemical reactions leading to the reduction of the electron acceptor Q_A, while the J to P phase of the transient is stongly affected by the subsequent dark reactions in the electron transport chain (Strasser *et al.*, 1999).

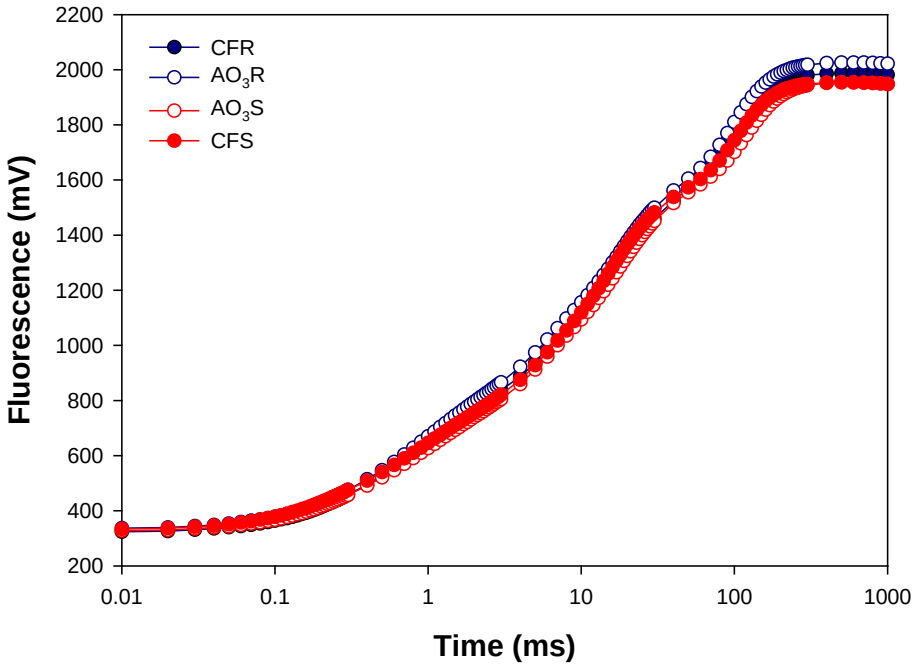

Figure 3.3: Average raw chlorophyll *a* fluorescence transients measured in intact leaves of resistant (R123) and sensitive (S156) *Phaseolus vulgaris* plants before fumigation commenced.

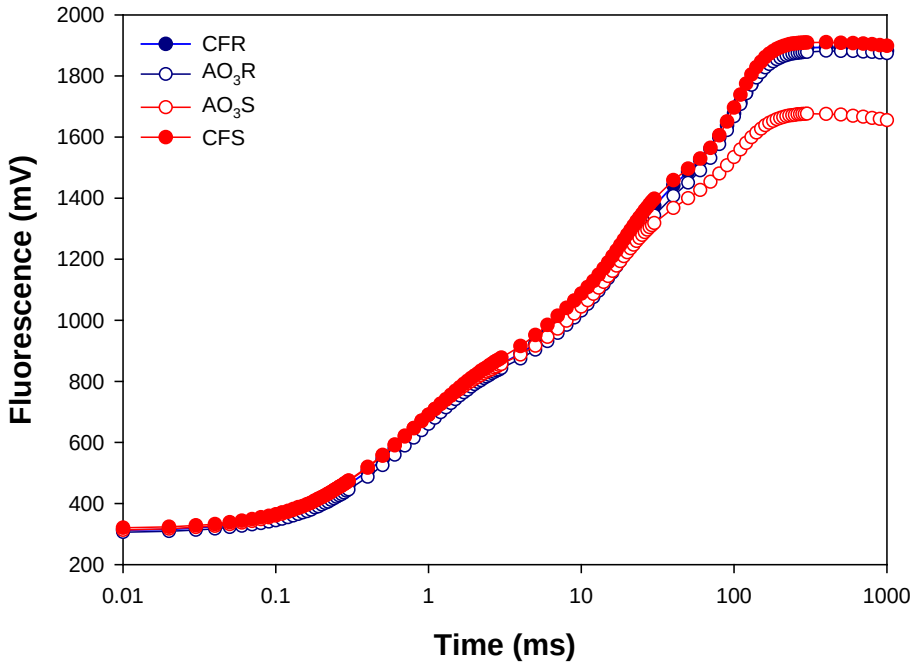

Figure 3.4: Raw chlorophyll *a* fluorescence transients measured in intact leaves of resistant (R123) and sensitive (S156) *Phaseolus vulgaris* plants after 25 days exposure to carbon filtered air (CF) and 80 nmol.mol^{-1} ozone (AO_3) respectively.

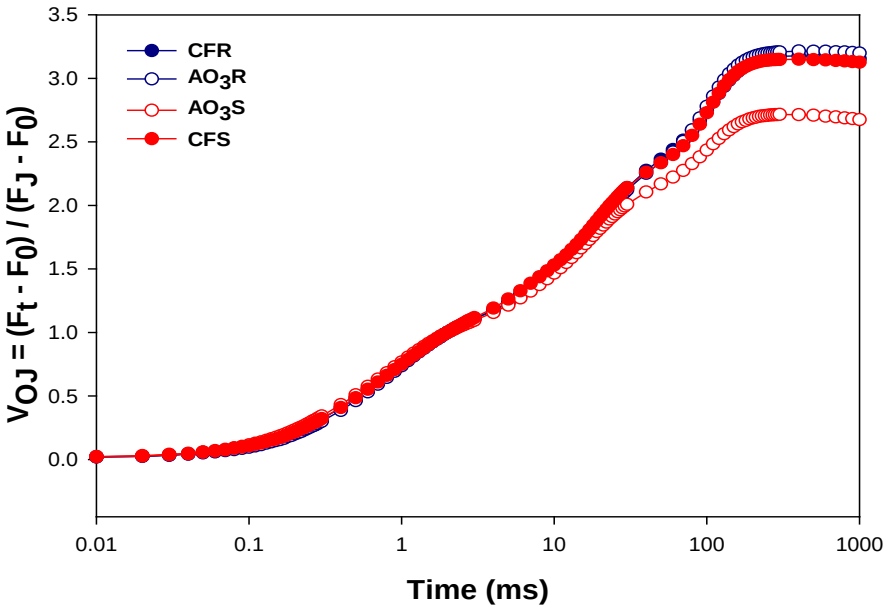

Figure 3.5: Average fast phase chlorophyll *a* fluorescence transients of resistant (R123) and sensitive (S156) *Phaseolus vulgaris* plants after 25 days exposure to filtered air (CF) and 80 nmol.mol^{-1} ozone (AO_3) respectively, double normalised between F_O (50 µs) and F_J (2 ms), indicating the relative change in the single turnover phase (0 – 2 ms) and the multiple turnover phase (2 ms – 1000 ms).

The average fast phase fluorescence transients were used to even further evaluate the differences in the response of the test plants. The average curves were normalised between the steps O (50 µs) and I (30 ms) and presented as relative variable fluorescence $V_{OI} = (F_t – F_0)/(F_I – F_0)$ vs. log time (**Figure 3.6**). The O-J part of the transient represents the single turnover photochemical event $Q_A \rightarrow Q_A^-$, as well as the reduction of intersystem electron carriers. The I-P part of the transient represents the reduction of PSI electron acceptors, such as Fd and $NADP^+$ (Yusuf *et al*., 2010). The effect of O_3 on the O-J and I-P phases of the transient of AO_3S is evident namely that O_3-induced changes occurred in both parts of the transient. In **Figure 3.7** and **3.7 insert** (linear scale) only the part with $V_{OI} \geq 1$ of the normalised curve of **Figure 3.6**, was plotted, in the 30 – 1000 ms time range. For each curve, the maximum amplitude of the fluorescence rise reflects the size of the pool of the end electron acceptors at the PS I acceptor side (Yusuf *et al*., 2010). **Figure 3.7** (insert) demonstrates that in the AO_3S plants had 10 % decrease in the pool size, while in the AO_3R plants a 3 % increase in pool size occurred. In **Figure 3.8** the fluorescence data were normalised between the steps I (30 ms) and P (peak), as $V_{IP} = (F_t – F_I)/(F_P – F_I)$, and

plotted on a linear scale in the 30 – 400 ms range. This normalisation, where the maximal amplitude of the rise was fixed at unity, facilitated a comparison of the reduction rates of the end electron acceptors' pool for the different treatments. The half-times of the kinetics are shown by the interception of the curves with the horizontal dashed line drawn at V_{IP} = 0.5 (half rise). The overall rate constant for reduction of e^--end acceptors is the inverse of the half-time. (Yusuf *et al.*, 2010). No significant decrease could be seen in the reduction rates of end electron acceptors of the different treatments (**Figure 3.8**).

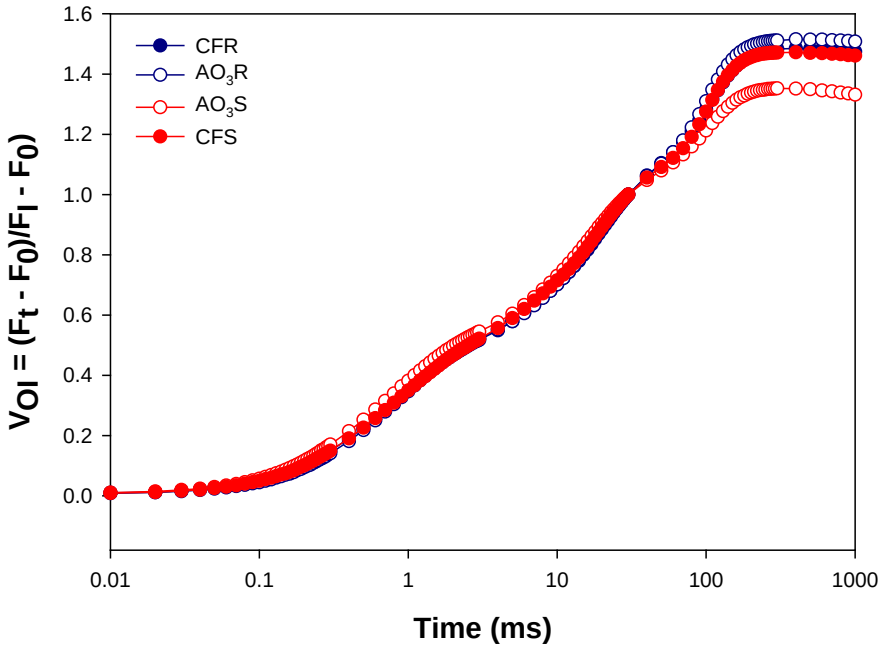

Figure 3.6: Average fast phase chlorophyll *a* fluorescence transients of resistant (R123) and sensitive (S156) *Phaseolus vulgaris* plants after 25 days exposure to filtered air (CF) and 80 nmolmol^{-1} ozone (AO_3) respectively double, normalised between F_O (50 µs) and F_I (30 ms).

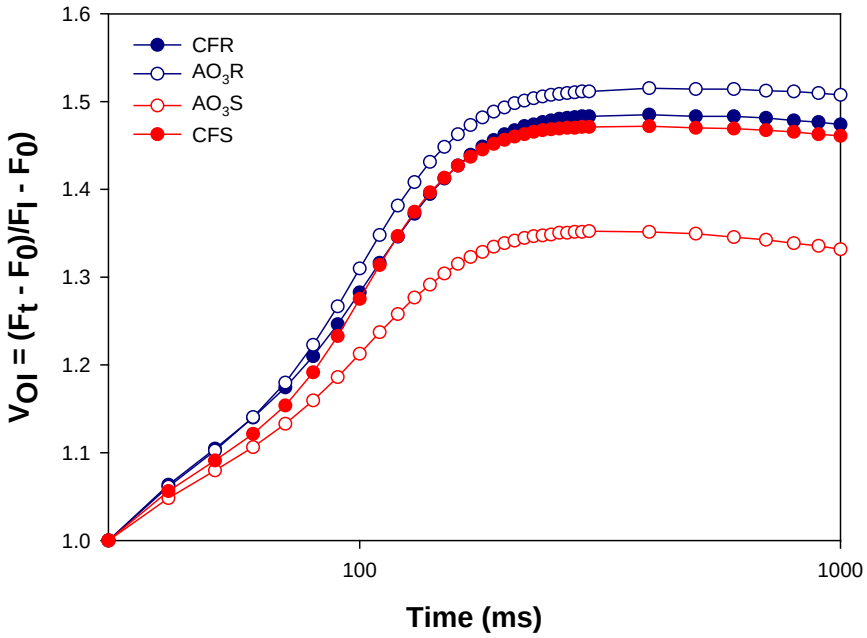

Figure 3.7: Average fast phase chlorophyll *a* fluorescence transients of resistant (R123) and sensitive (S156) *Phaseolus vulgaris* plants after 25 days exposure to filtered air (CF) and 80 nmolmol^{-1} ozone (AO_3) respectively normalised between F_O (50 µs) and F_I (30 ms), and the part VO-I ≥ 1 over the time range 30 – 1000 ms, plotted, showing the maximum amplitude of the rise reflecting the size of the end electron acceptor pool.

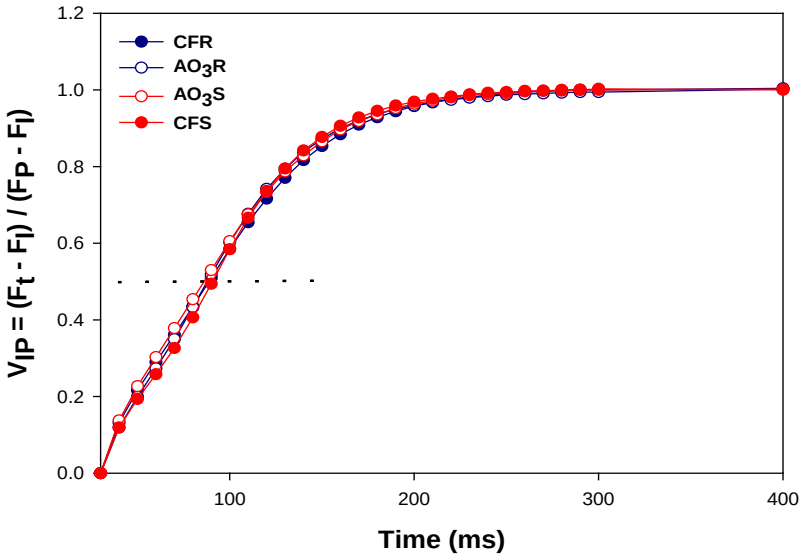

Figure 3.8: Average fast phase chlorophyll *a* fluorescence transients of resistant (R123) and sensitive (S156) *Phaseolus vulgaris* plants after 25 days exposure to filtered air (CF) and 80 nmolmol^{-1} ozone (AO_3) respectively normalised between F_I (30 ms) and F_M (peak), plotted on a linear scale in the 30 – 400 ms range with the maximum amplitude fixed at 1 to compare the reduction rate of the e- end acceptors of the different treatments.

The fluorescence transients depicted in **Figure 3.4** were also analysed by the JIP-test to deduce 10 structural and functional parameters of PS II function, quantifying the photosynthetic behavior of the different treatments 25 days after fumigation commenced. The values of the parameters are expressed relative to the control (CFR) (solid blue line) and plotted in a multiparametric radar plot (**Figure 3.9**). The 10 % decrease in active reaction centres per total absorption (RC/ABS) of the AO_3S plants can be attributed to the decrease of active oxygen evolving complexes. A decrease of RC/ABS indicates that the size of the PS II units is affected but in some of them the reaction centres have been deactivated, hence the corresponding units contribute towards absorption but not photochemistry (increase of apparent antenna size), or that the size of PS II units with active reaction centres increases (increase of functional antenna size (Luo *et al*., 2006) (See also **Figure 3.11**). All other quantum yields, TR_0/ABS, ET_0/ABS and RE_0/ABS, decreased by 15 %, 21 % and 23 %, respectively. The performance index ($PI_{ABS,total}$) of the AO_3S plants showed the most noticeable change, namely a 53 % decrease, since it expresses the overall potential for energy conservation that depends on all the efficiencies for the sequential energy transduction (**Figure 3.10**). **Figure 3.9** also indicates a concomitant increase of 10 % in antenna size (ABS/RC) which is the total absorption or total chlorophyll per active RC)

in the AO_3S plants. ABS/RC has been regarded as providing a measure of the apparent antenna size (Strasser & Strasser, 1995), based on the relation $TR_0/RC = \varphi_{P0}$ x ABS/RC. This increase may either mean that (i) a fraction of RCs was inactivated e.g. by being transformed to non-Q_A-reducing centres, or (ii) the functional antenna, i.e., the antenna that supplies excitation energy to active RCs, has increased in size. The increase in ABS/RC was accompanied by an increase of 8 % in the maximum trapping flux (TR_0/RC). This increase suggests that changes took place both in the fraction of RCs transformed to non-Q_A-reducing centres and in the functional antenna size (Yusuf *et al*., 2010). A decrease of 10 % in the electron transport per cross-section (ET_0/CS) in the AO_3S plants can be attributed to a decrease of 10 % in the density of PSII reaction centres per excited cross section (RC/CS).

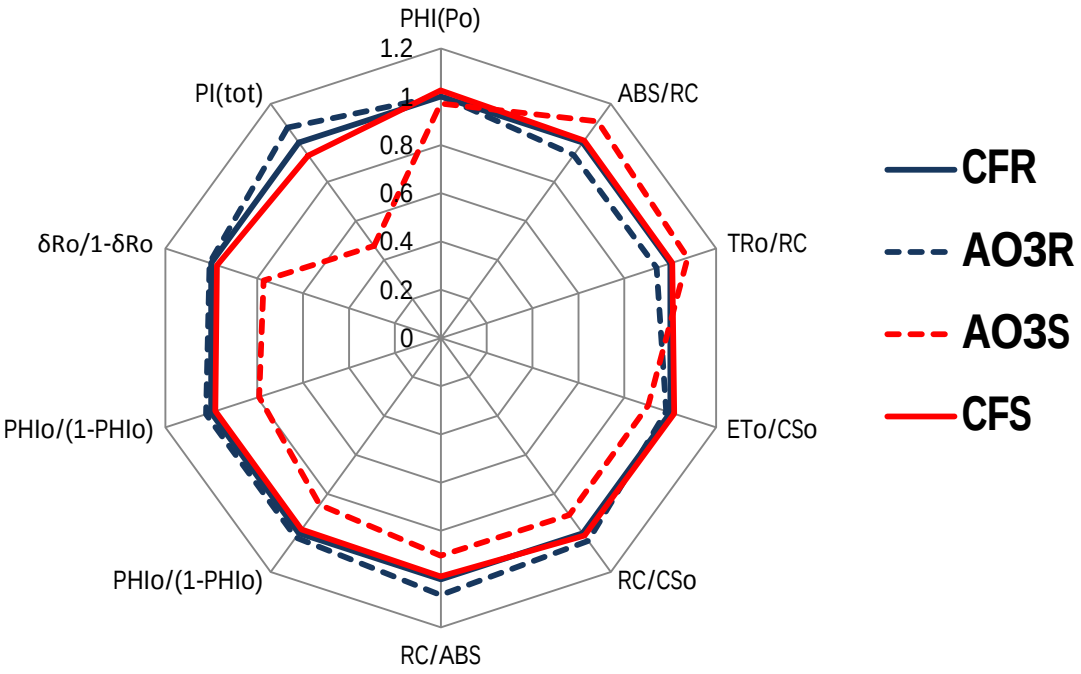

Figure 3.9: Functional and structural parameters of PS II deduced by the JIP analysis of fluorescence transients. For each parameter and for both plant genotypes the values were normalised to that of the control (CFR).

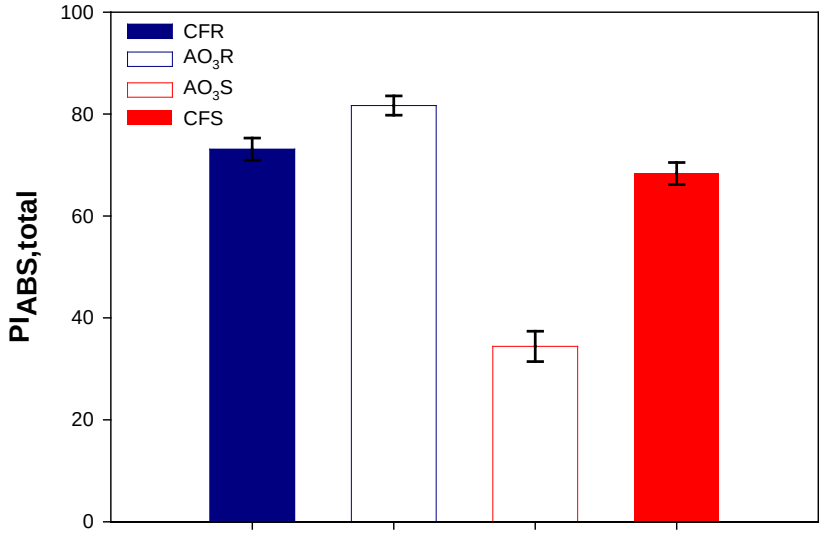

Figure 3.10: Performance index total ($PI_{ABS,tot}$) measured after 25 days of fumigation with filtered air (CF) and 80 nmolmol^{-1} ozone (AO_3) respectively.

The change in the derived energy fluxes per reaction centre (membrane model) (**Figure 3.11**, top) or per cross section (leaf model) (**Figure 3.11**, bottom) is displayed by the pipeline model. The leaf model provides a visualisation of the inactivation of RCs upon O_3 fumigation, while the membrane model demonstrates the associated increase of the ABS/RC, both as flux and as antenna size. The pipeline model can be seen as a dynamic model in which the value of each energy flux is expressed by the appropriately adjusted width of the corresponding arrows. Two types of models are shown; one dealing with the specific energy (per RC, Membrane model), and the other refers to the cross section of a leaf (per CS, Leaf Model). At the top of **Figure 3.11** (membrane model), the antenna size, which corresponds with ABS/CS of AO_3S (right) plants, increased when compared to that of the control plants (CFR - left). In the leaf model (**Figure 3.11** – bottom), the active reaction centres per cross section (RC/CS) are indicated by open circles. **Figure 3.11** shows that after 25 days of O_3 fumigation some of the RC's were deactivated (see closed circles in the leaf model), which resulting in an associated increase in the ABS/RC of the AO_3S plants, both as flux and as average antenna size. As a consequence of the above alteration, the AO_3S plants exhibited a much lower electron transport per leaf cross section compared to the control.

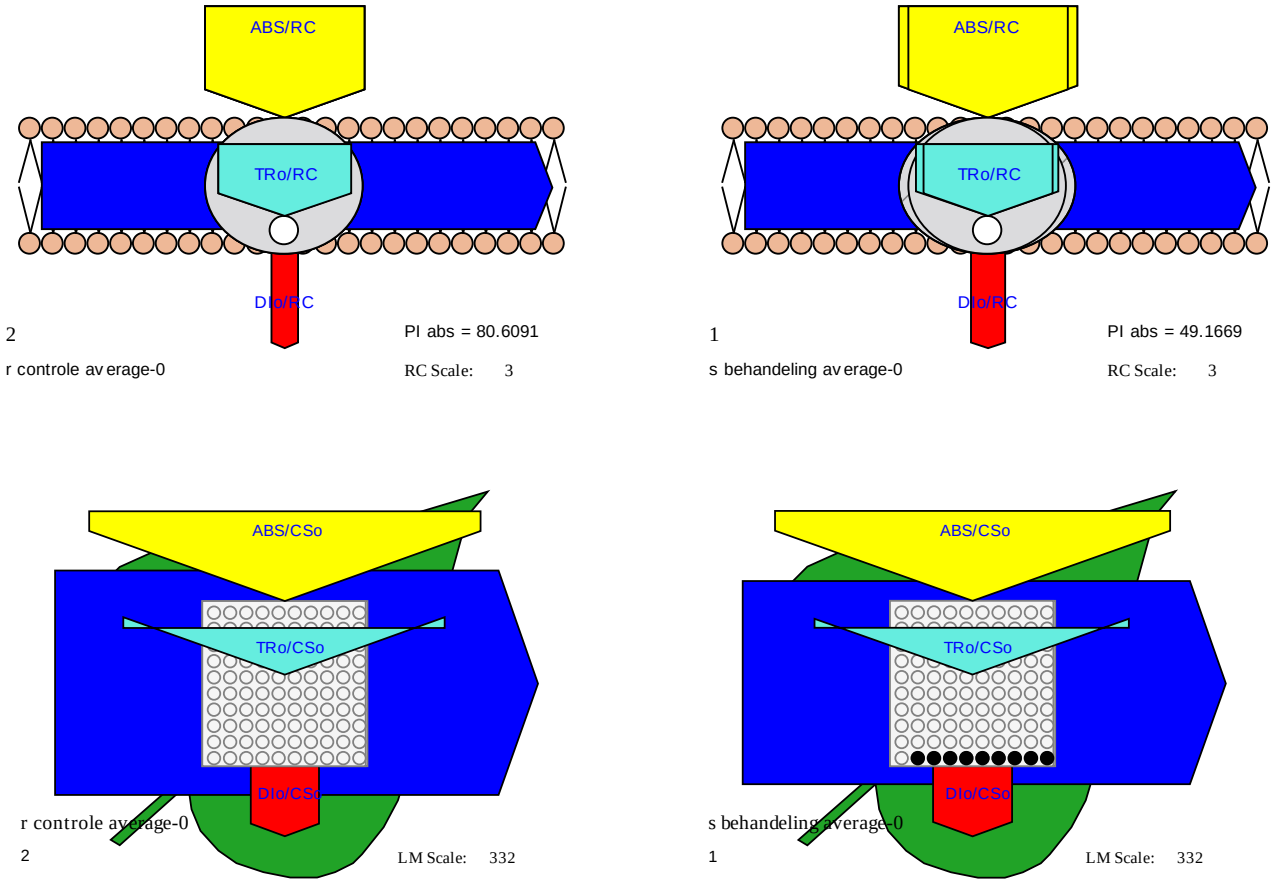

Figure 3.11: Energy pipeline models of the control plants (CFR) (left) and treatment plants (AO_3S) (right). The membrane models (top) represent the specific activities, expressed as fluctuations per reaction centre (RC). The leaf models (bottom) show the phenomenological fluctuations, expressed as per leaf cross section (CS). The relative magnitude of each activity or fluctuation is shown by the width of the corresponding arrow. The average antenna size is given as ABS/CS. This expresses the total absorption flux of PS II antenna chlorophyll divided by the number of active reaction centres. Thus, the antenna of PS II complexes with non-Q_A reducing RCs (heat sink centres) are graphically added to the antenna of the active reaction centres. The absorption and trapping by PS II units with heat sink centre is indicated as the hatched parts of the arrows ABS/CS and TR_0/RC. The antenna belonging to the PS II units with heat sink centres is drawn in black while the antenna which belongs to the active (Q_A reducing) centres is drawn in white. In the shaded zones of the model, the Q_A reducing RCs per cross section are indicated by open circles and the non-Q_A reducing RCs (heat sink or silent RCs) are indicated by the closed circles. The colouration of the foliage indicates the chlorophyll concentration per leaf cross section.

Further in-depth analysis of the fluorescence transients comprised normalisation of the average fast phase chlorophyll *a* fluorescence transients of the different treatments between the steps O (50 µs) and J (2 ms), as $V_{OJ} = (F_t - F_0)/(F_J - F_0)$ as well as between steps J (2 ms) and F_M (peak), as $V_{JP} = (F_t - F_J)/(F_P - F_J)$. The normalised fluorescence transients of the control (CFR) were then subtracted from the normalised fluorescence transients of the different treatments to obtain difference kinetics ($\Delta V = V_{treatment} - V_{control}$). The two difference kinetics were then plotted as ΔV_{OJ} and ΔV_{JP}, respectively (ΔV_{OJ} left and ΔV_{JP} right in **Figure 3.12**). The positive ΔV_K-band (at about 300 µs) appearing in the AO_3S plants is the consequence of an increase in fluorescence (**Figure 3.12** – left), probably due to the short-lived accumulation of reduced electron carriers such as $Pheo^-$, which, in turn, is caused by the dissociation of the OEC (oxygen evolving complex), resulting in an imbalance between the electron flow from the OEC to the RC and towards the acceptor side of PS II in the direction of PS I (Strasser, 1997). Uncoupling of the OEC enables an alternative internal electron donor such as ascorbate or proline (instead of H_2O) to donate electrons to PS II. This leads to a short-lived increase in the reduced Pheo/Q_A concentration, creating a ΔV_K-band appearing between 100 and 300 µs and increasing with intensity of the stress (De Ronde *et al*., 2004). The ΔV_K-band can also occur due to an increase of the functional PSII antenna size (Strasser et al., 2004). Note that the AO_3R plants exposed to the same O_3 concentration had a negative K-band, which points out that O_3 had no effect on the function of the OEC.

A positive ΔV_I-band also became visible between 2 ms and F_M (**Figure 3.12** – right) of the AO_3S plants after 25 days of exposure to O_3. The ΔV_I-band provides information on the activation state of feredoxin $NADP^+$ reductase (FNR) and possible inhibition of reduction of end electron acceptors such as $NADP^+$ and Fd due to a higher reduced state of the pool mixture of plastoquinone, cytochrome b/f and plastocyanin (Yusuf *et al*., 2010).

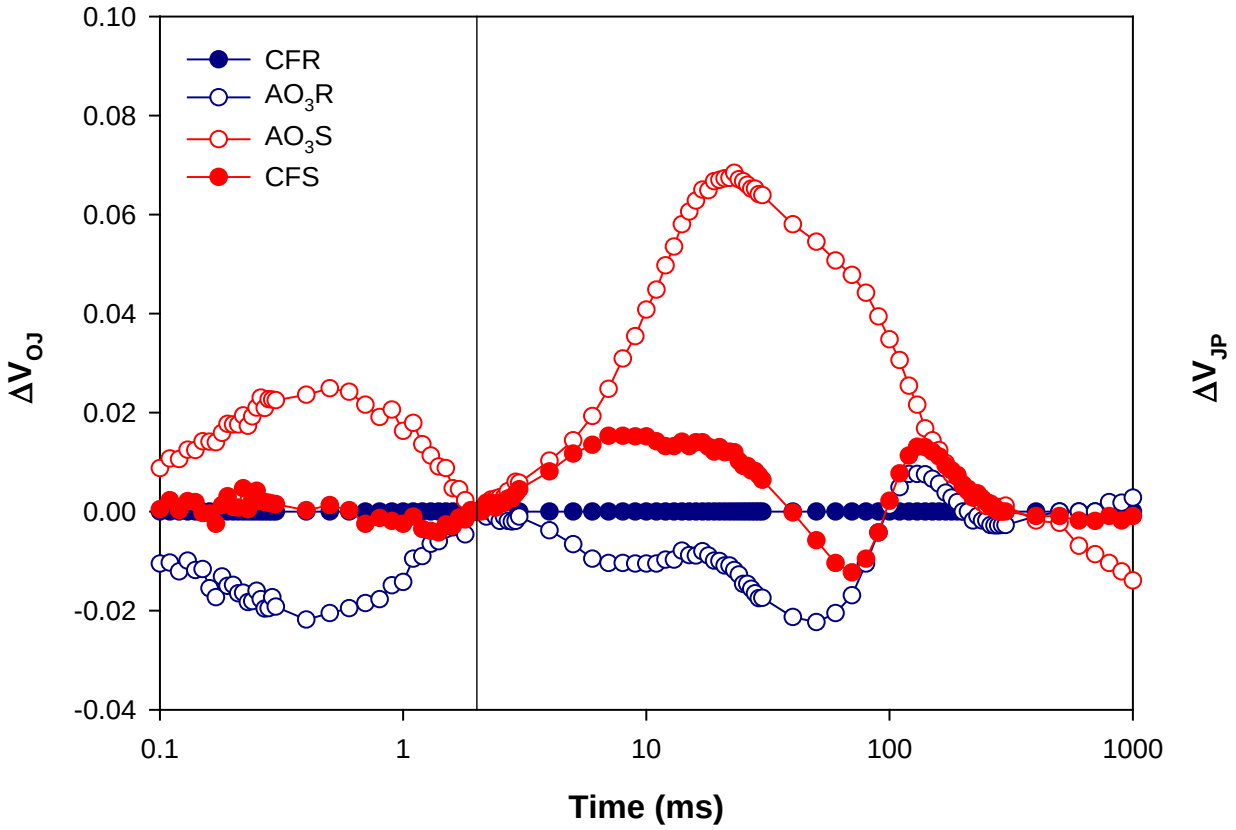

Figure 3.12: Difference in relative variable chlorophyll *a* fluorescence transients ($\Delta V = V_{treatment} - V_{controle}$) of resistant (R123) and sensitive (S156) *Phaseolus vulgaris* exposed to 80 nmolmol^{-1} ozone (AO_3) for 25 days respectively (expressed as V = f(t)) normalised between fluorescence extremes F_O (50 µs) and F_J (2 ms) as well as between F_J (2 ms) and F_P to obtain the ΔV_{O-J} and ΔV_{J-P} curves. ΔV_K and ΔV_I bands are indicated. Each curve represents the average of 48 measurements.

3.2.2 Effect of O_3 on photosynthetic gas exchange

In order to determine the effect of O_3 on the photosynthetic gas exchange of the test plants, several gas exchange parameters were derived from the A:C_i response curves (**Figure 3.13**). It is accepted that the most reasonable standard for comparing and characterizing the status of the photosynthetic apparatus on basis of gas exchange is a CO_2 response curve of the intact leaf (Lange et al., 1987). All the measurements were done on the same leaf of the respective different treated plants. All major photosynthetic gas exchange parameters were calculated and presented in **Table 3.2**. The actual assimilation rate (ambient conditions), A_{370}, occurs where we find the simultaneous solution of the demand function and the supply function, i.e. the operational point. The A_{370} value of the AO_3S test plants decreased by 57 % ($p<0.01$). The very small decrease of 3 % in the A_{370} of the AO_3R plants again showed that O_3 had almost no effect on the CO_2 assimilation at ambient CO_2 levels in this genotype. This drastic inhibition of CO_2 assimilation capacity in the AO_3S plants could be ascribed to the decrease in the CO_2 saturated rate of photosynthesis (J_{max}), which suggests that O_3 had an inhibitory effect on the regeneration capacity of RuBP. J_{max} of the AO_3S plants decreased by 61 % ($p<0.01$). The J_{max} values of the AO_3R and CFR test plants were remarkably similar, showing that O_3 at 80 nmol.mol^{-1} had no effect on CO_2 assimilation rate nor the regeneration capacity of RuBP. The carboxylation efficiency (CE; slope of the A:C_i response curve at $C_i \leq 200$ μmol.mol^{-1}) of the AO_3S plants decreased by a significant 75 %. The carboxylation efficiency expresses the rate of CO_2 assimilation in terms of the effective C_i and the capacity (CE) of the system to assimilate CO_2. Farquhar *et al.* (1980), suggested that at low CE, CO_2 assimilation follows the Michaelis-Menton kinetics and is determined by the RuBP saturated rate of the enzyme. The lower the carboxylation capacity, the less steep the slope of the demand function. The CE values of the CFR AO_3R and CFS test plants did not differ from each other. The CFR and AO_3R test plants had exactly the same CE value (**Figure 3.13** and **Table 3.2**). This indicates that O_3 had no effect on the carboxylation efficiency of the resistant plants exposed to elevated levels of 80 nmol.mol^{-1}. The Ci_{370} value of the AO_3S test plants was not effected when compared to the CFR test plants. This is an indication that the large decrease in A_{370} was due to mesophyll limitation rather than stomatal limitation. This fact is corroborated by the large increase in Γ and large decrease in CE in AO_3S plants. The supply function (Gs_{370}) of the AO_3S plants decreased by 36 % ($p<0.05$). The

supply function expresses the rate of CO_2 assimilation in terms of the difference in concentration between C_a and C_i (the driving force for inward movement of CO_2) and the prevailing stomatal conductance (g_{CO2}). Reduced stomatal conductance is rarely the main cause of reduced assimilation rates (Farquhar & Sharkey, 1982). However, the calculated percentage stomatal limitation (ℓ), suggests that reductions in assimilation rates in the AO_3S plants was the result of mesophyll limitation only. The ℓ of the AO_3S plants decreased by 37 % in comparison with the CFR plants. The ℓ of the AO_3R plants had an moderate increase of 9 %. Elevated O_3 of 80 nmolmol^{-1} caused a very pronounced decrease of 60 % ($p<0.01$) in the CO_2 assimilation rate at C_i = 370 µmol.mol^{-1} (A_0) of the AO_3S test plants when compared to the control plants (CFR) (**Table 3.2**). The AO_3R showed no O_3 induced effect in the CO_2 assimilation rate. The CO_2 assimilation rate of the CFS was 8 % higher compared to the CFR test plants. O_3 also lead to a 51 % decrease in the water use efficiency (WUE) of the AO_3S plants compared to the CFR plants. This decrease in WUE occurred in spite of a reduction in transpiration rate (E). E of AO_3S plants decreased by 30 % in comparison with the CFR plants. E of the AO_3R plants was not affected by elevated O_3.

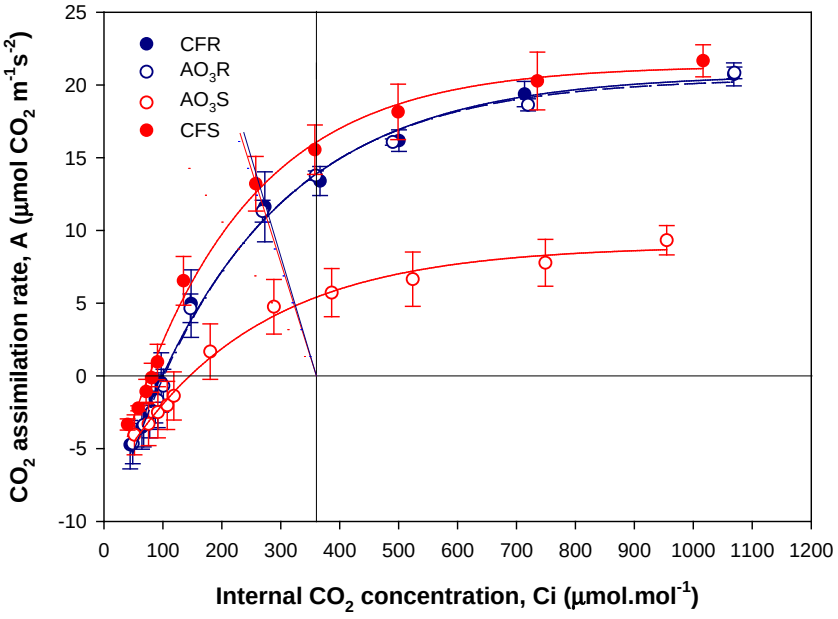

Figure 3.13: Average CO_2 assimilation rate (A) as a function of intercellular CO_2 concentration for leaves of R123 and S 156 *Phaseolus vulgaris* genotypes after 25 days exposure to filtered air (CF) and 80 nmol.mol^{-1} ozone (AO_3) respectively. Each value represents a mean (± SE) where n = 4.

Table 3.2: Mean values (± standard errors) of photosynthetic gas exchange parameters of leaves of R123 and S156 *Phaseiolus vulgaris* genotypes (n = 4 plants per treatment) 25 days after exposure to filtered air (CF) and 80 nmol.mol^{-1} ozone (AO_3) respectively. Symbols: E_{370}, transpiration rate at Ca = 370 mmol.m^{-2}.s^{-}1; A_{370}, rate of CO_2 assimilation at C_a = 370 µmol.mol^{-1}; Ci_{370}, intercellular CO_2 concentration at Ca = 370 µmol.mol^{-1}; A_0, rate of CO_2 assimilation at C_i = 370 µmol.mol^{-1};Gs_{370}, stomatal conductance at Ca = 370 µmol.mol^{-1}; CE, carboxylation efficiency at Γ; J_{max}, minimum rate of CO_2 assimilation; Γ, CO_2 compensation concentration; ℓ, percentage stomatal limitation of photosynthesis; WUE, water use efficiency, with * and ** indicating significant differences at p<0.05 and p<0.01, respectively, compared to the control plants (CFR).

	CFR	AO_3R	CFS	AO_3S
E (mmol.m^{-2}.s^{-1})	5.3 (1.12)	4.66 (0.48)	4.90 (0.86)	3.70 (0.63)
A_{370} (µmol.m^{-2}.s^{-1})	11.45 (1.2)	11.2 (1.2)	13.76 (1.38)	4.92 (1.27**)
Ci_{370} (µmol.mol^{-1})	295.75 (19.34)	270.0 (18.24)	256.16 (18.48)	292.2 (26.61)
A_0 (µmol.m^{-2}.s^{-1})	14.87 (1.24)	14.98 (0.76)	16.07 (0.94)	5.97 (0.85**)
Gs_{370} (µmol.m^{-2}.s^{-1})	259 (80.97)	203.25 (25.96)	274.66 (14.71)	165.2 (50.45*)
CE mol.m^{-2}.S^{-1})	0.056 (0.002)	0.056 (0.002)	0.061 (0.003)	0.014 (0.003**)
Jmax (µmol.m^{-2}.s^{-1})	20.25 (0.56)	20.17 (0.31)	20.95 (1.27)	7.87 (1.51**)
Γ (µmol.mol^{-1})	98 (4.57)	101.6 (5.64)	76.4 (2.78)	145.8 (6.35**)
ℓ (%)	22.99	25.23	14.37	17.73
WUE (µmol.mmol.$^{-1}$)	2.97 (0.23)	2.75 (0.24)	2.99 (0.13)	1,46 (0.55*)

3.3 Effect of O_3 on chlorophyll content index (CCI) in *Phaseolus vulgaris*

After 30 days of exposure to 80 nmol.mol^{-1} O_3 the AO_3S plants showed a decrease of 24 % in the CCI when compared to the CFR plants (**Figure 3.14**). The AO_3R plants showed an increase of 19 % in the CCI. The above finding corresponds well with the 10 % decrease in RC/CS_0 obtained from the fluorescence parameters measured (see **Figure 3.9**). There was a significant difference between both of the genotypes exposed to elevated O_3, when compared to the control plants (CFR).

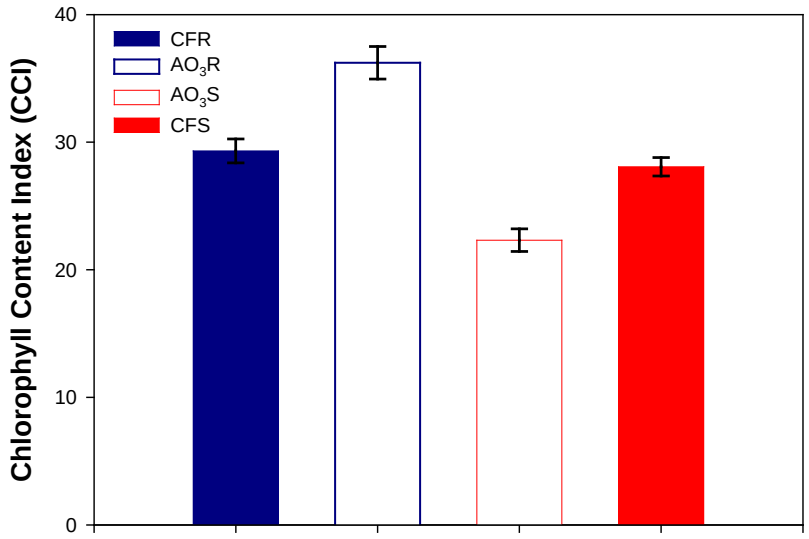

Figure 3.14: Chlorophyll content expressed as chlorophyll content index (CCI) of R123 and S156 *Phaseolus vulgaris* genotypes after 30 days exposure to carbon filtered air (CF) and 80 nmol.mol^{-1} ozone (AO_3) respectively.

Chapter 4

Results and discussion on: Interaction of ozone fumigation and drought on photosystem II function and photosynthetic gas exchange in *Pisum sativum* L. in open-top chambers

4.1 Verification of the water regime of the different treatments, i.e. "well watered (WW) and drought stressed (DS)":

4.1.1 Relative water content (RWC)

Following drought treatment, the relative water content (RWC) of *Pisum sativum* leaves ranged from 85 % in the drought stressed plants exposed to elevated O_3 concentrations (DSO_3), to 94 % in the well watered plants exposed to carbon filtered air (WWCF). The drought stressed control plants had a RWC of 86 %, while the WWO_3 plants had a 94 % RWC. The RWC of the test plants were compared to that of the WWCF plants. The DSCF and DSO_3 test plants revealed an 8 % and 9 % decrease in RWC when compared to the RWC of the WWCF plants (**Figure 4.1**). The above measurements confirmed that drought stress induced by using only one wick in the irrigation system, significantly reduced RWC values in the DSCF and DSO_3 test plants.

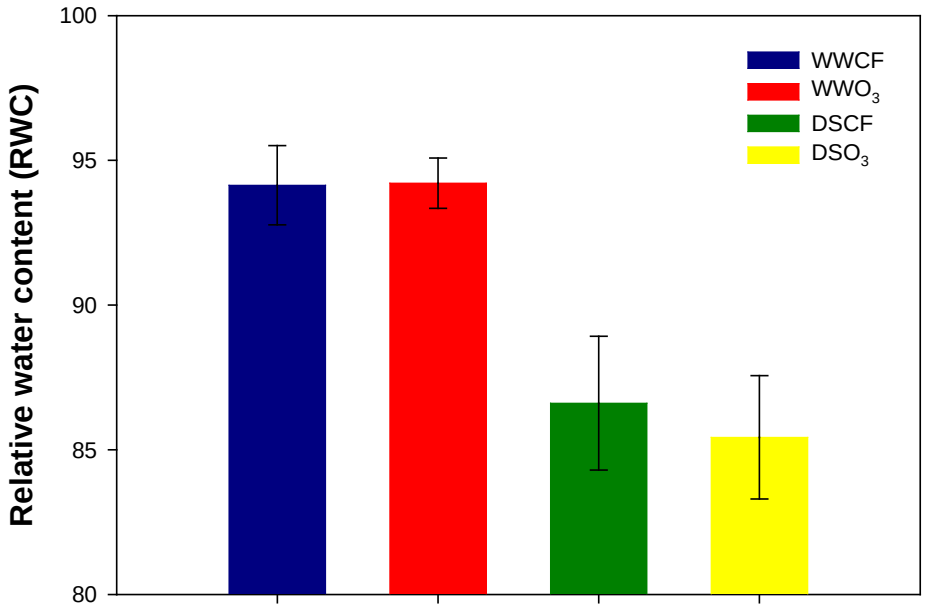

Figure 4.1: Effect of O_3 and drought stress (DS), singly and combined on the relative water content (RWC) of *Pisum sativum* plants 30 and 10 days after exposure to O_3 and drought stress, respectively.

4.1.2 Leaf water potential

After 30 days of fumigation with 80 nmol.mol^{-1} O_3 and 15 days of drought stress, the pre-dawn leaf water potential (Ψ_{PD}) (**Figure 4.2**) of the WWO_3 and DSO_3 test plants increased when compared to the value of -0.036 MPa (WWCF) to -0.1 and -0.15 MPa, respectively, while leaf water potential in drought stressed carbon filtered grown in the absence of O_3 remained nearly the same as the WWCF test plants. The leaf water potential measured over midday (Ψ_{MD}) for plants grown in drought stress was significantly higher than the control and corresponded in behaviour on crops such as soybean (Villalobos-Rodriquez and Shibles, 1985) and maize (Lal *et al*., 1987. The Ψ_{MD} of the DSCF and DSO_3 plants decreased by 33 % and 26 %, respectively. We found that withholding water, reduced stomatal conductance in both drought stressed plants (DSCF and DSO_3) which normally would lead to a less negative water potential, however under drought stress conditions available water in the soil is limited and results in a greater negative pressure inside the xylem. According to Vassey & Sharkey (1989) and Santos *et al*. (2006), low water potential due to mild drought stress, caused strong photosynthesis impairment in *Phaseolus vulgaris*. Although not significant, the water potential of the WWO_3 test plants

decreased by 6 % when compared to that of the WWCF plants, which could be attributed to a decrease in stomatal aperture (See **Figure 4.4 and 4.5**).

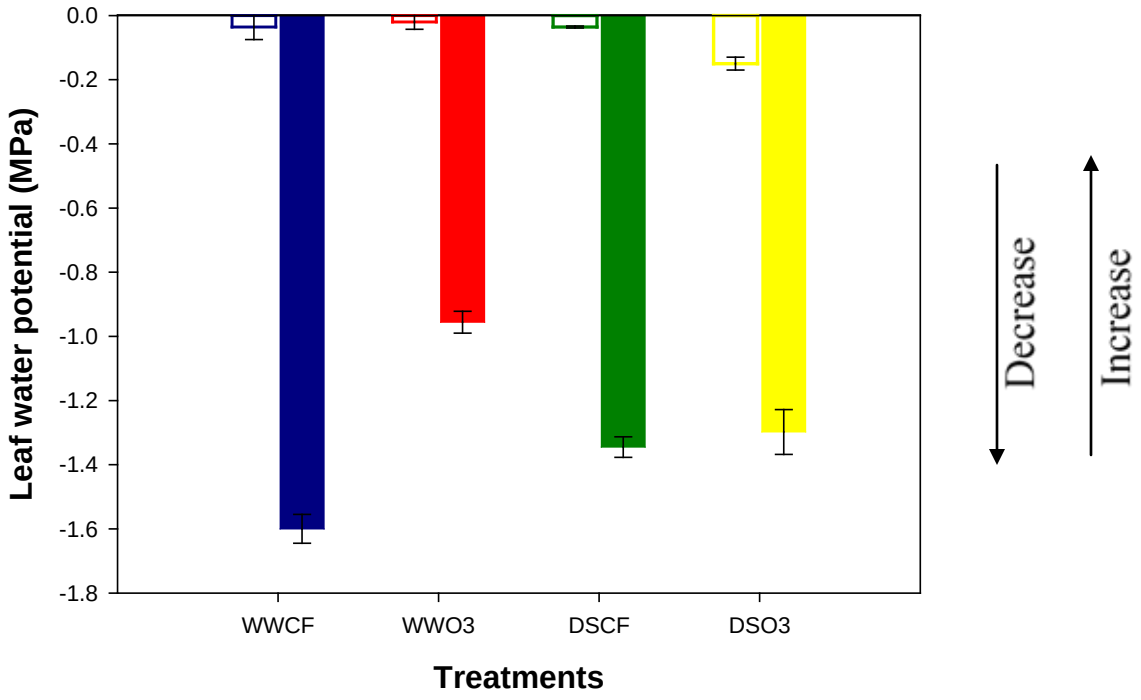

Figure 4.2: Leaf water potential (MPa) for *Pisum sativum* plants exposed to O_3 and drought stress (DS), singly and combined. Pre-dawn (open bars) and midday (solid bars) water potential was measured with a Scholander pressure chamber and each value represents a mean (±SE), where n = 4.

4.2 Growth

4.2.1 Plant development

Although no leaf damage was visible, a noticeable decrease in growth was evident in all the treated plants after 40 days of treatment when compared to the WWCF test plants (**Figure 4.3**). The decrease in growth was verified in the final biomass. The different treatments had no effect

on the time of flowering, abundance of inflorescence and pod formation when compared with the control (WWCF).

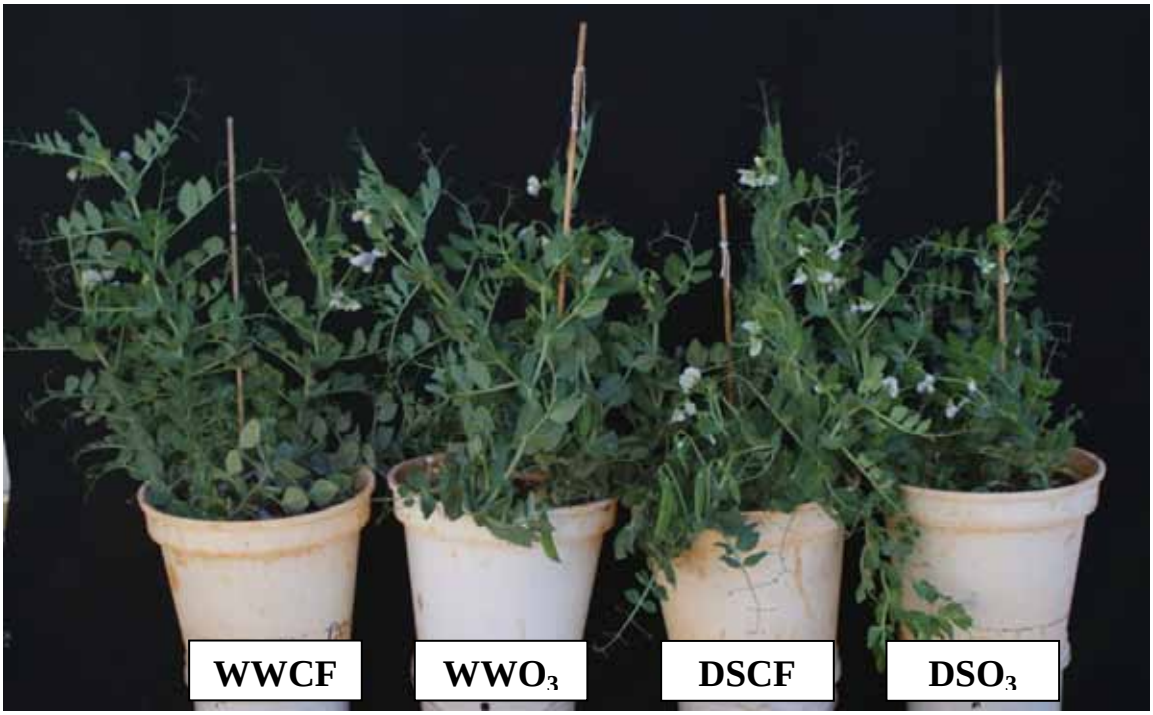

Figure 4.3: Well watered (WW) and drought stressed (DS) *Pisum sativum* plants 40 days after exposure to carbon filtered (CF) air and 80 nmolmol^{-1} ozone (O_3) respectively.

4.2.2 Effect of O_3 on the stomata of *Pisum sativum*

The response of the stomata with respect to the stomatal aperture of the different treatments differed markedly (**Figure 4.4**). Ozone and drought stress caused a decrease in stomatal apertures. The stomata of the WWCF test plants were the widest open and those of the DSO_3 test plants the smallest (**Figure 4.5**). The stomatal apertures of the WWO_3 test plants decreased by 36 % ($p < 0.05$), while the apertures of the two drought stressed plants, DSCF and DSO_3, by 45 % and 66 % ($p < 0.01$), respectively. The mentioned % decreases in stomatal apertures corresponded to the decreases in stomatal conductance of the respective treatments derived from the gas exchange data. The latter two parameters (stomatal aperture and G_{s370}) corroborated with the findings of Scheidegger *et al*. (1991), which found that O_3 induces partial stomatal closure

(Scheidegger *et al*., 1991), but with additional drought stress the effect on the stomata became more evident, as was evident in the DSO_3 test plants.

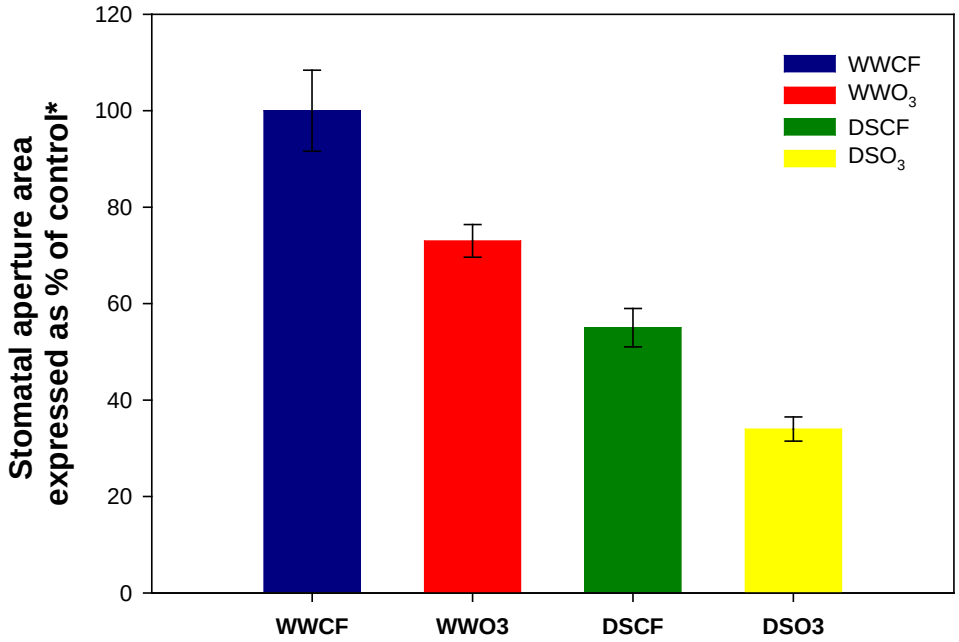

*stomatal aperture was calculated by weighing cut outs from scanning electron micrographs.

Figure 4.4: Influence of O_3 and drought stress singly and combined on the stomatal aperture of *Pisum sativum* plants 30 and 10 days after exposure to O_3 and drought stress, respectively.

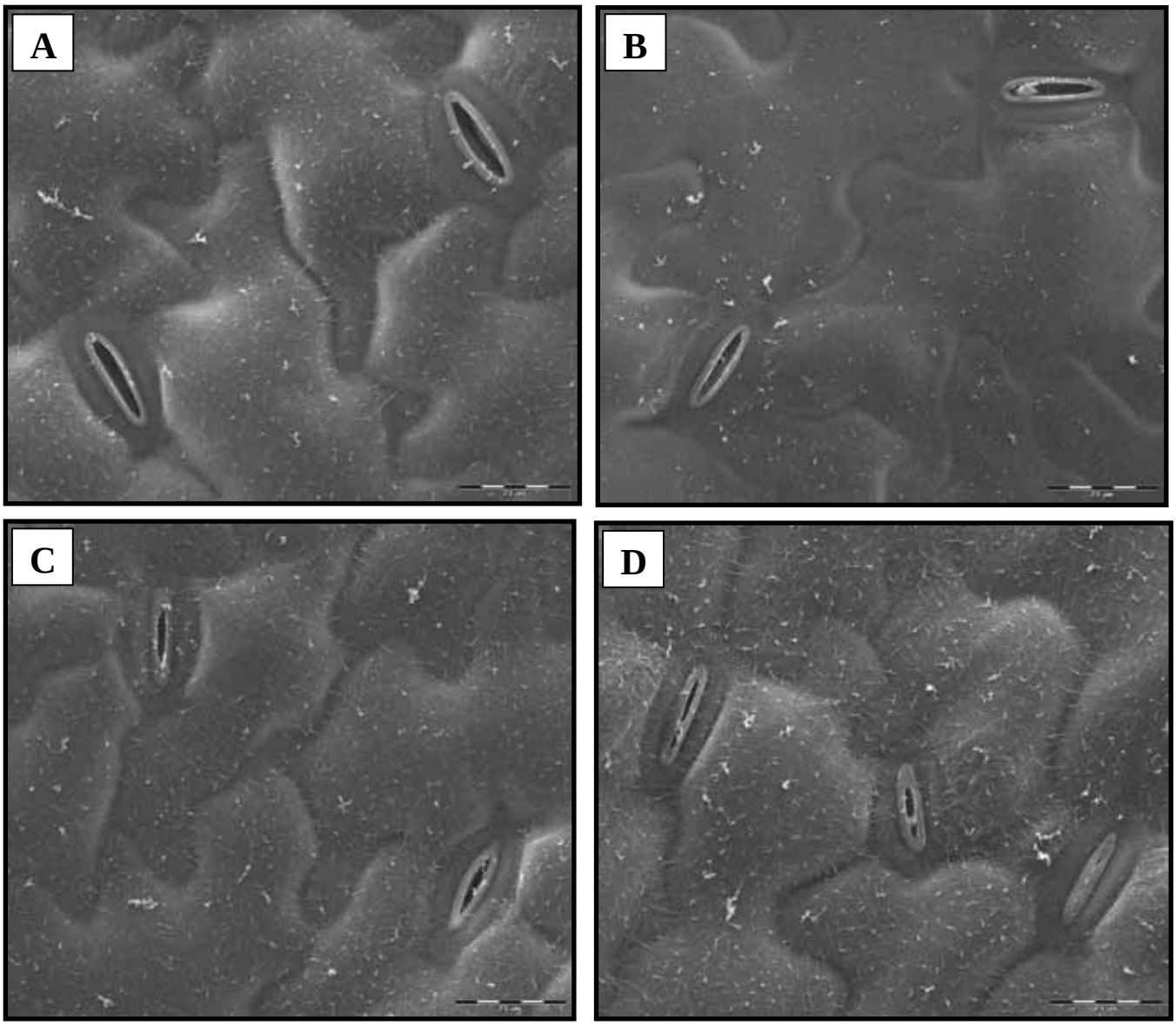

Figure 4.5: Scanning electron micrograph (SEM) of stomata on the abaxial epidermis of the surface of pea (*Pisum sativum*) leaves showing the effects of O_3 and drought stress, singly and combined. (A) WWCF plants, (B) WWO_3 plants, (C) DSCF plants and DSO_3 test plants.

4.2.3 Bio- and Root mass accumulation

The final biomass (dry mass) measured of all O_3 and drought (singly and combined) treatments was greatly reduced when compared to the WWCF test plants. The biomass of the WWO_3, DSCF and DSO_3 plants decreased by 23 %, 12 % and 24 %, respectively, with the decreases in WWO_3 and DSO_3 being statistically significant. A similar trend was recorded in the root mass with a marked decrease of 37 % occurring in the WWO_3 treatment. The 23 % decrease in biomass of the DSO_3 plants, however, was not statistically significant. An increase in root dry mass of 5 % occurred in the DSCF test plants. Several researchers (Pandey *et al.*, 1984; Sponchiado *et al.*, 1980) have hypothesised that the ability of a plant to change (i.e. increase) its root distribution in the soil is an important mechanism for drought avoidance. Merrill *et al*. (2002) showed that soybean and dry bean had the greatest root growth in the driest year in order to widen its absorption area and the least root growth in the wettest year.

Decreases in biomass are usually accompanied by reductions in photosynthesis as reported by Pausch *et al*. (1996) for *Glycine max.* The observations of reduction in plant growth (**Figure. 4.3**) correlated well with the biomass and root mass (**Figure 4.6**).

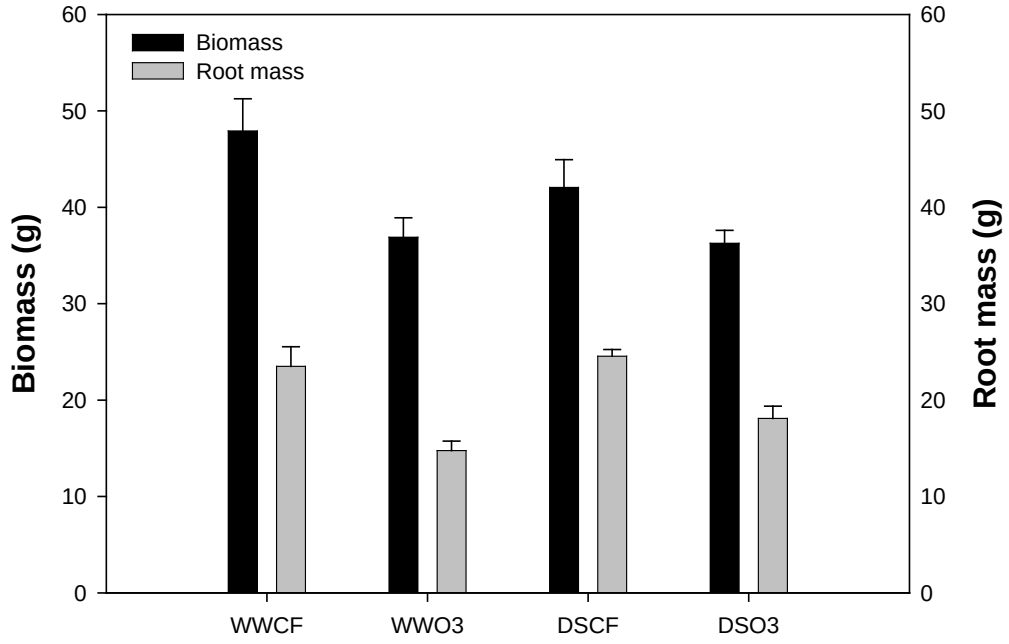

Figure 4.6: Effect of O_3 and drought stress (DS), singly and combined on the dry biomass above soil and root biomass of *Pisum sativum* plants.

4.3 Physiological response parameters

4.3.1 Effect of O_3 on fast phase chlorophyll a fluorescence kinetics

Average chlorophyll *a* fluorescence transients of dark adapted leaves of *P. sativum* are presented on a logarithmic time scale in **Figure 4.7** and **Figure 4.8**. These transients show the typical O-J-I-P fluorescence rise. The transients started from an initial level of F_0 and increased up to a maximum F_M (peak P). F_M can be considered as representing the maximum fluorescence yield, since the actinic light source of the fluorimeter (600 $W.m^{-2}$, peak at 650 nm) is high enough to ensure the closure of all the reaction centres. An important feature to point out is that the F_0 and F_M values of the chlorophyll *a* fluorescence transients of the test plants were remarkably similar before fumigation and drought stress commenced, indicating that the plants were physiologically homogenous (**Figure 4.7**). The low F_0 indicates that the plants were completely dark adapted, meaning that all the reaction centres were fully open. After 30 days of fumigation with 80 $nmol.mol^{-1}$ O_3 and 15 days of drought stress, the fluorescence transients of the controls and treatments began to differ (**Figure 4.8**). To compare the fluorescence transients they were normalised between F_0 (50 μs) and F_J (2 ms). This presentation revealed that the major effect of O_3 and drought stress probably occurred in the multiple turn-over events of PS II function of the treated plants, i.e. in the transition J (2 ms) to P (700 ms) (**Figure 4.9**). The transition from O to J represents the single turnover range of the transient (i.e. Q_A only reduced once) which reflects mainly photochemical reactions leading to the reduction of the electron acceptor Q_A, while the J to P part of the transient is strongly affected by the subsequent dark reactions in the electron transport chain (Strasser *et al*., 1999).

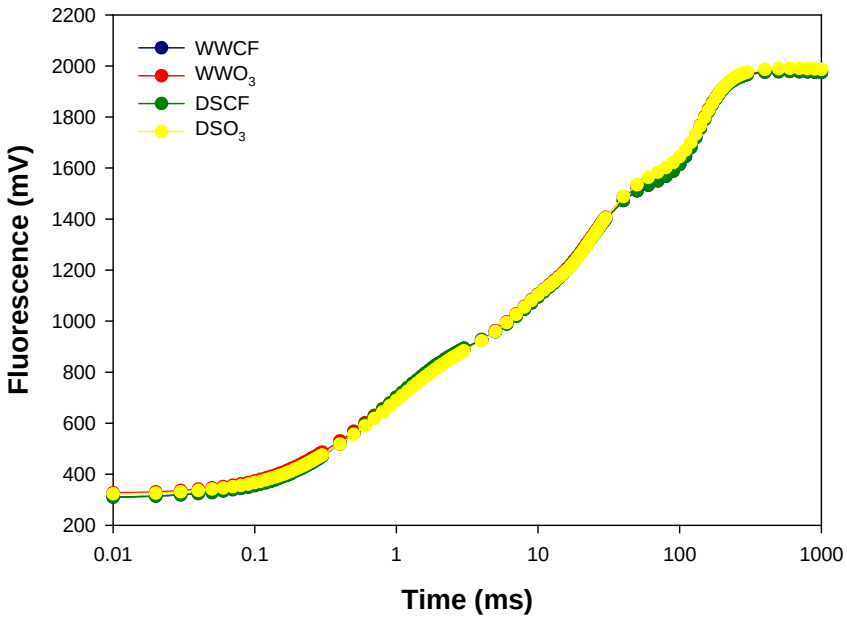

Figure 4.7: Raw chlorophyll *a* fluorescence transients measured in intact leaves of *Pisum sativum* plants before fumigation commenced demonstrating the physiological similarity of the test plants.

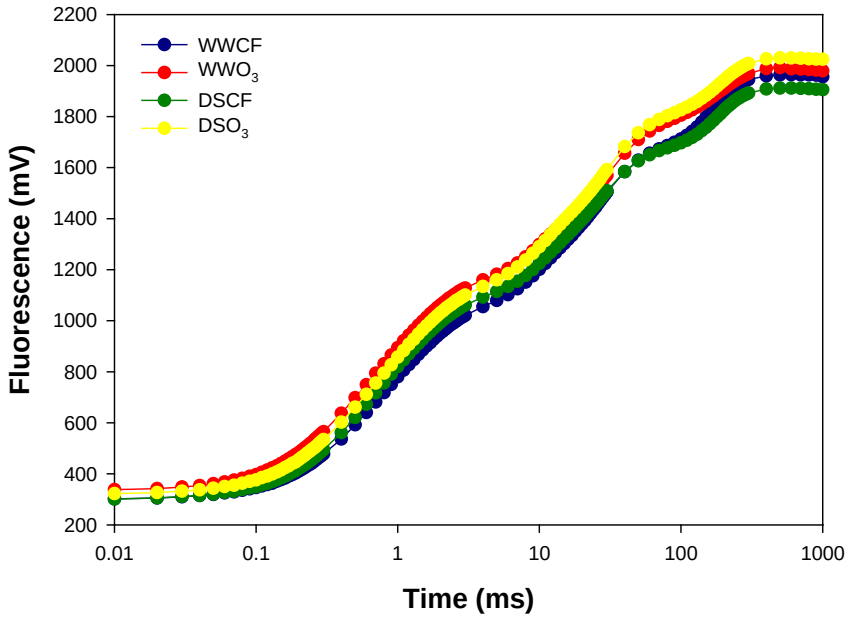

Figure 4.8: Raw chlorophyll *a* fluorescence transients measured in intact of well watered (WW) and drought stressed (DS) leaves of *Pisum sativum* plants after 30 days exposure to carbon filtered air (CF) and 80 nmolmol^{-1} ozone (AO_3) respectively.

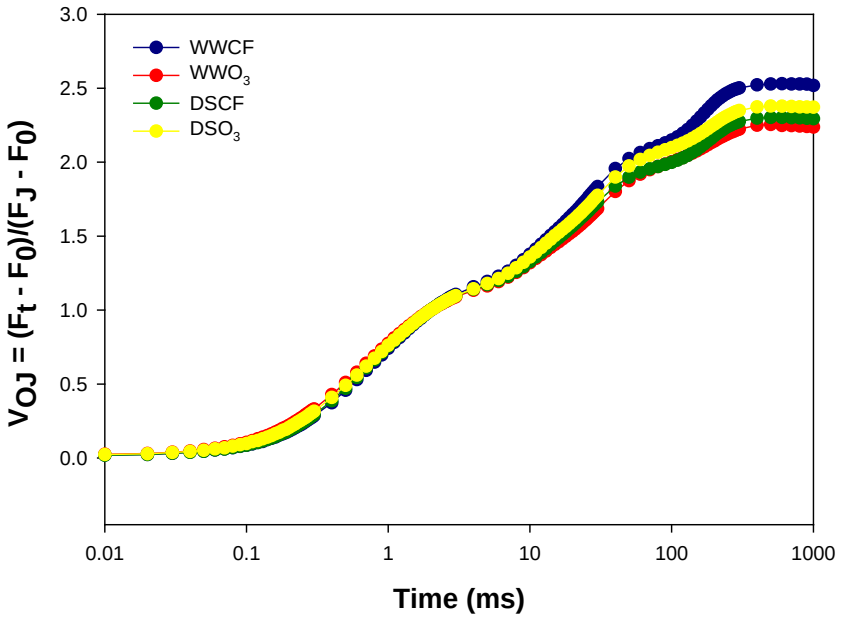

Figure 4.9: Average fast phase chlorophyll *a* fluorescence transients of well watered (WW) and drought stressed (DS) leaves of *Pisum sativum* plants after 30 days exposure to filtered air (CF) and 80 nmolmol^{-1} ozone (AO_3) respectively normalised between F_O (50 µs) and F_J (2 ms), indicating the relative change in the single turnover phase (0 – 2 ms) and the multiple turnover phase (2 ms – 1000 ms).

The average fast phase fluorescence transients were used for further in depth analysis of the differences in response of the test plants. The raw curves were normalised between the steps O (50 µs) and I (30 ms) and presented as relative variable fluorescence $V_{OI} = (F_t – F_0)/(F_I – F_0)$ vs. time (**Figure 4.10**). In **Figure 4.11** only the part with $V_{OI} \geq 1$ was plotted, in the 30 – 300 ms time range (linear scale). In the latter figure, the maximum amplitude of the fluorescence rise of each curve reflects the size of the pool of the end electron acceptors at the PS I acceptor side (Yusuf *et al.*, 2010). **Figure 4.11** demonstrates that the treatments WWO_3, DSCF and DSO_3 showed a 3 % decrease in the end electron acceptor pool size, when compared to the WWCF plants. **Figure 4.12** presents fluorescence data normalised between the steps I (30 ms) and P (peak) as $V_{IP} = (F_t – F_I)/(F_P – F_I)$ and plotted on a linear scale in the 30 – 400 ms range. This normalisation, where the maximal amplitude of the rise was fixed at unity, facilitated a comparison of the reduction rates of the end electron acceptors' pool in various treatments. Their half-times are shown by the interception of the curves with the horizontal dashed line drawn at $V_{IP} = 0.5$ (half rise) (Yusuf *et al.*, 2010). We observed that the plants which were fumigated with O_3 (WWO_3 and DSO_3), the overall rate constant (inverse of the half time) of the processes leading to the reduction of the end

electron acceptors was higher indicating that the regulation of the overall rate constant for the reduction of the end electron acceptor pool was independent of the regulation of the pool size (Yusuf *et al*., 2010).

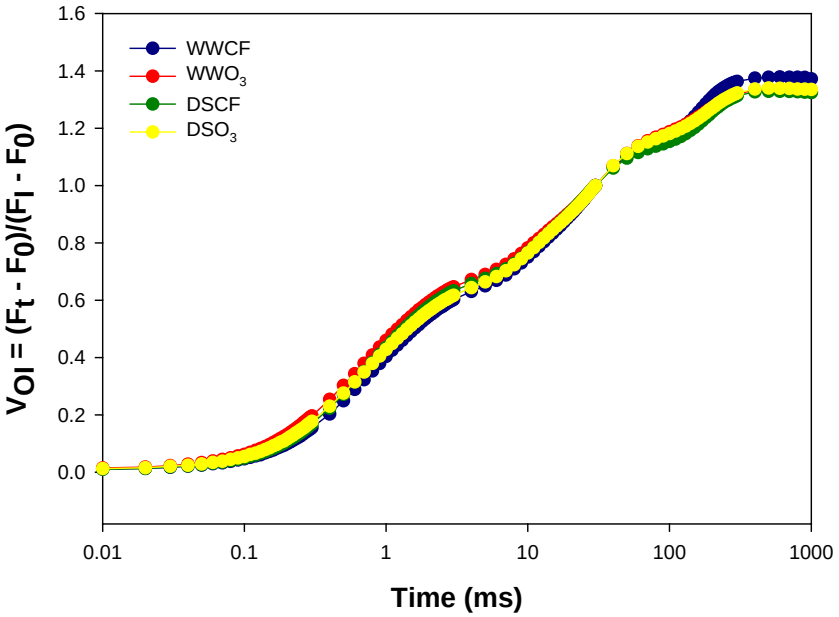

Figure 4.10: Average fast phase chlorophyll *a* fluorescence transients of well watered (WW) and drought stressed (DS) leaves of *Pisum sativum* after 30 days exposure to filtered air (CF) and 80 nmolmol^{-1} ozone (AO_3) respectively normalised between F_O (50 µs) and F_I (30 ms).

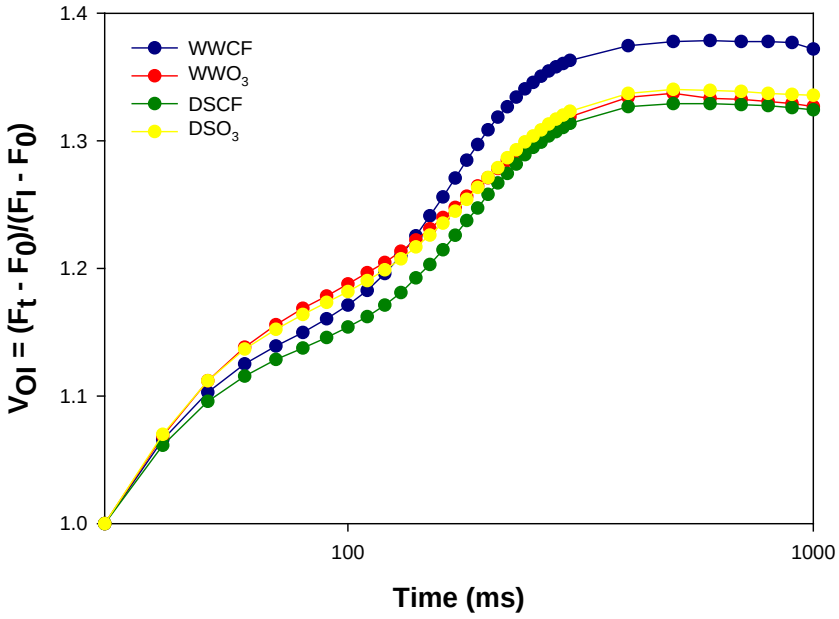

Figure 4.11: Average fast phase chlorophyll *a* fluorescence transients of well watered (WW) and drought stressed (DS) leaves of *Pisum sativum* plants after 30 days exposure to filtered air (CF) and 80 nmolmol^{-1} ozone (AO_3) respectively normalised between F_O (50 µs) and F_I (30 ms), plotted above 1 and 30 ms.

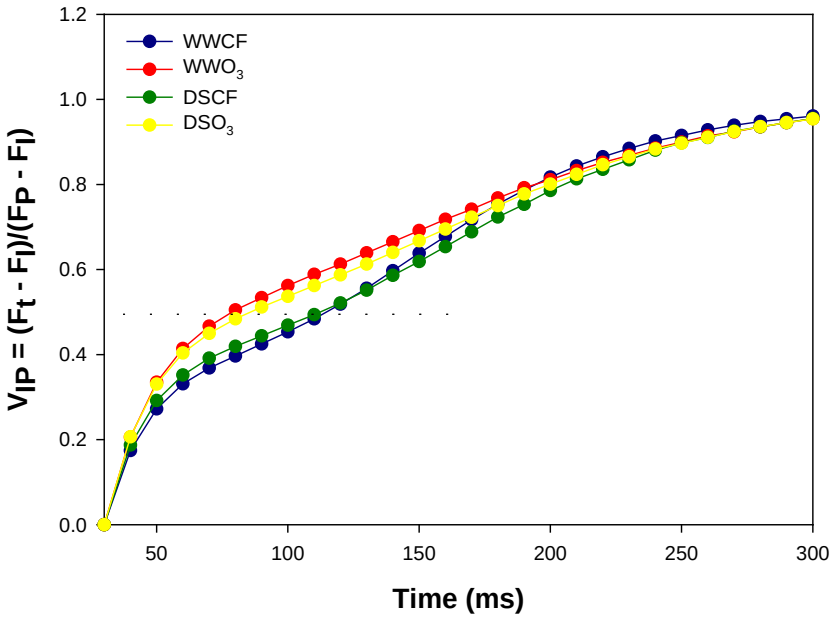

Figure 4.12: Average fast phase chlorophyll *a* fluorescence transients of well watered (WW) and drought stressed (DS) leaves of *Piusum sativum* plants after 30 days exposure to filtered air (CF) and 80 nmolmol^{-1} ozone (AO_3) respectively normalised between F_I (30 ms) and F_M (peak), plotted on a linear scale in the 30 – 300 ms range.

The fluorescence transients depicted in **Figure 4.8** was analysed by the JIP-test using the Biolyzer computer program to calculate 10 structural and functional parameters quantifying the PS II function of the different treatments 30 days after O_3 fumigation commenced. The values of these parameters are expressed relative to the control (WWCF i.e. solid blue line) and plotted in a multiparametric radar plot (**Figure 4.13**). Significant decreases ($p < 0.05$) of 15 % and 11 % occurred in the number of active reactive centres per total absorption (RC/ABS) of the WWO_3 and DSO_3 test plants, respectively. A decrease in RC/ABS corresponds to a decrease in the size of the chlorophyll antenna serving each RC (Strasser and Strasser, 1995). This large decrease can be attributed to the decrease of active (functional) oxygen evolving complexes, indicated by the positive ΔV_K-band (**Figure 4.14**). The RC/ABS (apparent antenna size) of the DSCF test plants was almost unaffected. Concurrently a significant ($p < 0.05$) increase in ABS/RC of 18 % and 11 %, and an increase of 15 % and 10 % in the specific trapping flux (TR_0/RC) (maximum trapping flux) occurred in the WWO_3 and DSO_3 test plants, respectively. The increases in antenna size and trapping flux compensated for the inactivation of reaction centres and may either mean that (i) a fraction of RCs is inactivated e.g. by being transformed to non-Q_A reducing centres, or (ii) the functional antenna, i.e., the antenna that supplies excitation energy to active RCs, has increased in size (Strasser & Strasser, 2004). Concomitantly all the other quantum yields were also affected, with a decrease of 13 % ($p < 0.05$), 4 % and 5 % in TR_0/ABS (φ_{P0}) occurring in the WWO_3, DSCF and DSO_3 test plants, respectively. The largest effect on the quantum yields was seen in the ET_0/ABS (φ_{E0}), where a significant ($p < 0.05$) 18 %, 15 % and 10 % decrease was observed in the WWO_3, DSCF and DSO_3 treatments, respectively. The two drought stressed treatments (DSCF and DSO_3) showed a significant ($p < 0.05$) decrease of 8 % and 9 % in the RE_0/ABS (φ_{RE}). The performance index ($PI_{ABS,tot}$) combines the latter four independent functional steps of photosynthesis namely that of: efficiency of light absorption RC/ABS; the performance due to the quantum efficiency of primary photochemistry (TR_0/ABS); the performance due to the quantum efficiency of the conversion of excited energy to electron transport (ET_0/ABS) and the performance due to the quantum efficiency of the reduction of end electron acceptors (RE_0/ABS). The $PI_{ABS,total}$ of the two O_3-treated (WWO_3 and DSO_3) test plants decreased by 36 % ($p < 0.01$) and 31 % ($p < 0.01$), respectively, while a significant ($p < 0.05$) decrease of 25 % was observed in the DSCF test plants relative to the WWCF control.

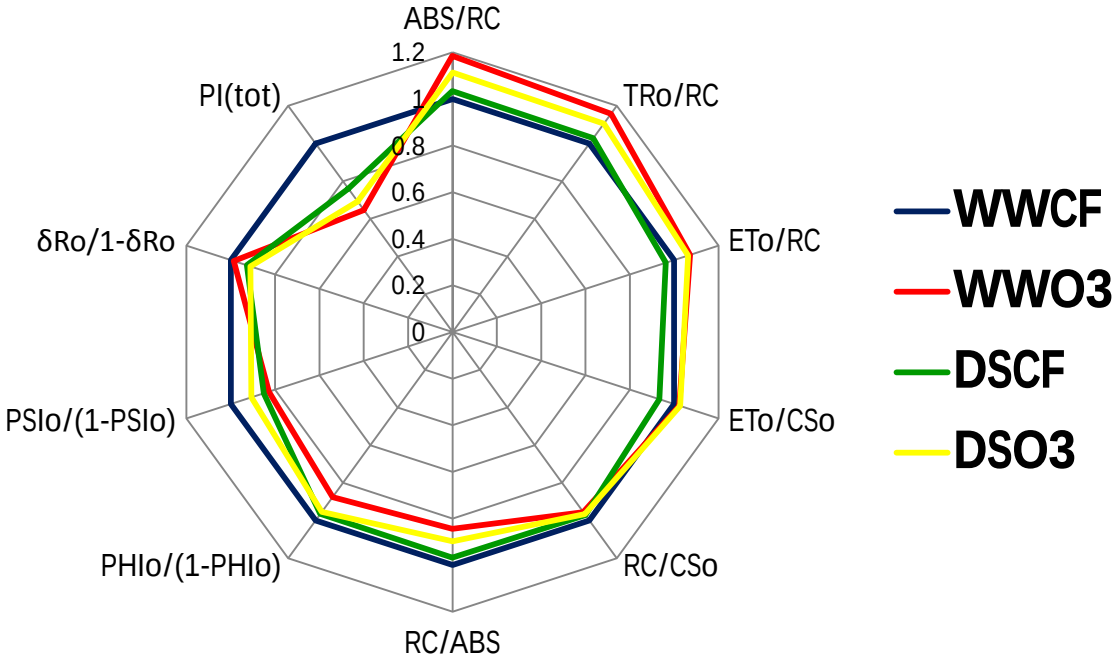

Figure 4.13: Functional and structural parameters of PS II deduced by the JIP analysis of fluorescence transients. For each parameter and for all the test plant genotypes the values were normalised to that of the control (WWCF).

To obtain the ΔV difference fluorescence spectra the average fast phase chlorophyll a fluorescence transients of the different treatments shown in **Figure 4.9**, were normalised between the steps O (50 µs) and J (2 ms), as $V_{OJ} = (F_t - F_0)/(F_J - F_0)$ as well as between steps J (2 ms) and F_M (peak), as $V_{JP} = (F_t - F_J)/(F_P - F_J)$. The normalised fluorescence transient of the control (WWCF) was then subtracted from the normalised fluorescence transients of the different treatments to obtain difference kinetics ($\Delta V = V_{treatment} - V_{control}$). The difference kinetics was then plotted as ΔV_{OJ} and ΔV_{JP}, respectively (ΔV_{OJ} left and ΔV_{JP} right in **Figure 4.14**). A significant positive ΔV_K-band (at about 300 µs) appeared in the O_3-treated test plants and a minor ΔV_K-band in the drought stressed plants. The positive ΔV_K-bands (**Figure 4.14** – left) are probably due to the short-lived accumulation of reduced electron carriers such as $Pheo^-$, which in turn is caused by the dissociation of the OEC (oxygen evolving complex), resulting in an imbalance between the electron flow from the OEC to the RC and towards the acceptor side of

PS II in the direction of PS I (Strasser, 1997). Uncoupling of the OEC enables an alternative internal electron donor such as ascorbate or proline (instead of H_2O) to donate electrons to PS II. This leads to a short-lived increase in the reduced Pheo/Q_A concentration, creating a ΔV_K-band appearing between 100 and 300 µs (De Ronde *et al*., 2004). The ΔV_K-band can also occur as due to an increase of the functional PS II antenna size (Strasser et al., 2004). The greatest effect was apparent in the WWO_3 test plants, which points at the protective properties associated with drought-induced stomatal closure occurring in the DSO_3 test plants. It has to be emphasized that although the effect of O_3 on the DSO_3 test plants was ameliorated, a prominent ~~Δ~~ V_K-band nevertheless appeared

So called ΔV_I-bands were also apparent between 2 ms and F_M (**Figure 4.14 – right**). A distinctive positive ΔV_I-band appeared in both the O_3-treated test plants. According to Schansker *et al.* (2006), fluorescence changes in the I-P phase may provide information on the inactivation state of ferredoxin $NADP^+$ reductase (FNR) and possible accumulation of end electron acceptors such as NADPH and Fd (red). The more inactive FNR is, the longer it takes to fully reduce the Q_A pool and reach F_m. The inhibition of the reduction of end electron explains the decrease observed in J_{max} and CE in the WWO_3 and DSO_3 test plants obtained from the CO_2-response curves.

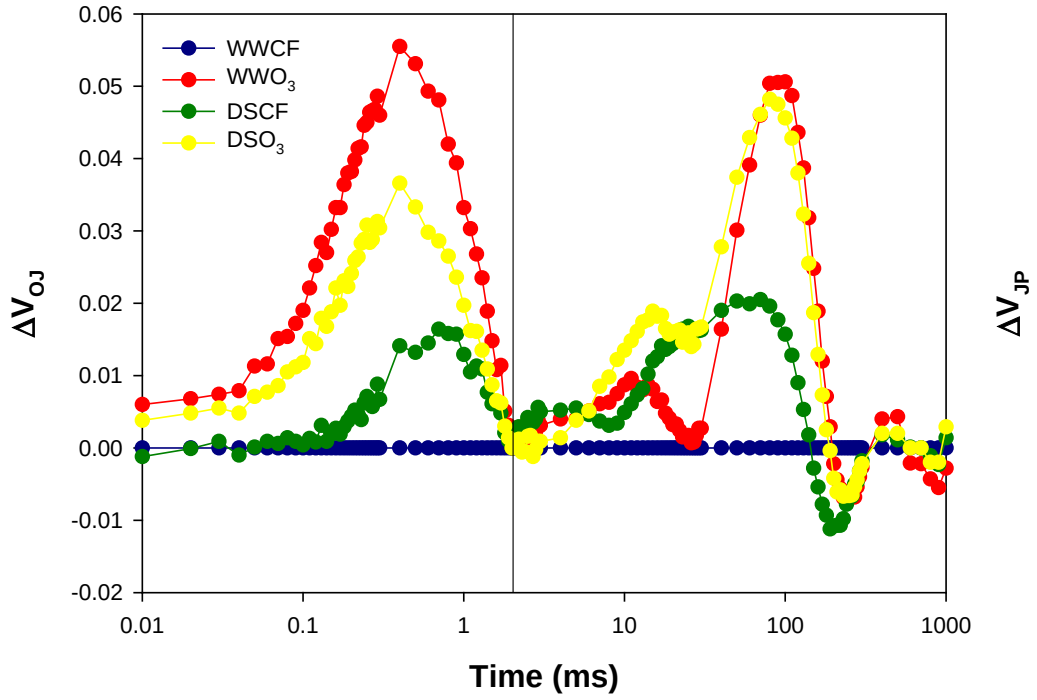

Figure 4.14: Difference in relative variable chlorophyll *a* fluorescence transients ($\Delta V = V_{treatment} - V_{control}$) of well watered (WW) and drought stressed (DS) leaves of *Pisum sativum* plants exposed to 80 nmolmol^{-1} ozone (AO_3) for 30 days respectively (expressed as V = f(t)) normalised between fluorescence extremes F_O (50 µs) and F_J (2 ms) as well as between F_J (2 ms) and F_P to obtain theΔV_{O-J} and ΔV_{J-P} curves. ΔV_K and ΔV_I bands are indicated. Each point represents the average of 48 measurements.

The performance index ($PI_{ABS,total}$) which is a multiparametric expression taking into consideration four independent parameters, namely efficiency of absorbtion of light energy (RC/ABS) (reaction centre density), quantum efficiency of trapping of excitation energy [φ_{Po} / (1- φ_{Po})], conversion of trapped excitation energy to electron transport [ψ_0 / (1- ψ_0)] and the probability for reduction of end electron acceptors [δ_0 / (1- δ_0)] (e.g. Fd) is the most sensitive parameter for detection and quantification of most stresses (Strasser *et al*., 1999; Smit *et al*., 2008). Under stress conditions the $PI_{ABS,total}$ of dark-adapted intact leaves, which indicates partial "potentials" for energy conservation is closely related to the final outcome of the plants activity, such as growth or survival. $PI_{ABS,total}$ is the most sensitive parameter of the JIP-test (Yusuf *et al*., 2010). After 1 week of fumigation with 80 nmol.mol^{-1} O_3 in the absence of drought stress no significant decreases in $PI_{ABS,total}$ were observed. At week 2, decreases in the $PI_{ABS,total}$

values of both O_3-treated test plants (WWO_3 and DSO_3) were observed. At this stage a statistically highly significant decrease of 24 % ($p < 0.01$) was observed in the WWO_3 test plants. After 21 days (week 3) of O_3 fumigation and 6 days of drought stress the DSCF showed a statistically non-significant decrease of 12 %. The $PI_{ABS,total}$ of the DSO_3 test plants showed a significant ($p < 0.05$) 24 % decrease, while a highly significant ($p < 0.01$) decrease of 42 % was observed in the WWO_3 test plants. This large difference in $PI_{ABS,total}$ between the DSO_3 and WWO_3 test plants could largely be attributed to the decrease in stomatal conductance, which led to a concomitant decrease in O_3 influx. After 4 weeks from onset of fumigation the $PI_{ABS,total}$ of the DSCF plants was still unaffected with a non-significant decrease of 5 %. A highly significant decrease ($p < 0.01$) of 27 % and 30 % occurred in both O_3 treated test plants (WWO_3 and DSO_3). From **Figure 4.14** it can be seen that a significant ($p < 0.05$) decrease of 24 % occurred after 5 weeks of fumigation in the DSCF test plants. It is important to note that these plants were only subjected to 20 days of drought treatment. The $PI_{ABS,total}$ of the WWO_3 and DSO_3 test plants decreased by 35 % and 31 %, respectively.

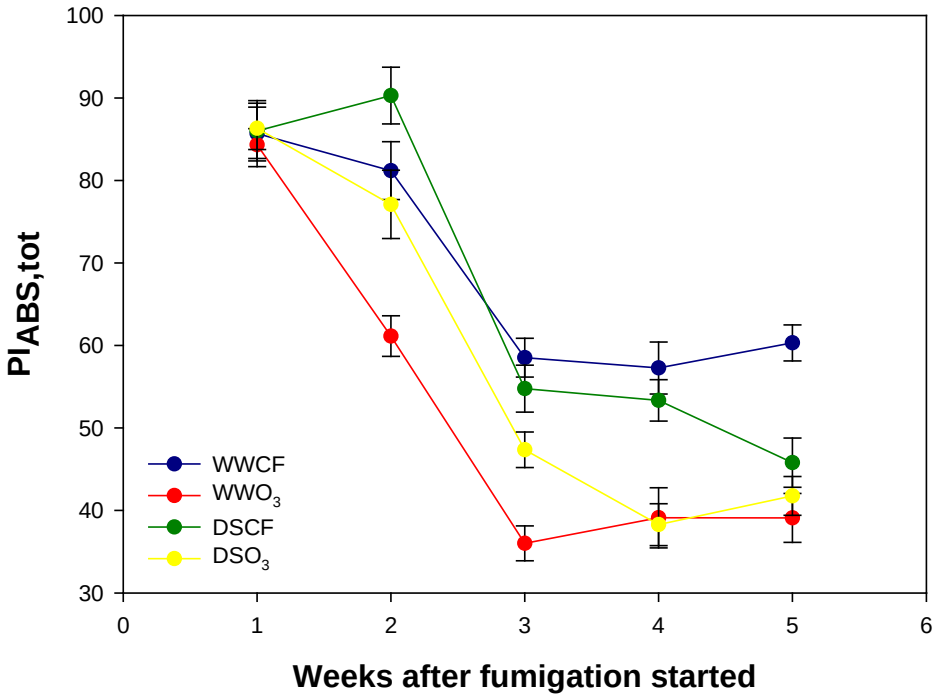

Figure 4.15: Performance index ($PI_{ABS,tot}$) measured after 7, 14, 21, 28 and 35 days exposure to filtered air (CF) and 80 nmolmol^{-1} ozone (AO_3) respectively

4.3.2 Effect of O_3 on photosynthetic gas exchange of *Pisum sativum*

Various gas exchange parameters were calculated from the A:Ci response curves to illucidate the physiological basis of the inhibition of CO_2 assimilation (**Table 4.1**). All the measurements were done on the same leaf on the respective differently treated plants. After 15 days of fumigation with CF air and 80 nmol.mol^{-1} O_3, and before drought stress was induced, the rate of CO_2 assimilation at C_a = 370 µmol.mol^{-1} (A_{370}) of the WWO_3 and DSO_3 plants decreased by 35 % and 25 % ($p < 0.05$), respectively. The A:Ci response curves of the two O_3 treatments (WWO_3 and DSO_3) were affected similarly (**Figure 4.16**). The carboxylation efficiency (CE; slope of the A:C_i response curve) displayed a decrease, although statistically not significant, of 12 % and 14 % in the WWO_3 and DSO_3 test plants respectively. This decrease in CE is attributed to a decrease in Rubisco activity which also resulted in the increase in the compensation concentration (Γ). The Γ of the WWO_3 and DSO_3 treatments increased by 29 % and 19 %, respectively, when compared to that of the control WWCF (**Table 4.1**). The Γ increase of the WWO_3 was statistically significant and strongly points at O_3-induced mesophyll limitation of CO_2 assimilation. The elevated O_3 concentration also caused a 16 % and 20 % decrease in A_0 (assimilation rate at C_i = 370 µmol.mol^{-1}) of the WWO_3 and DSO_3 test plants, respectively. This decrease was, however, not statistically significant. The concentration of CO_2 around the photosynthesising cells within the leaf i.e. C_i, depends on the concentration at the leaf surface and the stomatal conductance (Gs) to CO_2 (Jarvis & Sanford, 1986). In our data the decrease in stomatal conductance (Gs_{370}) of the WWO_3 and DSO_3 plants of 58 % ($p < 0.01$) and 36 % ($p < 0.05$), respectively, as well as the concomitant decrease in (C_{i370}) by 15 % and 11%, respectively, however shows evidence of stomatal limitation. The decrease in stomatal conductance (Gs) corresponded to the corresponding increase in the stomatal limitation (ℓ) calculated (**Table 4.1**). The maximum rate of CO_2 assimilation (J_{max}) of the WWO_3 and DSO_3 plants decreased by 14 % and 13 %, respectively. This inhibition of J_{max} could be ascribed to the decrease in the regeneration capacity of RuBP, once again pointing at mesophyll limitation. Our data thus shows that the O_3-induced decrease in A_{370} was a result of mesophyll and stomatal limitation. The water use efficiency (WUE) of the WWO_3 and DSO_3 plants remained fairly similar to that of the WWCF control plants due to similar decreases in A_{370} and E_{370}. E_{370} of the WWO_3 and DSO_3 plants decreased by 42 % ($p < 0.05$) and 28 % ($p < 0.05$) in comparison with to WWCF plants.

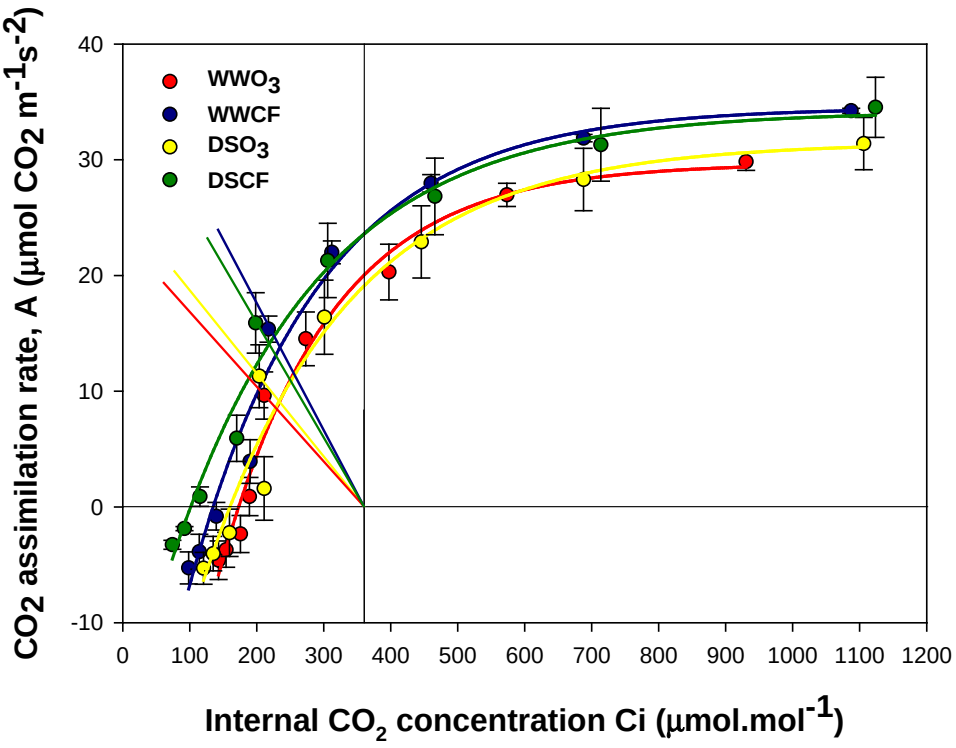

Figure 4.16: Average CO_2 (A:Ci) response curves i.e. assimilation rate (A) as a function of intercellular CO_2 concentration measured on intact leaves of *Pisum sativum* test plants after 15 days exposure to filtered air (CF) and 80 nmolmol^{-1} ozone (AO_3) respectively, before induction of drought. Each value represents a mean (± SE) where n = 4.

Table 4.1: Mean values (± standard errors) of photosynthetic gas exchange parameters of leaves of *Pisum sativum* (n = 4 plants per treatment) 15 days after exposure to filtered air (CF) and 80 nmol.mol^{-1} ozone (AO_3) respectively before induction of drought. Symbols: E_{370}, transpiration rate at Ca = 370 mmol.m^{-2}.s^{-1}; A_{370}, rate of CO_2 assimilation at C_a = 370 µmol.mol^{-1}; Ci_{370}, intercellular CO_2 concentration at Ca = 370 µmol.mol^{-1}; A_0, rate of CO_2 assimilation at C_i = 370 µmol.mol^{-1};Gs_{370}, stomatal conductance at Ca = 370 µmol.mol^{-1}; CE, carboxylation efficiency at Γ; J_{max}, minimum rate of CO_2 assimilation; Γ, CO_2 compensation concentration; ℓ, percentage stomatal limitation of photosynthesis; WUE, water use efficiency, with * and ** indicating significant differences at p<0.05 and p<0.01, respectively, compared to the control plants (WWCF).

	WWCF	WWO_3	DSCF	DSO_3
E_{370} (mmol.m^{-2}.s^{-1})	4.06 (0.39)	2.34 (0.41*)	4.0 (0.99)	2.91 (0.7*)
A_{370} (µmol.m^{-2}.s^{-1})	14.96 (1.42)	9.6 (2.07*)	15.56 (2.99)	11.26 (2.74*)
Ci_{370} (µmol.mol^{-1})	223.0 (6.11)	194 (8.54)	201 (17.07)	201.66 (17.07)
A_0 (µmol.m^{-2}.s^{-1})	23.46 (1.98)	20.1 (1.43)	23.46 (2.07)	19.5 (1.82)
Gs_{370} (µmol.m^{-2}.s^{-1})	307.66 (54.18)	127.33 (27.83*)	277 (46.17)	197 (84.52)
CE mol.m^{-2}.S^{-1})	0.10 (0.002)	0.089 (0.003)	0.090 (0.002)	0.087 (0.003)
Jmax (µmol.m^{-2}.s^{-1})	34.23 (0.60)	29.83 (1.58)	34.43 (1.92)	29.66 (2.17)
Γ (µmol.mol^{-1})	134.6 (5.64)	173.2 (6.35**)	101.8 (4.57)	159.9 (2.78)
ℓ (%)	36.06	52.23	33.78	41
WUE (µmol.mmol.$^{-1}$)	3.58 (0.03)	4.01 (0.28)	3.99 (0.22)	3.83 (0.05)

Gas exchange was also measured and the parameters calculated after 30 days of fumigation with 0 and 80 nmolmol^{-1} O_3 and 15 days of concomitant drought stress. It was evident from the A:Ci response curves of *Pisum sativum* (**Figure 4.17**) that the CO_2 assimilation rate at C_i = 370 µmol.mol^{-1} (A_0) of the WWO_3 test plants decreased substantially and significantly by 36 %. The combination between drought- and O_3 stress lead to a highly significant decrease of 51 % in A_0 of the DSO_3 test plants. This drastic decrease was also observed in the rate of CO_2 assimilation at

C_a = 370 µmol.mol^{-1} (A_{370}), showing a 35 % and 25 % decrease in (A_{370}) of the WWO_3 and DSO_3 test plants, respectively. The carboxylation efficiency (CE; slope of the A:C_i response curve at $C_i \leq 200$ µmol.mol^{-1}) displayed a highly significant decrease of 34 % and 41 % of the O_3 treated test plants (WWO_3 and DSO_3, respectively). This decrease in CE may be attributed to a decrease in Rubisco activity and this decrease also corroborated the increase in compensation concentration (Γ). The compensation point (Γ) of the respected treated plants increased when compared to the WWCF test plants. The Γ of the WWO_3 and DSCF treatments increased significantly by 19 % and 21 %, respectively, when compared to that of the control WWCF (**Table 4.2**). The Γ of the DSO_3 treatment increased drastically with a highly significant increase of 32 %, which strongly points at mesophyll limitation. Short-term stress generally seems to affect the regeneration of RuBP, possibly by distrupting electron transport, whereas long-term stress also affects Rubisco activity, and possibly also the balance between the PCR and PCO cycles (Jarvis & Sanford, 1986). As a result of the drought induced stress, a highly significant decrease in stomatal conductance was observed in both the drought stress test plants, with a 53 % and 59 % decrease in the DSCF and DSO_3 test plants, respectively. Although significant, a much less pronounced stomatal conductance decrease of 40 % was evident in the WWO_3 test plants. Singh *et al*. (2009), working on *Glycine max* exposed to the same O_3 concentration, observed similar, although not as pronounced reductions in stomatal conductance. Exactly the same trend was also observed in the Scanning Electron Microscopy **(Figure 4.5)**. The decrease in stomatal conductance (Gs) corresponded to the concomitant increase in the stomatal limitation (*l*) (**Table 4.2**). A significant decrease of 31 % and 23 % occurred in the maximum rate of CO_2 assimilation (J_{max}) of the WWO_3 and DSCF test plants, respectively. Although the DSO_3 test plants did not differ that much from the WWO_3 test plants with respect to the decrease in J_{max}, a highly significant decrease was observed in the DSO_3 test plants when compared to the control. The reduction in the J_{max} of the two O_3-treated test plants suggests that O_3 had an inhibitory effect on the regeneration capacity of RuBP. Although working on a non related species (*Quercus mongolica*), Wang *et al*. (2008, reported a similar decrease of 22 % in J_{max}, fumigated with exactly the same O_3 concentration (80 nmol.mol^{-1}) and exposure time (9 hours). The water use efficiency (WUE) of the two drought stress treatments, namely DSCF and DSO_3 plants increased by 21 % and 6 % respectively. This was mainly due to the decrease is stomatal conductance. With this increase in stomatal resistance a concomitant decrease in transpiration rate (E)

occurred, with a 28 %, 45 % decrease and a significant decrease of 47 % in the WWO_3, DSO_3 and DSCF test plants, respectively.

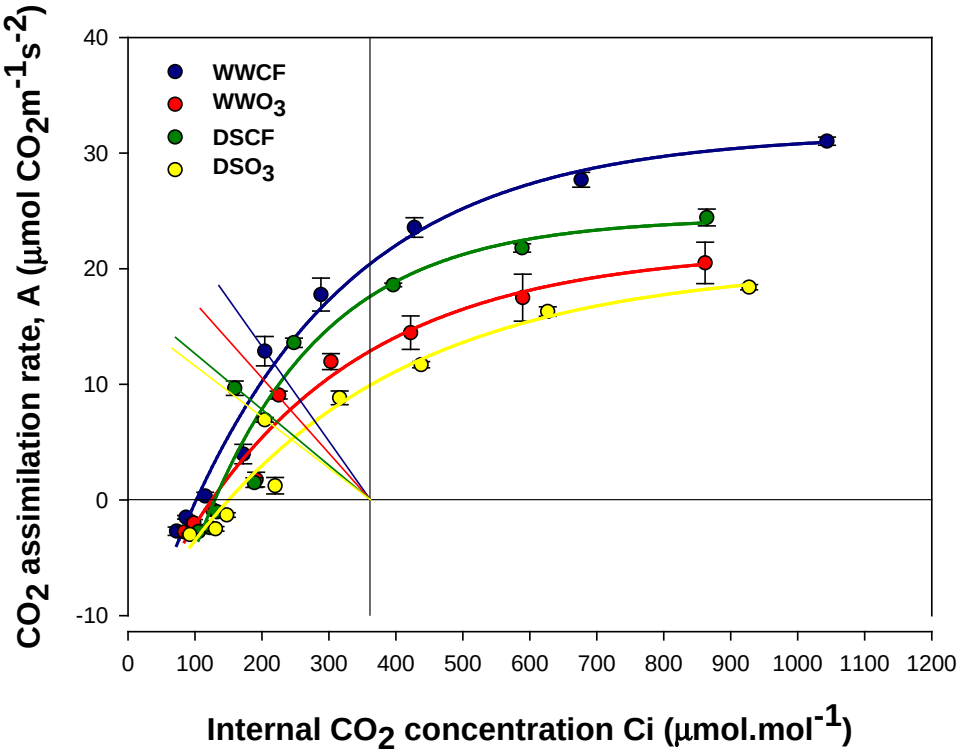

Figure 4.17: Average CO_2 response curves i.e. A:Ci response curves (assimilation rate (A) as a function of intercellular CO_2 concentration) of well watered (WW) and drought stressed (DS) leaves of *Pisum sativum* after 30 days exposure to filtered air (CF) and 80 nmolmol^{-1} ozone (AO_3) respectively. Each value represents a mean (± SE) where n = 4.

Table 4.2: Mean values (± standard errors) of photosynthetic gas exchange parameters of leaves of *Pisum sativum* (n = 4 plants per treatment) 30 days after exposure to filtered air (CF) and 80 nmol.mol^{-1} ozone (AO_3) respectively. Symbols: E_{370}, transpiration rate at Ca = 370 mmol.m^{-2}.s^{-1}, A_{370}, rate of CO_2 assimilation at C_a = 370 µmol.mol^{-1}; Ci_{370}, intercellular CO_2 concentration at Ca = 370 µmol.mol^{-1}; A_0, rate of CO_2 assimilation at C_i = 370 µmol.mol^{-1}; Gs_{370}, stomatal conductance at Ca = 370 µmol.mol^{-1}; CE, carboxylation efficiency at Γ; J_{max}, minimum rate of CO_2 assimilation; Γ, CO_2 compensation concentration; ℓ, percentage stomatal limitation of photosynthesis; WUE, water use efficiency, with * and ** indicating significant differences at p<0.05 and p<0.01, respectively, compared to the control plants (WWCF).

	WWCF	WWO_3	DSCF	DSO_3
E (mmol.m^{-2}.s^{-1})	3.32 (0.81)	2.4 (0.01)	1.75 (0.26*)	1.81 (0.06)
A_{370} (µmol.m^{-2}.s^{-1})	12.36 (1.52)	9.03 (0.37)	9.46 (0.94)	7.06 (0.20*)
Ci_{370} (µmol.mol^{-1})	191.33 (20.62)	209 (4.33)	153.33 (9.26)	200.66 (8.41)
A_0 (µmol.m^{-2}.s^{-1})	20.3 (1.41)	12.9 (1.21*)	17.5 (1.51)	9.93 (0.77**)
Gs_{370} (µmol.m^{-2}.s^{-1})	223.66 (85.69)	132.66 (1.33*)	104 (18.47**)	92.33 (8.18**)
CE mol.m^{-2}.S^{-1})	0.086 (0.002)	0.056 (0.003**)	0.083 (0.002)	0.050 (0.003**)
Jmax (µmol.m^{-2}.s^{-1})	29.66 (0.52)	20.4 (1.99*)	22.63 (2.25*)	19.56 (1.23**)
Γ (µmol.mol^{-1})	101.6 (4.17)	125.5 (8.75*)	128.5 (5.08*)	150.1 (13.99**)
ℓ (%)	39.41	55.73	53.37	28.9
WUE (µmol.mmol.$^{-1}$)	3.72 (0.10)	3.75 (0.17)	4.7 (0.18)	3.94 (0.03)

The relationship between stomatal conductance (G_s), transpiration (E) and CO_2 assimilation (A_{360}) of the different treatments are shown (**Figure 4.18**). Note that with a decrease in stomatal conductance, i.e. an increase in stomatal resistance, a decrease in transpiration and CO_2 assimilation occurs. After 30 days of fumigation with 80 nmol.mol^{-1} O_3 and 15 days of drought stress the effect of the different treatments observed. The relative combination of O_3 and drought to the decrease in A_{370}, E_{370} is clearly shown.

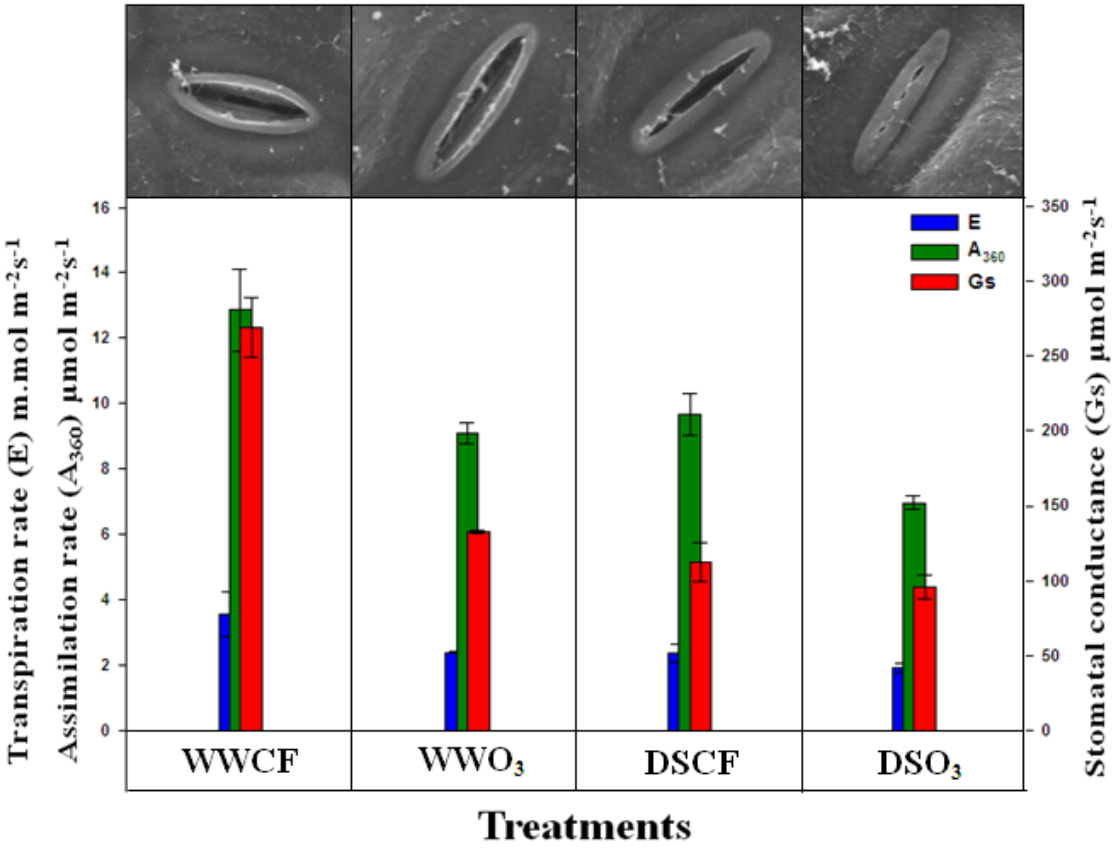

Figure 4.18: The effect of O_3 and O_3 in combination with co-stress drought, on CO_2 assimilation (A_{360}), transpiration rate (E) and stomatal conductance (G_s). Scanning electronmicrograph of the stomata corresponding to each of the treatments are shown.

4.4 Effect of O_3 on *in vitro* Rubisco activity in *Pisum sativum*

After 30 days of fumigation with 80 nmol.mol^{-1} O_3 and 15 days of concomitant drought treatment, the Rubisco activity in all of the treatments decreased when compared to the control (WWCF) (**Figure 4.19**)**.** The activity of Rubisco activase was determined by measuring the activation state (initial activity) of Rubisco. This measurement provides a valid estimate of the photosynthetic activity of the leaf because the activation state of Rubisco in the light is a direct consequence of the activity of Rubisco activase (Walker & Osmond, 1986). The total activity displays the activity of the fully carbamylated Rubisco. Although statistically non-significant ($p > 0.05$), the initial Rubisco activity of the DSCF test plants, calculated on a leaf basis, decreased by 19 %. A significant reduction ($p < 0.05$), of 33 % and 35 % in initial Rubisco activity was observed in the WWO_3 and DSO_3 test plants, respectively. A similar reduction was observed in the total Rubisco activity, with a non-significant reduction of 18 % occurring in the DSCF test plants. The two O_3-treated test plants, WWO_3 and DSO_3, showed a highly significant ($p < 0.01$) reduction of 31 % and 39 %, respectively. Not much is known about the response of Rubisco to drought stress, as different studies have produced conflicting results. Giménez *et al*. (1992) and Gunasekera & Berkowitz (1993), working on sunflower and tobacco, respectively, found little effect of drought on Rubisco. On the other hand Majumdar *et al*. (1991), found rapid and very early decreases in Rubisco activity in response to drought stress in soybeans. A decrease in Rubisco content is most likely to explain the decline in the rate of carboxylation (Pell *et al*., 1992; Pell *et al*., 1997). According to Mehta *et al*. (1992) the degradation of Rubisco as a result of O_3 stress can be attributed to the susceptibility of Rubisco to oxidative stress (ROS), which could explain the rapid decrease of 35 % and 25 % observed in A_{370} (CO_2 response curve: **Figure 4.16**) of the WWO_3 and DSO_3 test plants, respectively. It should be emphasised that the effect of O_3 on the activity Ribusco vary between species. However in general, it is acknowledged that Ribusco is a central target for O_3 adverse effects (Dizengremel, 2001). The decrease in initial Rubisco activity and total Rubisco activity in the WWO_3 and DSO_3 plants correspond to the decrease in CE and J_{max} for the same treatments determined through gas analyses.

.

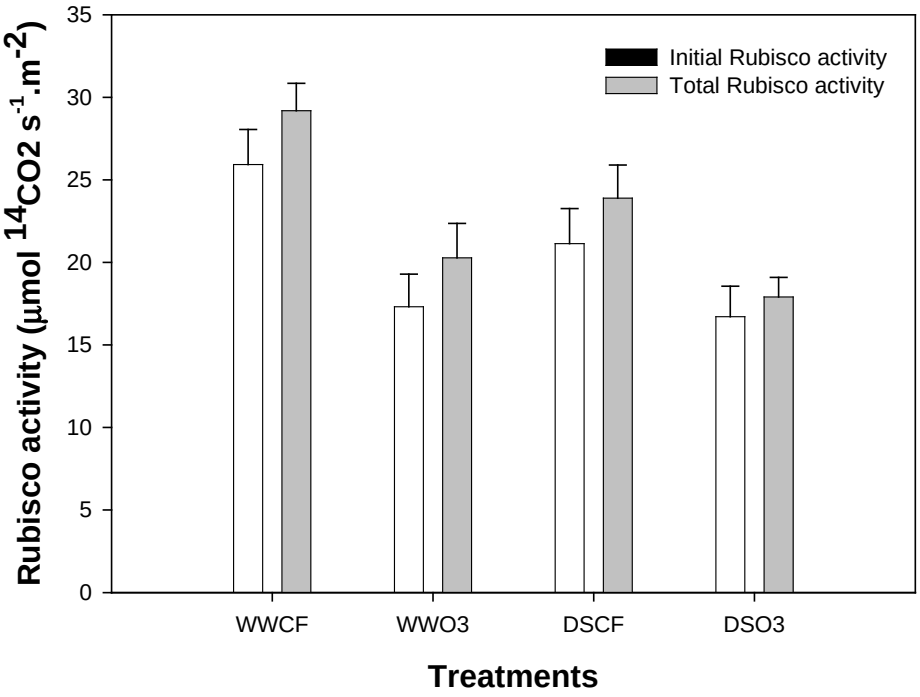

Figure 4.19 Initial (black bars) and total (grey bars) Rubisco activity measured in *Pisum sativum* after 30 days exposure to 80 nmol.mol^{-1} O_3 and 15 days of drought stress.

4.5 Effect of O_3 on chlorophyll content index (CCI) in *Pisum sativum*

Although no visual chlorosis occurred on the leaves at any time during the treatments, decreases in measured chlorophyll content index (CCI) values were observed (**Figure 4.20**). After 15 days of 80 nmol.mol^{-1} O_3 treatment, in the absence of drought stress, no significant differences in all of the treatments were observed when compared to the WWCF control plants. After 25 days of 80 nmol.mol^{-1} O_3 fumigation and 10 days of drought stress treatment, a significant decrease in CCI was observed in both the O_3 treated plants. The CCI values of the WWO_3 and DSO_3 test plants decreased by 9 % and 10 % respectively. Virtually no difference was observed in the DSCF test plants. After 35 days of 80 nmol.mol^{-1} O_3 fumigation and 20 days of drought stress treatment the CCI of all treatments decreased substantially, with a highly significant decrease occuring in the two O_3 treated plants and a significant decrease in the CFDS plants. Exposure to O_3 results in a reduction in chlorophyll content (Reigh, 1983). The CCI values of the WWO_3, DSO_3 and CFDS decreased by 33 %, 27 % and 16 %, respectively. The latter finding supports the fluorescence data excellently, explaining the decrease in $PI_{ABS,total}$ values as a result of a

decrease in the total amount of chlorophyll molecules per cross section (ABS/CS). A decrease in chlorophyll concentration results in less light energy absorbed per cross-section (CS) resulting in impairment of photosynthesis.

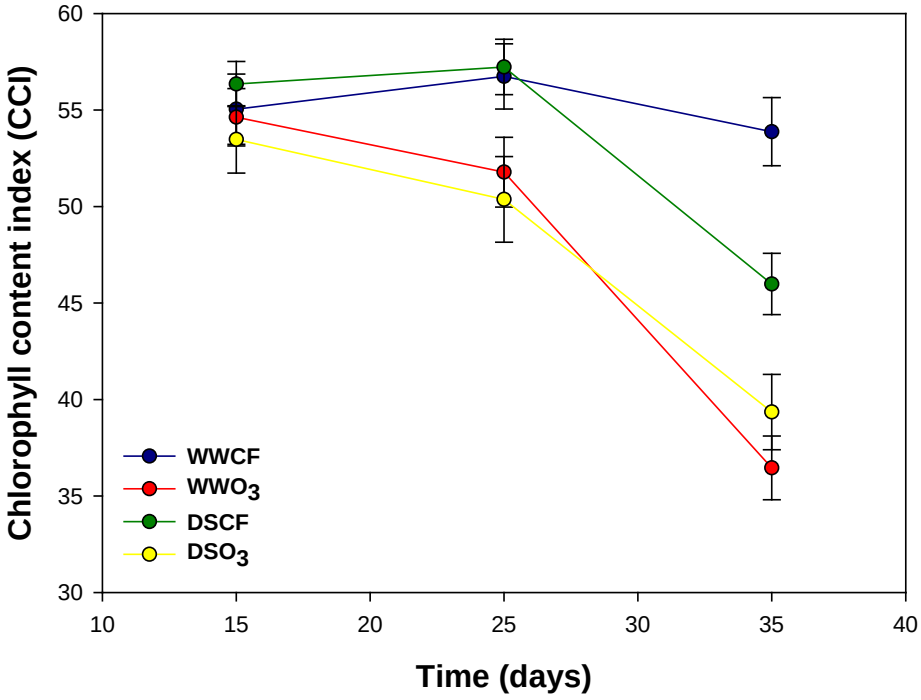

Figure 4.20: Average chlorophyll content index for leaves of *Pisum sativum* after 15, 25 and 35 days exposure to filtered air (CF) and 80 nmolmol^{-1} ozone (AO_3) respectively.

4.6 Effect of O_3 on Antioxidant metabolism

4.6.1 H_2O_2 content in leaves of *Pisum sativum*

After 20 days from onset of O_3 fumigation the WWO_3, DSCF and DSO_3 test plants showed a significant ($p < 0.05$) increase of 23, 40 and 31% in H_2O_2 concentration when compared to the WWCF test plants (**Figure 4.21**). The drought stressed plants at this point were only subjected to 5 days of drought treatment. The much higher H_2O_2 concentration in the two drought stressed plants (DSCF and DSO_3) are most likely caused by water stress through the action of abscisic

acid (ABA), which caused an increase in cytosolic Ca^{2+} concentration through H_2O_2-activated Ca^{2+} channels and from release from intracellular stores (Price *et al*., 1994; McAinish *et al*., 1996; Chen *et al*., 2003). ABA causes an increase in H_2O_2 production, which acts as a signaling intermediate in guard cells to promote stomatal closure (Price *et al*., 1994; McAinish *et al*., 1996; Murata *et al*., 2001; Chen *et al*., 2003). A similar trend occurred after 30 days of fumigation with O_3 and 15 days of concomitant drought stress. The H_2O_2 concentration of the WWO_3, DSCF and DSO_3 test plants increased by 30, 18 and 32 %, respectively, with the increases in the two O_3 treated plants (WWO_3 and DSO_3) being significant ($p < 0.05$). The lower H_2O_2 concentration in the DSCF plants after 30 days from onset of O_3 treatment (15 days drought stress) is most probably due to the higher levels of POD (**Figure 4.22**) as POD acts on H_2O_2. In general the H_2O_2 accumulation was more evident in the plants exposed to O_3 due to a lower turnover rate as a result of a slower response to excess H_2O_2 (Willekens *et al*., 1997).

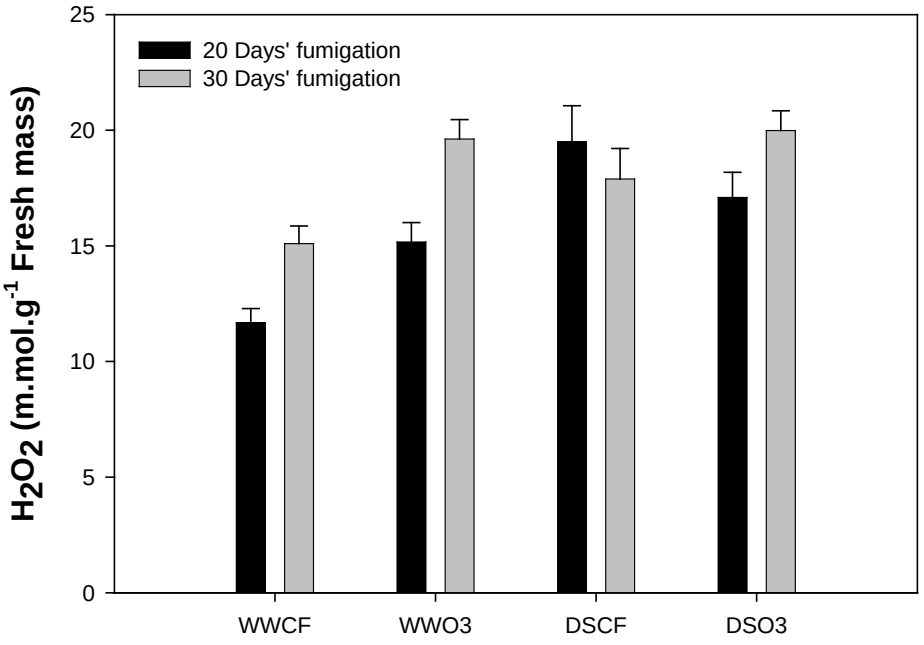

Figure 4.21: The concentration of H_2O_2 in leaves of *Pisum sativum* after 20 and 30 days exposure to filtered air (CF) and 80 nmolmol^{-1} ozone (AO_3) respectively.

4.6.2 POD concentration in leaves of *Pisum sativum*

After 20 days from onset of O_3 fumigation the WWO_3, DSCF and DSO_3 test plants showed a non-significant increase of 9, 23 and 10% in peroxidase activity when compared to the WWCF test plants (**Figure 4.19**). Peroxidase activity has been reported as an early response to O_3 stress (Curtis *et al*., 1976; Manes *et al*., 1990). The drought stressed treatments (DSCF, DSO_3) at this point in time were only subjected to 5 days of drought treatment. Drought stress leads to the formation of H_2O_2 (Mittler & Zilinskas, 1994), which can be detoxified via peroxidases, occurring throughout the cell having a high affinity for H_2O_2 (Jiménez *et al*., 1997). The two drought stressed treatments (DSCF and DSO_3), even though subjected to the same water regime, showed a significant difference in POD activity when compared to each other. The most likely explanation for the higher activity in the DSCF test plants could be due to the fact that the POD activity in the DSO_3 test plants reached its maximal activity under O_3-stress and that the additional drought stress caused the POD activity to steadily decline. After 30 days from onset of O_3 fumigation the WWO_3 and DSO_3 test plants showed a highly significant ($p < 0.01$) increase in POD activity of 40 and 41 %, respectively, when compared to that of the control. A significant increase ($p < 0.05$) in POD activity also occurred in the DSCF test plants. From this data it is clearly demonstrated that O_3 in combination with drought stress, does not have any additional influence on the POD activity. This finding can be confusing, as drought stress ameliorates the effect of O_3, however there is evidence that drought stress leads to an increase in the production of free radicals in leaves (Badiani *et al*., 1990; Quartacci and Navari-Izzo, 1992; Kronfuβ *et al*., 1998).

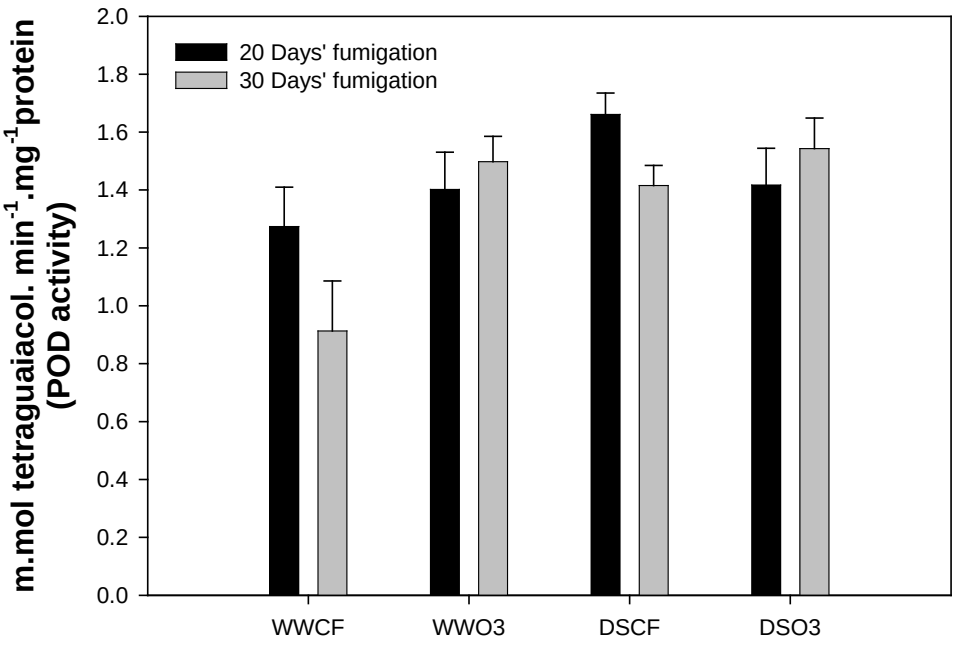

Figure 4.22: Effect of O_3 and drought stress, singly- or combined on the peroxidase activity after 30 days from onset of fumigation and 15 days of drought stress.

5. Synthesis and Conclusion

5.1 Studying ozone impacts in OTCs

The biological effects of O_3 on plants have been studied for more than 50 years (Brennan *et al*., 1969). The effect of O_3 on crops, include visible injury and changes in growth, biomass allocation, yield, reproduction and vitality, as have been reported by numerous studies. This study has contributed in resolving the physiological and biochemical effect of O_3 on photosynthesis. The data presented and discussed in Chapter 3, showed that O_3, even at moderately low concentration of 80 nmol.mol^{-1}, have pronounced effects on photosynthesis and growth of the O_3 sensitive genotype of *Phaseolus vulgaris* (S156) and *Pisum sativum* and in some cases without concomitant visual symptoms. Both crops showed a similar response regarding the decrease in photosynthetic rate. By interpreting the CO_2 gas exchange and chlorophyll a fluorescence induction kinetics data measured in parallel, we could explain the basis of O_3 constraints on the test plants. Open-top chambers may alter some aspects of plant growth, but as noted in the 1996 O_3 AQCD (U.S. Environmental Protection Agency, 1996), evidence from the comparative studies of OTCs done by Olszyk *et al*. (1986) suggested that, since significant differences were found for fewer than 10 % of the growth parameters measured, the responses were, in general, essentially the same regardless of exposure system used and chamber effects did not significantly affect responses. Heagle *et al*. (1988) concluded: "Although chamber effects on yield are common, there are no results showing that this will result in a change in yield response to O_3. The available evidence thus suggests that chamber effects do not fundamentally alter the responses of plants to O_3 and OTCs can be used as a useful tool for testing species sensitivity, studying the physiological basis of responses and developing O_3-response relationships.

5.2 Growth and development

5.2.1 *Phaseolus vulgaris*

In *Phaseolus vulgaris* the O_3 treatment applied affected the growth height negatively. This observation was also reflected by biomass and yield data.

Growth of the S156 genotype of *P. vulgaris* subjected to 80 nmol.mol^{-1} O_3 (AO_3S) was suppressed and after 35 days of fumigation a marked effect was evident. Visible damage appeared after 12 days. Burkley *et al*. (2005) observed similar symptoms in the same genotype fumigated at 48 nmol.mol^{-1} in OTCs. The R123 genotype of our experiment, treated at the same O_3 concentration as the S156 genotype however showed much less severe symptoms, which were restricted to older leaves.

5.2.2 *Pisum sativum*

Although no leaf damage was visible in the case of the *Pisum sativum* test plants, a noticeable decrease in growth height occurred in all treated plants after 40 days of treatment when compared to the well watered carbon filtered WWCF (control) test plants. The decrease in growth was also reflected by the final biomass.

5.3 Biomass

Biomass production of *Pisum sativum* decreased in all the experimental plants when compared to the control (WWCF). The well watered, O_3-treated (WWO_3) and drought-stressed, O_3-treated (DSO_3) test plants showed a significant and very similar decrease in shoot dry mass of 23 % and 24 %, respectively. It was expected that the drought co-stress in the DSO_3 test plants would have lead to a larger decrease in biomass when compared to the drought stressed carbon filtered (DSCF) test plants (which showed a 12 % decrease). This was however not the case and must be attributed to closure in stomata in the drought stressed plants that ameliorated some of the harmful effects of O_3. Thus the hypothesis set about the decrease in stomatal conductance due to drought stress could be proved by this investigation.

The elevated O_3 concentration affected root mass negatively showing a significant decrease of 37 % for WWO_3 and a non-significant decrease of 23 % for DSO_3 relative to the CFWW treatment. Sanz *et al.* (2005) reported an up to a 45 % reduction in root biomass of *Trifolium subterraneum* after O_3 exposure in open-top chambers. The decrease in root mass may mainly be ascribed to a decrease in carbon translocation to roots and retaining photosynthate in shoots possibly for injury repair (Blum *et al*., 1983; Grantz *et al*., 2006; Guidi *et al*., 2009). Both treatments of the drought stressed test plants (DSCF and DSO_3), when compared to their respective well watered parallels (WWCF and WWO_3) showed a moderate increase in root biomass, although not statistically significant. The drought stressed induced increase in root biomass in our data correspond to data obtained by Merrill *et al*. (2002) on *Glycine max*. This extra investment in root biomass production could provide a mechanism to ensure better acquisition of mineral nutrients and water to maintain photosynthesis during drought stress periods (Deepak & Agrawal, 2001).

5.4 Yield

The reduction in yield of O_3 sensitive *Phaseolus vulgaris* genotype (S156) in our study was also reported in previous studies. Brunschön-Harti *et al*. (1995) found a 56 % reduction in final pod mass when the S156 genotype was exposed to 9 hours mean O_3 concentration as low as 32 $nmol.mol^{-1}$. Tingey *et al*. (2002), also reported a 57 % reduction in pod dry weight of the S156 genotype exposed to 75.7 $nmol.mol^{-1}$ O_3 for 8 hours daily. In the present study we found that the S156 genotype suffered a highly significant decrease of 58 % in final pod weight relative to the CFR test plants. Therefore, the O_3-induced yield reduction found was quantitatively consistent with findings of previous studies (Burkley & Eason, 2002; Heagle *et al*., 2002; Burkley *et al*., 2005; Flowers *et al*., 2007). Greater sensitivity of S156 in our experiments, may be due to germplasm differences or other differences in experimental set-up and protocols. The resistant genotype, R123, which previously had been characterised as tolerant to O_3 in our study was found to be moderately sensitive to 80 $nmol.mol^{-1}$ O_3, with a highly significant decrease of 32 % in seed yield, compared to the CFR control plants. The huge decrease in both the O_3 treated genotypes (AO_3S and AO_3R) was due to the decrease in total number of pods and number of seeds per pod in the test plants. Both these parameters contributed to the final decrease in yield. Reduction in final biomass can often be attributed to a lower CO_2 assimilation rate, which proved

to be the case in the S156 genotype (57 % decrease in A_{370}). A recent meta-analysis done on *Glycine max*, exposed to elevated O_3 concentrations of 70 nmol.mol^{-1}, revealed that the percentage decrease in carbon assimilation was the same as the percentage decrease in yield loss (Morgan *et al*., 2003). With the present study the latter finding was corroborated by our data showing a 57 % decrease in biomass and a 57 % decrease in CO_2 assimilation rate. Although the R123 genotype showed no decrease in CO_2 assimilation rate, the seed yield was however lower.

5.5 Chlorophyll content

Exposure to O_3 reduced the chlorophyll content index (CCI) of *Phaseolus vulgaris* and *Pisum sativum.* The CCI of the S156 *Phaseolus vulgaris* genotype exposed to elevated O_3 concentration of 80 nmol.mol^{-1} for 35 days, decreased by a significant 24 % compared to the CFR plants. The CCI of the R123 genotype exposed to the same O_3 concentration however increased significantly, i.e. by 19 %. Not much work has been done on the effect of O_3 on chlorophyll content of *Phaseolus vulgaris.* This higher CCI value maintained by the AO_3R test plants may be the reason for the resistant properties as the amount of solar radiation absorbed by a leaf is largely a function of the foliar concentration of photosynthetic pigments. Reduced concentrations of chlorophyll can directly limit photosynthetic potential and hence primary production (Curran *et al*., 1990; Filella *et al*., 1995). Singh *et al*. (2009), working with *Glycine max* found a significant positive correlation between chlorophyll content and photosynthesis. The above finding corresponds well with the 10 % decrease in RC/CS_0 obtained from the fluorescence parameters measured.

Although no visual O_3 effect, such as chlorotic damage, could be detected on *Pisum sativum* test plants, a decrease in the chlorophyll content index (CCI) values was observed. After 15 days of fumigation at 80 nmol.mol^{-1} O_3, no significant differences in CCI in any of the treatments were observed with respect to the control (WWCF). Drought treatment commenced after 15 days of fumigation. After 25 days of fumigation, including 10 days of drought, no effect on the CCI values could be detected in the CFDS test plants. At this point in time, CCI values of WWO_3 and DSO_3 test plants decreased by 9 % and 10 % respectively. Virtually no difference in CCI was observed in the DSCF test plants when compared to the WWCF test plants. After 35 days of O_3

treatment including 20 days of drought stress, the CCI values of all the treatments decreased significantly. The CCI value of the CFDS test plants decreased by 16 % whereas the decrease in the DSO_3 test plants was as high as 27 %. On the other hand the WWO_3 test plants which were only subjected to O_3-stress, showed the largest decrease in CCI, namely 33 %. The reduction in chlorophyll content due to the elevated O_3 concentration is in accordance with findings made by Heagle *et al*., (1994) on white clover. It is known that although O_3 can hardly reach the chloroplast, the oxidative stress (ROS) induced by O_3, apparently has effects on the photosynthetic apparatus particularly at the membrane level (Heath, 1994a). This includes oxidation of the chloroplast pigments.

5.6 Photosynthesis

5.6.1 Photosynthesis of *Phaseolus vulgaris*

Results of this study convincingly demonstrated that the physiological and biochemical inhibition of photosynthesis in the S156 and R123 *Phaseolus vulgaris* genotypes, are located at different sites within the chloroplasts, as indicated in the schematic presentation shown in **Figure 5.1.** Inhibition of photosynthesis by O_3 in the S156 genotype could mainly be ascribed to mesophyll limitation, i.e. constraints on PS II function, photosynthetic electron transport, reduction of end electron acceptors such as NADPH and the key Calvin-Benson cycle enzyme, Rubisco. The physiological and biochemical basis of O_3 inhibition of photosynthesis in the *Phaseolus vulgaris* genotypes used and the possible sites of inhibition, are discussed with reference to the experimental data and the scheme presented in **Figure 5.1.**

1. In the S156 genotype, the stomatal conductance decreased (i.e. stomatal resistance increased) upon fumigation at 80 $nmol.mol^{-1}$ O_3, resulting in less CO_2 entering the leaf, which limited the total carbon available for the plant for incorporation into starch and sugars.

   As the internal or mesophyll resistance to O_3 uptake is very low (Taylor *et al*., 1982; Laisk *et al*., 1989), the majority of the O_3 flux is controlled by the stomatal movements. Reich & Amundson (1985) argued that species with higher stomatal conductances were more affected by O_3. Temple (1990) on the other hand found that

conductances were relatively uniform in tomato and that there was no relationship between maximum conductance and the resistance of the cultivars to O_3. The majority of reports however found that O_3 induces stomatal closure (Darrall, 1989; Heath, 1994b; Singh *et al*., 2009). Various studies (Reigh & Amundson, 1985; Reigh, 1987; Farage *et al.*, 1991) argue that the lower stomatal conductance is caused by a decrease in CO_2 assimilation and hence an increase in C_i.

The high stomatal limitation (ℓ) of 37 % occurring in the AO_3S plants in our study, suggests that O_3 may have had a direct effect on the guard cells, potentially through changes in intra- and extracellular calcium concentration, resulting in stomatal closure rather than as a result of effects on photosynthesis (Moldau *et al*., 1990; McAinsh *et al*., 2002). As the stomata are at the point of entry of O_3 and thus exposed to the highest concentration (Heath, 1994a).

2. In the S156 genotype the carboxylation efficiency (CE) decreased by a highly significant 75 % when compared to the CFR control plants. Thus reduction in CE and the concomitant highly significant reduction (57 %) in CO_2 assimilation rate (A_{370}), indicate that substantial non-stomatal (mesophyll) limitation of photosynthesis occurred in S156. The decrease in CE may be attributed to the direct oxidative stress on the enzymes of the Calvin-Benson cycle or to indirect effect caused by membrane disorders (Gian *et al*., 1998). Our data show that the ozone-induced decrease in CE in the S156 genotype was partially due to a decrease in the activity and/or concentration of Rubisco. Von Caemmerer & Farquhar (1981) presented evidence that CE is also dependent on the regeneration of RuBP (ribulose 1:5 bisphosphate). The regeneration of RuBP is furthermore dependent on reducing equivalent from the light reactions (see point 4 and 5 below). Studies of Pell *et al*., (1992) and Pell *et al*., (1997) on O_3 effects on ribulose bisphosphate carboxylase/oxygenase also showed that a decrease in Rubisco activity (such as in our AO_3S plants) was responsible for a decrease in CE and A_{370}. Thus the hypothesis with regards to the activity of RuBP is thus proven.

3. The reduction in the maximum CO_2 assimilation rate (J_{max}) in the S156 genotype decreased by a highly significant 61 % compared to the CFR control plants. The J_{max}

is a measure of the regeneration capacity of RuBP (Farquhar & Sharkey, 1982). The reduction in J_{max} is usually limited by the supply of NADPH and ATP and therefore dependant on electron transport capacity of the leaf. Farquhar *et al*. (1980) have linked RuBP regeneration to electron transport. This finding explains the concomitant substantial decrease in CE in S156.

4. Analysis of the normalised fluorescence curves of the S156 genotype support the gas exchange data and revealed a hidden positive ΔV_K-band. The ΔV_K-band is probably due to the short-lived accumulation of reduced electron carriers, most possibly Pheo-, which, in turn, is caused by the dissociation of the OEC (oxygen evolving complex), resulting in an imbalance between the electron flow from the OEC to the RC and towards the acceptor side of PS II in the direction of PS I (Strasser, 1997; De Ronde *et al*., 2004). The ΔV_K-band can also occur as a result of an increase of the functional PSII antenna size (Strasser *et al*., 2004). The uncoupling of the OEC from PS II disrupts electron flow in the photosynthetic electron transport chain, resulting in decrease in the quantity of NADPH and ATP formed. This inhibited the linear electron transport capacity and formation of reducing equivalents, which corresponds to the decrease in CE and RuBP regeneration capacity as well as to the increase in Γ.

5. The appearance of a dominant positive ΔV_I-band in the ΔV chlorophyll *a* fluorescence transient of the O_3-treated S156 genotype relative to its control suggested that the main inhibition in this case might be located further down from the reduced intersystem electron acceptors of the photosynthetic electron transport chain near PS I and end-electron acceptors. The appearance of a positive ΔV_I-band points at a decrease in the activation state of ferredoxin $NADP^+$ reductase (FNR) and a possible accumulation of end electron acceptors such as Fd (red) and NADPH (Tsimilli-Michael & Strasser, 2008; Yordanov *et al*., 2008). Due to the high energy demand for the regeneration of RuBP the latter inhibition and subsequent reduction in end electron acceptors (NADPH) may well be responsible for the reduction in RuBP regeneration (Hopkins & Hüner, 2004) in O_3-stressed S156. No positive ΔV_I band

occurred in the R123 genotype exposed to elevated O_3, which points out the resistant properties of this genotype.

Our data show that the O_3 sensitivity of S156 is mainly due to a weakness of the photosynthetic apparatus and electron transport chain. Especially PS II function, including the OEC, proved to be very vulnerable. With respect to the O_3 sensitivity of S156, our data is in accordance with the contention that the main protein of PS II CD1 is easily disrupted (Grotjohann *et al*., 2004). R123 has a superior O_3 tolerance probably due to a much more stable PS II structure. Thus the aim was met regarding as to why the resistant genotype is more tolerant to elevated O_3.

5.6.2 Photosynthesis of *Pisum sativum*: O_3 and drought interaction

Although no visible O_3 damage was observed on the leaves of *Pisum sativum*, photosynthesis was largely inhibited. This observation stresses the notion that physiological strain in plants is an important early indicator of O_3 injury.

A decrease in stomatal conductance of O_3 fumigated *Pisum sativum* plants acted as protective measure to minimise entry of O_3 into plants. Drought stress resulted in lower stomatal conductance and lower O_3 influx into the leaves, though at the same time impeding entry of much needed CO_2, drought stress partly protected the plants from the harmful effects of O_3. This reasoning is in accordance with the findings of Dobson *et al*., 1990; Fincher & Alscher, 1992; Freer-Smith *et al*., 1989; Havranek & Wieser, 1993; Wieser and McKee *et al*., 1997, which all demonstrated that withholding water reduces stomatal conductance.

It has frequently not been clear whether the effect of O_3 acts directly upon the stomata, or whether photosynthetic CO_2 uptake is reduced so that substomatal CO_2 concentration rises and stomatal closure then occurring in consequence. Farage *et al.* (1991), concluded that, in the early stages of treatment, O_3 exerted some direct effects on the stomata, but later the primary action of the pollutant was on the carboxylation efficiency (CE) within the mesophyll. Matyssek & Sandermann (2003), have suggested that carbon gain was less limited by reduced stomatal conductance than by the decline in capacity for CO_2 fixation in the mesophyll. These data,

together with our results, suggest that effects of O_3 on the stomata and gas exchange are very complex. Our data strongly suggests that the primary action of O_3 was on PS II function and photosynthetic electron transport. The duration of exposure to the pollutant, and the environmental conditions, may alter the nature of the response.

From the data presented in Chapter 4 on the effect of O_3 on fast phase chlorophyll *a* fluorescence kinetics, it is apparent that photosynthesis in *Pisum sativum* plants was markedly affected by O_3 at different sites within the chloroplast. The well watered and drought stressed O_3-treated test plants behaved similarly with regard to inhibition of the electron transport chain. Since drought stress alone induced similar responses by the defense system against oxidative stress as O_3 did, the results suggest that O_3 applied prior to drought stress may have had a ”hardening effect” against drought stress, enabling the plants to cope with the additional stress better. This finding corresponded to the findings of Kronfuß *et al*. (1998). According to our data, the stomata played an important role in protecting the drought stressed plants against oxidative O_3, but at the same time it also restricts CO_2 entering the leaf leading to reduced photosynthesis. The proposed sites of inhibition discussed below are numbered in **Figure 5.1** with reference to the experimental data and the scheme represented in **Figure 5.1.**

1. After 15 days of O_3 treatment in the absence of drought stress, the stomatal conductance of the *Pisum sativum* test plants exposed to 80 ppb O_3 (WWO_3 and DSO_3), decreased. According to Moldau *et al*. (1990) and McAinsh *et al*. (2002), this decrease was solely attributed to the direct O_3-induced effect on the guard cells. Despite the slight stomatal closure and concomitant decrease in E, the water use efficiency (WUE) was almost unaffected because A_{370} was equally affected. After 30 days of O_3 treatment, a change in the effect on the stomatal mechanism could be detected, due to the 15 days of drought stress treatment. Both the drought treated test plants (DSCF and DSO_3) showed a highly significant decrease in stomatal conductance, which corresponded to the scanning electron micrographs (SEM) taken in parallel revealing marked closure of the stomatal aperture. Drought stress thus had the largest influence on closure of the stomata, resulting in a decrease of the O_3 flux into the leaves. The effect of O_3 on stomatal conductance can vary from stomatal closure (Mansfield, 1998; McAinsh *et al*., 2002) to increased stomatal conductance

(Barnes *et al*., 1990; Grulke *et al*., 2007). The present study showed that O_3 led to a significant decrease in stomatal conductance in the WWO_3 test plants. The decrease was however not as prominent as in the case of the drought treated test plants. The cause of this stomatal closure was possibly not related to dysfunctional guard cells, but rather caused by a decrease in photosynthesis and increase in C_i (Farage *et al*., 1991).

2. In the well watered-, drought stressed O_3-treated *Pisum sativum* plants a decline in A_{370} could have been related to a reduction in carboxylation efficiency (CE). The CE of the WWO_3 and DSO_3 test plants decreased drastically by 34 % and 41 %, with respect to the control. Since the carboxylation efficiency corresponds directly to the Rubisco activity, the marked effect of O_3 on CE found in this experiment, could have resulted from a decrease in either the amount or the activity of Rubisco. Our data corresponds with the findings of Farage *et al*. (1991), namely that stomatal closure is predominantly secondary to a loss of carboxylation efficiency and that a decline in A_{370} is a function of both stomatal conductance and carboxylation efficiency. According to Ort *et al*. (1994) and Cornic & Massacci (1996), stomatal closure was generally accepted to be the main determinant for decreased photosynthesis under mild to moderate drought. However, evidence has been accumulating that shows that Rubisco activity is impaired under drought stress (Medrano *et al*., 1997; Medrano *et al*., 2002). The CE of the drought DSCF test plants did not decrease, which indicates that the 37 % decrease in A_{370} could mainly be attributed to the decrease in stomatal conductance and not to mesophyll limitations.

3. The reduction in the maximum CO_2 assimilation rate (J_{max}) of the well watered- and drought stressed-O_3 treated test plants decreased significantly. The J_{max} indicates the maximum electron transport capacity and the regeneration capacity of RuBP (Farquhar & Sharkey, 1982). This reduction in J_{max} of the WWO_3 and DSO_3 (31 and 34 %) test plants, shows that the production of ATP and NADPH required for the regeneration of RuBP, was severely affected. This notion is further corroborated by the fluorescence data measured in parallel, which revealed constraints in the

photosynthetic electron transport chain resulting in a decrease in the production of end-electron acceptors such as NADPH, necessary to promote glyceraldehyde–3–phosphate dehydrogenase and ATP needed by phosphoglycerate kinase and Ribulose–5–phosphate kinase. Although the carboxylation efficiency of the DSCF test plants was not affected, the J_{max} showed a significant decrease. Decreased capacity for RuBP regeneration has been shown to be an early response to drought stress, decreasing much earlier than CE (von Caemmerer & Farquhar, 1984; Escalona *et al*., 1999). It is still not well understood why RuBP regeneration decreases under water stress, but Tezara *et al*. (1999), have suggested that decreased ATP synthesis through ATPase impairment would lead to reduced RuBP regeneration.

From all the discussed data regarding CO_2-gas exchange, it is clear that drought stress ameliorates the total effect that O_3 has on the photosynthetic ability of the *Pisum sativum* test plants. It is however, more complicated since drought stress itself has an effect on the photosynthesis of plants. In the present study the drought effect as a stress factor was not as severe as the effect of O_3, but with a more severe drought effect the outcome may be different.

4. In depth analysis of the chlorophyll fluorescence transients by obtaining the difference in variable fluorescence transients between treatments and controls, revealed positive ΔV_K-bands occurring in all of the treated plants after 30 days of O_3-fumigation and 15 days of drought stress. The ΔV_K-band (50 µs – 2 ms) is probably due to the short-lived accumulation of reduced electron carriers such as Pheo-, which, in turn, is caused by the dissociation of the OEC (oxygen evolving complex), resulting in an imbalance between the electron flow from the OEC to the RC and towards the acceptor side of PS II in the direction of PS I (Strasser, 1997). The greatest effect was apparent in the WWO_3 test plants, which again points at the protective properties associated with drought-induced stomatal closure. Although not completely protected against O_3, some amelioration of the negative effect occurred.

5. A second, so calledΔ V_I-band appeared in the region between 2 ms and F_m, which indicates inhibition of reduction of end electron acceptors such as NADPH (Tsimilli-

Michael & Strasser, 2008; Yordanov *et al*., 2008). This band was particularly prominent, and remarkably similar in the two O_3-treated test plants (WWO_3 and DSO_3), which explains the marked decrease in J_{max} and CE in the WWO_3 and DSO_3 test plants.

5.7 Antioxidative metabolism

Increasing evidence suggests that some antioxidant systems of plants act as important tolerance mechanisms against O_3 and drought stress. Increases in cytosolic and apoplastic peroxidase activity (POD) in response to O_3 are often observed, but the reasons and outcomes of these changes have yet to be fully explained and understood. Increased POD activity is frequently correlated with O_3 injury. Enhanced POD activities have been associated with induced resistance of plants to drought stress (Ruiz-Lozano, 2003). Tingey *et al*. (1975) observed a 35 % decrease in POD activity of soybeans immediately following O_3 exposure; however, within 24 to 48 h, activity have increased significantly and was above the control level and remained there throughout the remainder of the study. In our *Pisum sativum* study, a drastic increase of 40 and 41 % was observed in the POD activity in the WWO_3 and DSO_3 test plants, respectively. This was mainly due to the 30 and 32 % increase in H_2O_2 concentration within the leaves of the WWO_3 and DSO_3 test plants. It is this increase in ROS (H_2O_2) which diffuses in al cellular compartments and reacts with constituents, leading to damages to the physiological and biochemical reactions in absence of visible symptoms of injury.

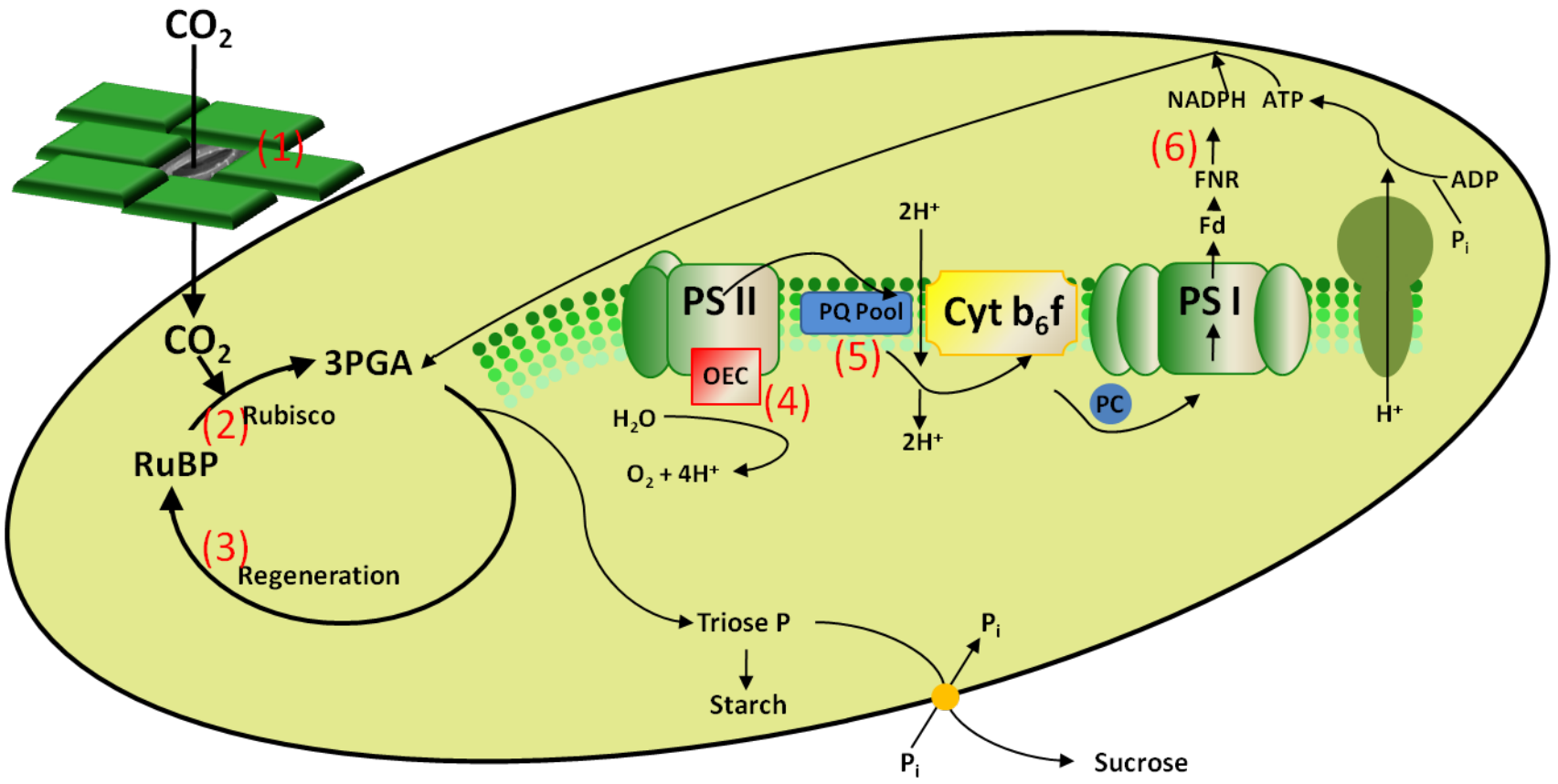

1. **Stomatal conductance**
2. **Inhibition of Rubisco**
3. **Maximum electron transport rate/regeneration capacity of RuBP**
4. **Inhibition or uncoupling of the OEC**
5. **Inhibition of the intersystem e^- transport chain**
6. **Reduction of end electron acceptors**

4.8 Future perspectives

In conclusion, this study demonstrated that elevated O_3 levels of 80 nmol.mol^{-1} affected the physiology of the two plants immensely. Although the aims of this study were reached, there is still an urgent requirement for further field-based studies, which include open-top studies, to assess the impact of O_3 under local agricultural conditions in southern Africa. This will enable the development of guidelines which are appropriate for crops of the developing world and may lead to more resistant cultivars.

Recommendations for possible practical application and future research, based on the results of this study, include the following:

- In South-Africa, air pollutant emission standards have not been established for agricultural regions. Since drastic effects were found at moderately low O_3 concentration of 80 nmol.mol^{-1}, the use of different lower concentrations will enable us to determine the actual thresholds of affects on these two crops.
- We only commenced measuring the peroxidase activity (POD) and H_2O_2 concentration after 20 days of O_3 exposure. Since the antioxidant system in biological systems are seen as an early response to oxidative stress. Therefore to better understand the antioxidant system a more detailed study is needed monitoring POD activity and H_2O_2 levels from onset of fumigation.
- By using the JIP-test as rapid diagnostic tool for assessing and screening O_3 tolerance in various genotypes, recommendations could be made regarding the selection of genotypes for cultivation in particular regions where tropospheric O_3 levels are high.

References

Adams, R.M., Glyer, J.D., McCarl, B.A., 1988. The NCLAN economic assessment: approaches and findings and implications. [In:] Heck, W.W., Taylor, O.C., Tingey, D.T., (eds.), Assessment of Crop Loss from Air Pollutants. Elsevier, London, pp. 473-504.

Agrawal, M. 2005. Effects of air pollution on agriculture: An issue of national concern. National Academy of Sciences, India. 28. 93-106.

Agrawal, M., Singh, B., Rajput, M., Marshall, F., Bell, J.N.B., 2003. Effect of air pollution on periurban agriculture: A case study. Environmental Pollution. 126: 323-329.

Anon, 2005. Ozone Monitor. Operational Manual. 2B Technologies, Inc. p 28.

Anon, 2009. Effects of Ozone Air Pollution on Plants. USDA, Agricultural Research Service. (Web:) www.usda.gov/ Date of access 29 June 2009.

Ashmore, M.R., 2005. Assessing the future global impacts of ozone on vegetation. Plant, Cell and Environment. 28: 949-964.

Ashmore, M.R., Bell, J.N.B., 1991. The role of ozone in global change. Annals of Botany. 67: 39-48.

Ashmore, M.R., Marshall, F.M., 1999. Ozone impacts on agriculture: an issue of global concern. Advances in Botanical Research. 29: 32-49.

Ashmore, M.R., Wilson, R.B., 1994. Critical levels of air pollution for Europe. Proceedings of a workshop. Egham, UK, March 1992. Creative Press, Reeding, UK.

Badiani, M., Debiasi, M.G., Artemi, F., 1990. Catalase, peroxidase and superoxide dismutase activities in seedlings submitted to increasing water deficit. Agrochimia. 34: 90-102.

Barnes, J.D., Eamus, J.D., Davison, A.W., Ro-Poulsen, H., Mortensen, L., 1990. Persistent effects of ozone on needle water-loss and wettability in Norway Spruce. Environmental Pollution. 63: 345-363.

Bell, J.N.B., Treshow, M., 2002. Introduction. [In:] Bell, J.N.B., Treshow, M., eds. Air Pollution and Plant Life. 2nd ed. John Wiley & Sons, West Sussex, UK. p.23-41.

Bender, J., Weigel, H.J., 2002. Ozone stress impacts on plant life. [In:] Ambasht, R.S., Ambasht, N.K., eds. Modern trends in applied terrestrial ecology. Kluwer Academic Publishers, New York. 369pp.

Bergmeyer, H.U., 1974. Methods of Enzymatic Analysis 2nd edition. Academic Press, New York. pp 1468-1472.

Bernacchi, C.J., Leakey, A.D.B., Heady, L.E., Morgan, P.G., Dohleman, F.G., McGrath, J.M., Gillespie, K.M., Wittig, V.E., Rogers, A., Long, S.P., Ort, D.R., 2006. Hourly and seasonal variation in photosynthesis and stomatal conductance of soybean grown at future CO_2 and ozone concentrations for 3 years under fully open-air field conditions. Plant, Cell and Environment. 29: 2077-2090.

Black, V.J., Black, C.R., Roberts, J.A., Steward, C.A., 2000. Impact of ozone on the reproductive development of plants. New Phytologist. 147: 421-447.

Blum, U., Mrozek, E., Johnson, E. 1983. Investigation of ozone (O3) effects on 14C distribution in ladino clover. Environmental and Experimental Botany. 23: 369-378.

Bolhar-Nordenkampf, H.R., Öquist, G., 1993. Chlorophyll fluorescence as a tool in photosynthesis research. [In:] Hall, D.O., Scurlock, J.M.O., Bolhàr-Nordenkampf, H.R., Leegood, R.C., Long, S.P. eds. Photosynthesis and Production in a Changing Environment. Chapman & Hall, London. p464.

Botha, A.T., Moore, L.D., Visser, J.H., 1990. *Gladiolus* and bean plants as biomonitors of air pollution impacts in the Cape Town area. Proceedings of the First IUAPPA Regional Conference on Air Pollution: Towards the 21st Century. 24-26 October 1990. Pretoria. Vol 1, paper 18.

Bradford, M.M., 1976. A rapid and sensitive method for the quantification of microgram quantities of protein utilizing the principle of protein dye binding. Analytical Biochemistry. 72: 248-254.

Brennan, T., Frenkel, C., 1977. Involvement of hydrogen peroxide in the regulation of senescence in pear. Plant Physiology. 59: 411-416.

Brennan, P.C., Fritz, T.E., Flynn, R.J. 1965. Pasteurella pneumotropica: cultural and biochemical characteristics and its association with disease in laboratory animals. Laboratory Animal Care. 15: 307-312.

Brunschön-Harti, S., Fangmeier, A., Jäger, H.J. 1995. Influence of ozone and ethylenediurea (EDU) on growth and yield of bean (Phaseolus vulgaris L.) in open-top field chambers. Environmental Pollution. 90: 89-94.

Buckland, S.M., Price, A.H., Hendry, G.A.F., 1991. The role of ascorbate in drought-treated *Cochlearia atlantica* Pobed. and *Armeria maritime* (Mill.) Willd. New Phytologist. 119: 155-160

Buckenham AH, Parry MA, Whittingham CP, Young AT (1981). An improved open-topped chamber for pollution studies on crop growth. Environmental Pollution, (Ser. B), 2: 475-82.

Burkley, K.O., Eason, G., 2002. Ozone tolerance in snap bean is associated with elevated ascorbic acid in the leaf apoplast. Plant Physiology. 114: 387-394.

Burkley, K.O., Miller, J.E., Fiscus, E.L., 2005. Assessment of ambient ozone effects on vegetation using snap bean as a bioindicator species. Journal of Environmental Quality. 34: 1081-1086.

Castagna, A., Ranieri, A., 2009. Detoxification and repair process of ozone injury: From O_3 uptake to gene expression adjustment. Environmental Pollution. 157: 1461-1469.

Chameides, W.L., 1989. The chemistry of ozone deposition on plant leaves: role of ascorbic acid. Environmental Sciences and Technology. 23: 595-600.

Chameides, W.L., Kasibhata, P.S., Yienger, J., Levy, H., 1994. Growth of continental-scale metro-plexes, regional pollution and world food production. Science. 264: 74-77.

Chen, Z., Young, T.E., Ling, J., Chang, S-C., Gallie, D.R., 2003. Increasing vitamin C content of plants through enhanced ascorbate recycling. Proceedings of the National Academy of Sciences, USA. 100: 3525-3530.

Convile, R.N., 2002. Emissions, dispersion and atmospheric transformation. [In]: Bell, J.N.B., Treshow, M., (eds.) Air Pollution and Plant Life. 2nd ed., John Wiley & Sons, West Sussex, UK. p.23-41.

Cope, W.G., 2010. Exposure classes, toxicants in air, water, soil, domestic and occupational settings. [In]: Hodgson, E., (eds.) Textbook of modern toxicology. 4th ed. John Wiley & Sons Hoboken, New Jersey.

Cornic, G., Massacci, A. 1996. Leaf photosynthesis under drought stress. [In:] Baker, N.R. eds. Photosynthesis and the environment. The Netherlands, Kluwer Academic Publishers.

Crutzen, P.J. 1975. Physical and chemical processes which control the production, destruction, and distribution of ozone and some other chemically active minor constituents. GARP Publications Series 16, World Meterological Organization, Geneva, Switzerland

Curran, P.J., Dungan, J.L., Gholz, H.L. 1990. Exploring the relationship between reflectance red edge and chlorophyll content in slash pine. Tree Physiology. 7: 33-48.

Curtis, C.R., Howell, R.K., Kremer, D.F., 1976. Soybean peroxidases from ozone injury. Environmental Pollution. 11: 189-194.

Darrall, N.M. 1989. The effect of air pollutants on physiological processes in plants. Plant, Cell and Environment. 12: 1-30.

De Ronde, J.A., Cress, W.A., Krüger, G.H.J., Strasser, R.J., van Staden, J., 2004. Photosynthetic response of transgenic soybean plants containing the Arabidopsis P5CR gene, during heat and drought stress. Journal of Plant Physiology. 161: 1211-1224.

Deepak, S.S., Agrawal, M. 2001. Influence of elevated CO2 on the sensitivity of two soybean cultivars to sulphur dioxide. Environmental and Experimental Botany. 46: 81-91.

Degl'Innocenti, E., Vaccà, C., Guidi, L., Soldatini, G.F., 2003. CO_2 photoassimilation and chlorophyll fluorescence in two clover species showing different response to O_3. Plant Physiology and Biochemistry. 41: 485-493.

Dizengremel, P. 2001. Effects of ozone on the carbon metabolism of forest trees. Plant Physiology and Biochemistry. 39:729-742.

Dobson, M.C., Taylor, G., Freer-Smith, P.H. 1990. The control of ozone uptake by *Picea abies* (L.) Karst. and *P. sitchensis* (Bong.) Carr. during drought and interacting effects on shoot water relations. New Phytologist. 116: 465-474.

Dunin, F.X., Greenwood, E.A.M., 1986. Evaluation of the ventilated chamber for measuring evaporation from a forest. Hydro. Proc. 1: 47-62.

Emberson, L.D 2003. Air pollution impacts on crops and forests: An Introduction. [In:] Emberson, L., Ashmore, M., Murray, F., eds. Air Pollution Impacts on Crops and Forests. Imperial College Press, London. p3-29.

Emberson, L.D., Agrawal, M., Wahid, A., Murray, F., Ashmore, M., Pleijel, H., 2003. Air pollution impacts on forests in developing countries. Environmental News. 9: 1-6.

Escalona, J.M., Flexas, J., Medrano, H. 1999. Stomatal and non-stomatal limitations of photosynthesis under water stress in field-grown grapevines. Australian Journal of Plant Physiology. 26: 421-433.Farage, P.K., Long, S.P., Lechner, E.G., Baker, N.R. 1991. The sequence of change within the photosynthetic apparatus of wheat following short term exposure to ozone. Plant Physiology. 95: 529-535.

Farquhar, G.D., Schulze, E-D., Küppers, M. 1980. Response to humidity by stomata of Nicotiana gluuca L. and Corylus avellana L. are consistent with the optimisation of carbon dioxide uptake with respect to water loss. Australian Journal of Plant Physiology. 7:315-327.

Farquhar, G.D., Sharkey, T.D., 1982. Stomatal concuctance and photosynthesis. Annual Review of Plant Physiology. 33: 317-345.

Farquhar, G.D., von Caemmere, S., Berry, J.A. 1980. A biochemical model of photosynthetic CO2 assimilation in leaves of C3 species. Planta. 149: 78-90.

Farquhar, G.D., von Caemmerer, S., 1980. Electron transport limitations on the CO2 assimilation rate of leaves: A model and some observations in Phaseolus vulgaris L. In: Abstracts of the Fifth International Congress on Photosynthesis, Hallkidiki (Greece), p 176.

Feister, U., Warmbt, W., 1985. Long-term measurements of surface ozone in German democratic republic. Journal of Atmospheric Chemistry. 5: 1-21.

Filella, I., Serrano, L., Serra, J., Peńuelas, J. 1995. Evaluating wheat nitrogen status with canopy reflectance indices and discriminant analysis. Crop Science. 35: 1400-1405.

Fincher, J., Alscher, R.G. 1992. The effect of long-term ozone exposure on injury in seedlings of red spruce (*Picea rubens* Sarg.). New Phytologist. 120: 49-59.

Fiscus, E.L., Booker, F.L., Burkey, K.O., 2005. Crop responses to ozone: uptake, models of action, carbon assimilation and partitioning. Plant, Cell and Environment. 28: 997-1011.

Flowers, M.D., Fiscus, E.L., Burkley, K.O., Booker, F.L., Dubois, J-J.B., 2007. Photosynthesis, chlorophyll fluorescence, and yield of snap bean (Phaseolus vulgaris L.) genotypes differing in sensitivity to ozone. Environmental and Experimental Botany. 61: 190-198.

Force, L., Critchley, C., van Rensen, J.J.S., 2003. New fluorescence parameters for monitoring photosynthesis in plants. Photosynthesis Research. 78: 111.

Fox, C. B. 1873. Ozone and Antozone, their history and natur. J. and A, Churchill, London, 329 pp.

Foyer, C.H., Descourvieres, P., Kunert, K.J., 1994. Protection against oxygen radicals: an important mechanism studied in transgenic plant. Plant, Cell and Environment. 17: 507-523.

Freer-Smith, P.H., Dobson, M., Taylor, G., 1989. Factors controlling the rates of O_3 uptake by spruce and beech. [In:] Bucher, J.B., Bucher-Wallin, I., eds. Air pollution and forest decline. Proceedings of the 14th international meeting for specialists in air pollution effects on forests ecosystems, IUFRO P2.05, Interlaken, Switzerland, 2-8 October 1988. EAFV, Birmensdorf, pp 407-409.

Fuhrer, J., Achermann, B., eds. 1994. Critical levels for ozone: a UNECE workshop report. FAC report 16. Liebefeld-Bern, Switzerland: Swiss Federal Research Station for Agricultural Chemistry and Environmental Hygiene.

Fuhrer, J., Booker, F., 2003. Ecological issues related to ozone: agricultural issues. Environment International. 29: 141-154.

Fuhrer, J., Sharby., Ashmore, M.R., 1997. Critical Levels of Ozone Effects on Vegetation in Europe. Environmental Pollution. 97: 91-106.

Fumagalli, I., Gimeno, B.S., Velissariou, D., De Temmerman, L., Mills, G., 2001. Evidence of ozone-induced adverse effects on crops in the Mediterranean region. Atmospheric Environment. 35: 2583-2587.

Fumagalli, I., Mignanego, L., Mills, G., 2003. Ozone biomonitoring with clover clones: yield loss and carryover effect under high ambient ozone levels in northern Italy. Agricultural Ecosystem Environment. 95: 119-128.

Gaspar, T., Penel, C., Thorpe, T., Greppin, H. 1982. Peroxidases 1970-1980. A survey of their biochemical and physiological roles in higher plants. University of Genéve, Switzerland.

Gian, F.S., Giacomo, L., Ferruccio, F., Cristina, N., Lucia, G. 1998. Photosynthesis of two polar clones under long-term exposure to ozone. Plant Physiology. 104: 707-712.

Giménez, C., Mitchell, V.J., Lawlor, D.W., 1992. Regulation of photosynthesis rate of two sunflower hybrids under water stress. Plant Physiology. 98: 516-524.

Grantz, D.A., Gunn, S., Vu, H-B. 2006. O3 impacts on plant development: a meta-analysis of root/shoot allocation and growth. Plant, Cell and Environment. 29: 1193-1209.

Grotjohann, I., Jolley, C., Fromme, P. 2004. Evolution of photosynthesis and oxygen evolution: Implication from structural comparisons of photosystem I and II. Phys. Chem. Phys. 6: 4743-4753.

Grulke, N.E., Neufeld, H.S., Daviso, A.W., Roberts, M., Chappelka, A,H., 2007. Stomatal behavior of ozone-sensitive and –insensitive coneflowers (*Rudbeckia laciniata* var. *digitata*) in Great Smoky Mountains National Park. New Phytologist. 173: 100-109.

Grünhage, L., Jäger, H.J., 1994. Influence of the atmospheric conductivity on the ozone exposure of plants under ambient conditions: considerations for establishing ozone standards to protect vegetation. Environmental Pollution. 85: 125-129.

Guiderian, R., Tingey, D.T., Rabe, R., 1985. Effects of photochemical oxidants in plants. [In:] Guderian, G., eds. Air pollution by photochemical oxidants. Springer, Berlin Heidelberg, pp 129-333.

Guidi, L., Degl'Innocenti, E., Martinelli, F., Piras, M. 2009. Ozone effects on carbon metabolism in sensitive and insensitive Phaseolus cultivars. Environmental and Experimental Botany. 66: 117-125.

Gunasekera, D., Berkowitz, G.A., 1993. Use of transgenic plants with ribulose-1,5-bisphosphate carboxylase oxygenase antisense DNA to evaluate the rate limitation of photosynthesis under water-stress. Plant Physiology. 103: 629-635.

Havranek, W.M., Wieser, G., 1993. Zur Ozontoleranz der Lärche (*Larix decidue* Mills.). Forstw Centralbl. 112: 56-64.

Heagle, A.S., Body, D.E., Heck, W.W., 1973. An open-top field chamber to assess the impact of air pollution on plants. Journal of Environmental Quality. 2: 365-372.

Heagle, A.S., Kress, L.W., Temple, P.J., Kohut, R.J., Miller, J.E., Heggestad, H.E. 1988. Factors influencing ozone dose-yield response relationships in open-top field chamber studies. [In:] Heck, W.W., Taylor, O.C., Tingey, D.T. eds. Assessment of crop loss from air pollutants: proceedings of an international conference; October, 1987; Releigh, NC; New York, NY: Elsevier Applied Science; pp. 141-179.

Heagle, A.S., Miller, J.E., Burkley, K.O., Eason, G., Pursly, W.A., 2002. Growth and yield responses of snap bean to mixtures of carbon dioxide and ozone. Journal of Environmental Quality. 31. 2008-2014.

Heagle, A.S., Miller, J.E., Sherril, D.E. 1994. A White clover system to estimate effects of tropospheric ozone on plants. Journal of Environmental Quality. 23: 613-621.

Heagle, A.S., Philbeck, R.B., Ferrel, R.E., Heck, W.W. 1989. Design and performance of large, field exposure chamber to measure effects of air quality on plants. Journal of Environmental Quality. 18: 361-368.

Heath, R.L. 1994a. Alteration of plant metabolism by ozone exposure. [In:] Alscher, R.G., Wellburn, A.R., eds. Plant response to the gaseous environment. Chapman and Hall, London, pp 121-145.

Heath, R.L. 1994b. Possible mechanisms for inhibition of photosynthesis by ozone. Photosynthesis Research. 39: 439-451.

Heyneke, E., Strauss, A.J., Strasser, R.J., Krüger, G.H.J. 2011. Open-top chamber facility to study air pollution impacts in South Africa. Part II: SO2-drought interactions on yield, photosynthesis and symbiotic nitrogen fixation on soybean. South African Journal of Plant and Soil. 4 (In press).

Holland, M., Kinghorn, S., Emberson, L., Cinderby, S., Ashmore, M., Mills, G.,Harmens, H., 2006. Development of a framework for probabilistic assessment of the economic losses caused by ozone damage to crops I Europe. Part of the UNECE International Cooperative Program on Vegetation. Contract Report EPG 1/2/205. CEH Project NO: C02309NEW. 49pp

Holland, M., Mills, G., Hayes, F., Buse, A., Emberson, L., Cambridge, H., Cinderby, S., Terry, A., Ashmore, M., 2002. Economic assessment of crop yield losses from ozone exposure. The UNECE International Cooperative Programme on Vegetation. Contract EPG1/3/170. Centre for Ecology and Hydrology and UK Department for Environment, Food and Rural Affairs.

Holmes, J.R., 1994. Estimated cost of ozone damage to California crops. Air Resources Board, California Environmental Protection Agency Research Notes, pp. 94-118.

Hopkins, W.G., Huner, N.P.A., 2004. Introduction to Plant Physiology 3rd ed. John Wiley & Sons, Inc. New York. p557

Hopkins, W.H., Hüner, N.P.A. 2004. Introduction to Plant Physiology 3rd edition. Wiley & Sons Inc. Hoboken. pp. 557.

Horsman, D.C., Wellburn, A.R., 1975. Synergistic effect of SO_2 and NO_2 polluted air upon enzyme activity in pea seedlings. Environmental Pollutant. 8: 123-133.

Horsman, D.C., Wellburn, A.R., 1977. Effects of SO_2 polluted air upon enzyme activity in plants originating from areas with different annual mean atmospheric SO_2 concentrations. Environmental Pollutant. 13: 33-39.

Houzeau, A. 1858. Preuve de la presence dans L' atmosphere dun nouveau principe gazeux 1'oxygéne naissant. Acadamy of Science. 46: 89-91.

Jarvis, P.G., Sandford, A.P., 1986. Temperate Forests. [In:] Baker, N.R., Long, S.P. eds. Photosymthesis in contrasting environments. Elsevier, Amsterdam, The Netherlands.

Jenkin, M.J., Clemitshaw, K.C., 2000. Ozone and other secondary photochemical pollutants: chemical processes governing their formation in the planetary boundary layer. Atmospheric Environment. 34: 2499-2527.

Jiménez, A., Hernández, J.A., Del Río, L.A., Sevilla, F., 1997. Evidence for the presence of the ascorbate-glutathione cycle in mitochondria and peroxisomes of pea (Pisum sativum) leaves. Plant Physiology. 114: 275-285.

Jones, H.G. 1983. Plants and Microclimate. Cambridge University Press, 323p.

Kangasjarvi, J., Jaspers, P., Kollist. H., 2005. Signaling and cell death in ozone-exposed plants. Plant, Cell and Environment. 28:1021-1036.

Kanofsky, J., Sima, P., 1991. Singlet oxygen production from the reaction of ozone with biological molecules. Journal of Biological Chemistry. 266: 9039-9042.

Kärenlampi, L., Sharby, L., (eds.) 1996. Critical levels for ozone in Europe: Testing and Finalising the Concepts. University of Kuopio, Finland. 363p.

Kautsky, H., Appel, W., Amann, H., 1960. Chlorophyllfluoreszenz und Kohlensäureassimilation. XIII. Die Fluoreszenzkurve und die Photochemie der Plflanze. Biochemische Zeitschrift. 332: 227-292.

Kautsky, H., Hirsch, A., 1934. Chlorophyllfluoreszenz und Kohlensäureassimilation. Das Fluoreszenzverhalten grüner Pflanzen. Biochemische Zeitschrift. 274: 423-434.

Keys, A.J., Parry, M.A.J., 1990. Ribulose bisphosphate carboxylase/oxygenase and carbonic anhydrase. Methods in Plant Biochemistry. 3: 1-15.

Kleinman, L.I., Daum, P.H., Imre, D., Lee, Y.-Y., Nunnermacker, L.J., Springston, S.R., Weinstein-Loyd, J., Rudolph, J., 2002. Ozone production rate and hydrocarbon reactivity in 5 urban areas: A cause of high ozone concentration in Houston. Geophysical Research Letters. 29: 1-4.

Kley, D., Kleinmann, M., Sanderman, H., Krupa, S., 1999. Photochemical oxidants, state of the science. Environmental Pollution. 100: 19-42.

Kronfuß, G., Polle, A., Tausz, M., Havranek, W.M., Wieser, G. 1998. Effects of ozone and mild drought stress on gas exchange, antioxidants and chloroplast pigments in current-year needles of young Norway spruce [Picea abies (L.) Karst.]. Trees, 12: 482-489.

Krüger, G.J.H., TsimillI-Michael, M., Strasser, R.J., 1997. Light stress provokes plastic and elastic modifications in structure and function of Photosystem II in camellia leaves. Physiologa Plantarum. 101: 265-277.

Lacasse, N.L. Treshow, M., 1976. Diagnosing Vegetation Injury Caused by Air P!ollution. U.S. Environmental Protection Agency Handbook.

Lafitte, R., 2002. Relationship between leaf relative water content during reproductive stage water deficit and grain formation in rice. Field Crop Research. 76: 165-174.

Laisk, A., Kull, O., Moldau, H., 1989. Ozone concentration in leaf intercellular air spaces is close to zero. Plant Physiology. 90: 1163-1167.

Laisk, A., Kull, O., Molday, H. 1989. Ozone concentration in leaf intercellular air spaces is close to zero. Plant Physiology. 90: 1163-1167.

Lal, R., Maurya, P.R., Yeboah, S.O., 1987. Effects of no-tillage and ploughing on efficiency of water use in maize and cowpea. Experimental Agriculture. 14: 113-120.

Lange, O.L., Harley, P.C., Beyshlag, W., Tenhunen, J.D., 1987. Gas exchange methods for characterizing the impact of stress on leaves. [In:] Tenhunen, J.D., F.M. Catarino, O.L. Lange, and W.C. Oechel (eds.). 1987. Plant Response to Stress - Functional Analysis in Mediterranean Ecosystems. NATO Advanced Science Institute Series. Springer-Verlag, Berlin-Heidelberg-New York-Tokyo, pp. 668.

Lavorel, J., Etienne, A.L., 1977. In vivo chlorophyll fluorescence. Topics in Photosynthesis. 2: 203-268.

Lawlor, D.W. 1993. Photosynthesis 2nd ed. Longman Scientific & Technical. UK, p 318.

Lee, D.S., Kohler, I., Grobler, E., Rohrer, F., Sausen, R., Gallardo-Klenner, L., Olivier, J.J.G., Dentener, F.J., 1997. Estimation of global NO_x emissions and their uncertainties. Atmospheric Environment. 31: 1735-1749.

Lee, E.H., Jersey, J.A., Gifford, C., Bennet, J., 1984. Differential ozone tolerance in soybean and snapbeans: analysis of ascorbic acid in O_3-susceptible and O_3-resistant cultivars by high performance liquid chromatography. Environmental and Experimental Botany. 24: 31-41.

Lefohn, A.S., eds. 1992. Surface ozone exposures and their effects on vegetation. Lewis Publishers, Chelsea.

Long, S.P. 1983. Whole plant photosynthesis and productivity. [In:] Coombs, J., Hall, D.O. eds. Techniques in bioproductivity & photosynthesis. Pergamon Press, Oxford, England. p171.

Long, S.P., Hällgren, J.-E., 1993. Measurement of CO_2 assimilation by plants in the field and the laboratory. [In:] Hall, D.O., Scurlock, J.M.O., Bolhàr-Nordenkampf, H.R., Leegood, R.C., Long, S.P. eds. Photosynthesis and production in a changing environment. Chapman & Hall, London. pp 129-167.

Luo, T., Deng, W-Y., Chen, F. 2006. Study on cold-rersistance ability of *Jatropha curcas* growing in different ecological environments. Ata. Sci. Nat. Univ. NeiMongol. 37: 446-449.

MacNevin, W.M., Uron, P.F., 1953. Seperation of hydrogen peroxide from organic hydroperoxides. Analytical Chemistry. 25: 1760-1761.

Mage, D., Ozolins, G., Peterson, P., Webster, A., Orthofer, R., Vandeweerd, V., Gwynne, M., 1996. Urban air pollution in megacities of the world. Atmospheric Environment. 30: 681-686.

Majumdar, S., Ghosh, S., Glick, B.R., Dumbroff, E.B., 1991. Activities of chlorophyllase, phosphenolpyruvate carboxylase and ribulose-1,5-bisphosphate carboxylase in the primary leaves of soybean during senescence and drought. Physiologia Plantarum. 81: 473-480.

Malhorta, S.S., Khan, A.A., 1984. Biochemical and physiology impact of major pollutants. [In:] Treshow, M., (eds.) Air pollution an plant life. John Wiley & Sons, New York, pp 113-157.

Mandl, R.D., Weinstein, L.H., McCune, D.B., Keveny, M., 1973. A cylindrical, open-top chamber for exposure of plants to air pollutants in the field. Journal of Environmental Quality. 2: 371-376.

Manes, F., Federico, R., Cortiello, M., Angelini, R., 1990. Ozone induced increase of peroxidase activity in tobacco (Nicotiana tabacum L. cv. Burley 21) leaves. Phytopath. Medit, 29: 101-106.

Mansfield, T.A. 1998. Stomatal and plant water relations: does air pollution create problems? Environmental Pollution. 101: 1-11.

Marshall, F.M., 2002. Effects of air pollution in developing countries. [In:] Bell, J.N.B., Treshow, M., eds. Air Pollution and Plant Life. 2nd ed. West Sussex, John Wiley & Sons. p.23-41.

Marshall, T.C., Slate, J., Kruuk, L., Pemberton, J.M., 1998. Statistical confidence for likelihood-based paternity inference in natural populations. Molecular Ecology. 7: 639-655.

Marsili-Libelli, S., 1996. Simplified kinetics of tropospheric ozone. Ecological modeling. 84: 233-244.

Massmann, W.J., Grantz, D.A., 1995. Estimating canopy conductance to ozone uptake from observations of evapotranspiration at the canopy scale and at the leaf scale. Global Change Biology. 1: 183-198.

Matyssek, R., Sandermann, H. 2003. Impact of O_3 on trees: an ecophysiological perspective. Progress in Botany. 64: 349-404.

McAinish, M.R., Clayton, H., Mansfield, T.A., Hetherington, A.M., 1996. Changes in stomatal behavior and guard cell cytosolic free calcium in response to oxidative stress. Plant Physiology. 111: 1031-1042.

McAinsch, M.R., Evans, N.H., Montgomery, L.T., North, K.A., 2002. Calcium signaling in stomatal responses to pollutants. New Phytologist. 153: 441-447.

McCormick, J., 1997. Acid Earth – The Pollitics of Acid Pollution. 3rd ed. Earthscan Publications Ltd, London. 190pp.

McKee, I.M., Bullimore, J.F., Long, S.P., 1997. Will elevated CO_2 concentrations protect the yield of wheat from ozone damage? Plant Cell Environment. 20: 77-84.

Medrano, H., Escalona, J.M., Bota, J., Gulías, J., Flexas, J. 2002. Regulation of photosynthesis of C3 plants in response to progressive drought: Stomatal conductance as a reference parameter. Annals of Botany. 89: 895-905.

Medrano, H., Parry, M.A., Socias, X., Lawlor, D.W. 1997. Long term water stress inactivates Rubisco in subterranean clover. Annals of Applied Biology. 131: 491-501.

Mehta, R.A., Fawcett, T.W., Porath, D., Mattoo, A.K., 1992. Oxidative stress causes rapid membrane translocation and in vivo degradation of ribulose-1,5-bisphosphate carboxylase/oxygenase. Journal of Biological Chemistry. 267: 2810-2816.

Merrill, S.D., Tanaka, D.L., Hanson, J.D., 2002. Root length growth of eight crop species in Haplustoll soils. Soil Science Society of America Journal. 66: 913-923.

Miller, J.E., 1998. Effects of photosynthesis, carbon allocation and plant growth associated with air pollution stress. [In:] Heck, W.W., Taylor, O.C., Tingey, D.T., (eds.), Assessment of crop loss from air pollutants. Elsevier Applied Science, London. pp287-314

Mittler, R., Zilinskas, B.A., 1994. Regulation of pea cytosolic ascorbate peroxidase and other antioxidant enzymes during the progression of drought stress and following recovery from drought. The Plant Journal. 5: 397-405.

Moldau, H., 1998. Hierarchy of ozone scavenging reactions in the plant cell wall. Physiologia Plantarum. 104: 617-622.

Moldau, H., Sõber, J., Sõber, A. 1990. Differential sensitivity of stomata and mesophyll to sudden exposure of bean shoots to ozone. Photosynthetica. 24: 446-458.

Morgan, P.B., Ainsworth, E.A., Long, S.B. 2003. Elevated O3 impact on soybeans: a meta-analysis of photosynthetic, biomass, and yield responses. Plant, Cell and Environment. 26: 1317-1328.

Murata, Y., Pei, Z.M., Mori, I.C., Schroender, J., 2001. Abscicic acid activation of plasma membrane Ca(2+) channels in guard cells requires cytosolic NAD(P)H and is differentially disrupted upstream and downstream of reactive oxygen species production in abi1-1 and abi2-1 protein phosphatase 2C mutants. Plant, Cell and Environment. 13: 2513-2523.

Musselman, R.C., Massmann, W.J., 1999. Ozone flux to vegetation and its relationship to plant response and ambient air quality standards. Atmospheric Environment. 33: 65-73.

Nilsen, E.T., Orcutt, D.M., 1996. Physiology of plants under stress: Abiotic factors. John Wiley & Sons, Inc. Canada. p689.

Nussbaum, S., Remund, J., Rihm, B., Mieglitz, K., Gurtz, J., Fuhrer, J., 2003. High-resolution spatial analysis of stomatal ozone uptake in arable crops and pastures. Environmental International. 29: 358-392.

OLGEAR. Installation & Operation Manual

Ollerenshaw, J.H., Lyons, T., Barnes, J.D., 1999. Impact of ozone on the growth and yield of field-grown winter oilseed rape. Environmental Pollution. 104: 53-59.

Olszyk, D.M., Bytnerowicz, A., Kats, G., Dawson, P.J., Wolf, J., Thompson, C.R. 1986. Crop effects from air pollutants in air exclusion systems vs field chambers. Journal of Environmental Quality, 15:417-422.

Ort, D.R., Oxborough, K., Wise, R.R. 1994. Depressions of photosynthesis in crops with water deficits. [In:] Baker, N.R., Bowyer, J.R. eds. Photoinhibition of photosynthesis: from molecular mechanisms to the field. Oxford, BIOS Scientific Publishers.

Pammenter, N.W. 1989. Research letter. Clarification of an apparent anomaly in the supply function associated with the response of carbon assimilation to carbon dioxide determined using con-ventional field equipment. South African Journal of Science. 85:271-272.

Pandey, R.K., Herrera, W.A.T., Pendleton, J.W., 1984. Drought response of grain legumes under irrigation. III. Plant growth. Agronomy Journal. 76: 557-560.

Paoletti, E., Grulke, N.E., 2005. Does living in elevated CO_2 ameliorate tree response to ozone? A review on stomatal responses. Environmental Pollution. 137: 483-493.

Papageorgiou, J., 1975. Chlorophyll fluorescence: an intrinsic probe of photosynthesis. [In:] Govindjee, X.U.C. eds. Bioenergetics of Photosynthesis. Academic Press, New York. pp 319-371.

Pausch, R.C., Mulchi, C.L., Lee, E.H., Forseth, I.N., Slaughter, L.H., 1996. Use of 13C and 15N isotopes to investigate O3 effects on C and N metabolism in soybeans. Part I. C fixation and translocation. Agriculture, Ecosystems and Environment. 59: 69-80.

Pell, E.J., Eckardt, N., Enyedi, A.J., 1992. Timing of ozone stress and resulting status of ribulose bisphosphate carboxylase/oxygenase and associated net photosynthesis. New Phytologist. 120: 397-405.

Pell, E.J., Schlagnhaufer, C.D., Arteca, R.N. 1997. Ozone-induced oxidative stress: mechanisms of action and reaction. Plant Physiology. 100: 264-273.

Peńarrubia, L., Moreno, J., 1999. Molecular mechanisms of plant responses to elevated levels of tropospheric ozone. [In:] Pessarakli, M., eds. Handbook of Plant and Crop Stress. 2nd ed. Taylor & Francis, New York. p.769-793.

Polle, A., Rennenberg, H., 1993. Significance of antioxidants in plant adaptation to environmental stress. [In:] Fowden, L., Mansfield, T., Stoddart, J., eds. Plant Adaptation to Environmental Stress. Chapman and Hall, London, UK. pp. 263-271.

PORG, 1997. Ozone in the United Kingdom. Fourth Report of the UK Photochemical Oxidants Review Group, Department of Environment, Transport and Regions, London.

Price, A.H., Taylor, A., Ripley S.J., Griffiths, A., Trewavas, A.J., Knight, M.R. 1994. Oxidative signals in tobacco increase cytosolic calcium. Plant, Cell and Environment. 6: 1301-1310.

Quartacci, M.F., Navari-Izzo, F., 1992. Water stress and free radical mediated changes in sunflower seedlings. Journal of Plant Physiology. 139: 621-625.

Queensland Government. Environment and Resource Management. 2010. Environment Management. http://www.derm.qld.gov.au/environmental_management/air/air_quality_monitoring/air_pollutants/ozone/. Date of use: 22 February 2010.

Reich, P.B., Amundson, R.G. 1985. Ambient levels of ozone reduce net photosynthesis in tree and crop species. Science. 230: 556-570.

Reich, P.B. 1983. Effects of low concentrations of O3 onnet photosynthesis, dark respiration, and chlorophyll content in aging hybrid poplar leaves. Plant Physiology. 73: 291-296.

Reigh, P.B. 1987. Quantifying plant responses to ozone: a unifying theory. Tree Physiology. 3: 63-91.

Reinert, P.B., Eason, G., 2000. Genetic control of O3 sensitivity in a cross between two cultivars of snap bean. Journal of American Society of Horticulture Science. 125: 222-227.

Richards, B.L., Middleton, J.T., Hewitt, W.B., 1958. Air pollution with relation to agronomic crops. V. Oxidant stipple of grape. Agronomy Journal. 50: 559-561.

Rodriguez-Maribona, B., Tenorio, J.L., Conde, J.R., Averbe, L., 1992. Correlation between yield and onsmotic adjustment of peas (Pisum sativum L.) under drought stress. Field Crops Research. 29: 15-22

Rogerson, C., 2000. Coping with Vulnerability in Africa: Urban agriculture and poverty alleviation. Africa Insight. Volume 30 (3-4), 66-72.

Rorich, R.P., Galpin, J.S., 1998. Air Quality in the Mpumalanga Highveld region, South Africa. South African Journal of Science. 94: 109-114.

Ruiz-Lozano, J.M. 2003. Arbuscular mycorrhizal symbiosis and alleviation of osmotic stress: new perspective for molecular studies. Mycorrhiza. 13: 309-317.

Santos, M.G., Ribeiro, R.V., Oliveira, R.F., Machado, E.C., Pimentel, C., 2006. The role of inorganic phosphate on photosynthesis recovery of common bean after mild water deficit. Plant Science. 170: 659-664.

Sanz, J., Muntifering, R.B., Bermejo, V., Gimeno, B.S., Elvira, S. 2005. Ozone and increased nitrogen supply effects on the yield and nutritive quality of Trifolium subterraneum. Atmospheric Environment. 39: 5899-5907.

Schansker, G., Srivastava, A., Govindjee., Strasser, R.J., 2003. Characterization of the 820-nm transmission signal paralleling the chlorophyll a fluorescence rise (OJIP) in pea leaves. Functional Plant Biology. 30: 785-796.

Schansker, G., Tóth, S.Z., Strasser, R.J., 2005. Methhylviologen and dibromothymo-quinone treatments of pea leave reveal the role of photosystem I in the Chl a fluorescence rise OJIP. Biochimica et Biophysica Acta. 1706: 250-261.

Schansker, G., Tóth, S.Z., Strasser, R.J., 2006. Dark-recovery of the Chl a fluorescence transient (OJIP) after light adaption: The qT-component of non-photochemical quenching is related to an activated photosystem I acceptor side. Biochimica et Biophysica Acta. 1757: 787-797.

Scheidegger, C., Günthardt-Goerg, M.S., Matyssek, R., Hatvani, P., 1991. Low-temperature scanning electron microscoppy of birch leaves after exposure to ozone. Journal of Microscopy. 161: 85-95.

Schenone, G., 1993. Impacts of air pollutants on plants in hot, dry climates. [In:] Jackson, M.B., Black, C.R., eds. Interacting Stresses on Plants in a Changing Climate. Global Environmental Change, Springer-Verlag, Berlin. p139-152.

Scholander, P.F., Hammel, H.T., Hemmingsen, E.A., Bradstreet, E.D., 1964. Hydrostatic pressure and osmotic potential in leaves of mangroves and some other plants. Proceedings of the National Academy of Science, United States, 52: 119-125.

Scholes, M.C., Olbrich, K.A., van Rensburg, E., 1996. The environ-mental impact of atmospheric pollution in the industrial Highveld and adjacent regions: crops, indigenous vegetation and commercial forests. [In:] Held, G., Gore, B.J., Surridge, A.D., Tosen, G.R., Turner., C.R., & Walmsey, R.D. eds. Air pollution and its impacts on the South-African Highveld. Environmental Scientific Association, Cleveland.

Scholes, R.J. & Scholes, M.C. 1998. Natural and Human-related Sources of Ozone-forming trace gases in southern Africa. South African Journal of Science. 94: 422-425.

Schönbein, C.F., 1840. Recherches sur la naturew d l' odeur qui se manifeste dans certaines actions chimique. Comptes Rendus de l'Académie des Sciences. 10: 706-710.

Sillman, S., 1999. The relation between ozone, NOx and hydrocarbons in urban and polluted rural environments. Atmospheric Environment. 33: 1821-1845.

Sillman, S., He, D., 2002. Theoretical results concerning O_3-NO_x-VOC chemistry and NO_x-VOC indicators. Journal of Geophysical Research. 107: 4659–4673.

Singh, E., Tiwari, S., Agrawal, M. 2009. Effects of elevated ozone on photosynthesis and stomatal conductance of two soybean varieties: a casestudy to assess impacts of one component of predicted global climate change. Plant Biology. 11: 101-108.

Singsaas, E., Ort, D.R., DeLucia, E.H., 2001. Variation in measured values of photosynthetic quantum yield in ecophysiology studies. Oecologia. 128: 15-23.

Smirnoff, N. 1993. The role of active oxygen in the response of plants to water deficit and desiccation. New Phytol, 125: 27-58.Park, NC: Office of Air Quality Planning and Standards; report no. EPA/452/R-96/007. Availible from: NTIS, Springfield, VA; PB96-203435/XAB. Available: http://www.epa.gov/ttn/naaqs/standards/ozone/s_O3_pr_sp.html (11 March 2011).

Smit, M.F., van Heerden, P.D.R., Pienaar, J.J., Weissflog, L., Strasser, R.J., Krüger, G.H.J., 2008. Effect of trifluoroacetate, apersistant degradation product of fluorinated hydrocarbons, on Phaseolus vulgar is and Zea Mays. Plant Physiology and Biochemistry. 47: 623-634.

Sponchiado, B.N., White, J.W., Castillo, J.A., Jones, P.G., 1980. Root growth of four common bean cultivars in relation to drought tolerance in environments with contrasting soil types. Experimental Agriculture. 25: 249-257.

Srivastava, A., Strasser, R.J., 1997. Constructive and destructive actions of light on the photosynthetic apparatus. Journal of Science. 56: 133-148.

Strasser, B.J., Strasser, R.J., 1995. Measuring fast fluorescence transients to address environmental questions: The JIP-test. [In:] Mathis, P. eds. Photosynthesis: From Light to Biosphere. Kluwer Academic Publishers, Dordrecht. Vol 5, pp 977-980.

Strasser, R.J, Tsimilli-Michael, A, Pêcheux, M., 1999. Polyphasic chlorophyll a fluorescence transients in plants and cyanobacteria. Journal of Photochemistry and Photobiology. 61: 32-42.

Strasser, R.J., 1997. Donor side capacity of photosystem II probed by chlorophyll a fluorescence transients. Photosynthesis Research. 52: 147-155.

Strasser, R.J., Govindjee, X.U.C., 1992. On the OJIP fluorescence transient in leaves and DI mutants of Chlamydomonas reinhardtii. [In:] Murata, N. eds. Research in Photosynthesis. Kluwer Academic Publishers, Dordrecht. pp. 29-32.

Strasser, R.J., Tsimilli-Michael, M., 2001. Stress in plants, from daily rhythm to global changes, detected and quantified by the JIP-test. Chimie Bouvelle (SRC), 75: 3321-3326.

Strasser, R.J., Tsimilli-Michael, M., Srivastava, A., 2004. Analysis of the chlorophyll a Fluorescence Transient. [In:] Papageorgiou, G., Govindjee, X.U.C. eds. Chlorophyll a fluorescence a signature of photosynthesis. Springer, Dordrecht, the Netherlands. pp818.

Taylor, G.E., Tingey, D.T., Ratsch, D.T. 1982. Ozone flux in Glycine max (L.) Merr. Sites of regulation and relationship to leaf injury. Oecologia. 53: 179-186.

Taylor, S.E., Terry, N., 1984. Limiting factors in photosynthesis. V. Photochemical energy supply co-limits photosynthesis at low values intercellular CO_2 concentration. Plant Physiology. 75: 82-86.

Temple, P.J. 1990. Growth and yield responses of processing tomato (Lycopersicon esculentrum Mill.) cultivars to ozone. Environmental and Experimental Botany. 30: 283-291.

Tezara, W., Mitchell, V.J., Driscoll, S.D., Lawlor, D.W. 1999. Water stress inhibits plant photosynthesis by decreasing coupling factor and ATP. Nature. 401: 914-917.

Thorp, C.E., 1955. Physical and pharmacological properties. In Bibliography of Ozone Technology. John Swift Company, Chicago, IL, 160pp.

Tingey, D.T. Anderson, C.P., 1991. The Physiological basis of Differential plant sensitivity to changes in atmospheric quality. [In:] Taylor, G.E., Pitelka L.F. Clegg, M.T., (eds.). Ecological genetics and air pollution. Springer-verlag, New York. p.209-235.

Tingey, D.T., Fites, R,C., Wickliff, C. 1975. Activity changes in selected enzymes from soybean leaves following ozone exposure. Physiol. Plant. 33: 316-320.

Tingey, D.T., Rodecap, K.D., Lee, E.H., Hogsettm W.E., Gregg, J.W. 2002. Pod development increases the ozone sensitivity of Phaseolus vulgaris. Water Air Soil Pollution. 139: 325-341.

Tsimilli-Michael, M., Pêcheux, M., Strasser, R.J., 1999. Light and heat stress adaptation of the symbionts of coral reef and temperature foraminifers probed in hospite by chlorophyll a fluorescence kinetics O-J-I-P. Zeitschrift für Naturforchung88m;p, 54C: 671-680.

Tsimilli-Michael, M., Strasser, R.J. 2008. In vivo assessment of stress impact on plants' vitality: applications in detecting and evaluating the beneficial role of mycorrhization on host plants. [In:] Varma, A. eds. Mycorrhiza: State of the Art, Genetics and Molecular Biology, Eco-Function, Biotechnology, Eco-Physiology, Structure and Systematics, 3rd ed. Springer, pp679-703.

U.S. Environment Protection Agency. 1996. Review of national ambient air quality standards for ozone: assessment of scientific and technical information OAQPS staff paper. Research Triangle

UNDP, 1998. Human Development Report 1998. United Nations Development Program. Oxford University Oress, New York.

UNECE, 1988. ECE critical levels workshop report. Bad Harzburg, Germany, 14-18 March 1988. Final draft report.United Nations - Economic Commission for Europe.

UNEP, 2000. Global Environment Outlook. United Nations Environmental Programme, Global State of the Environment Report 2000. Oxford University Press, New York.

Vahisalu, T., Kollist, H., Wang, Y.F. 2008. *SLAC1* is required for plant guard cell S-type anion function in stomatal signaling. Nature. 452: 487-493.

van Huyssteen, S.M., 2003. Impacts of ozone on the photosynthetic and metabolic properties of *Zea mays*. MSc thesis. University of the Free State.

van Tienhoven, A.M. 2000. Forestry problems in Africa. [In:] Innes, J.L., Haron, A.H. (eds.) Air Pollution and the Forests of Developing and Rapidly Industrializing Countries. DCABI Publishing, Wallingford, UK. 262pp.

van Tienhoven, A.M., Scholes, M.C., 2003. Air Pollution Impacts on Vegetation in South Africa. [In:] Ashmore, M., Emberson, L., Murray, F., (Eds.), Air Pollution impacts on crops and forests – a global assessment. Air pollution reviews Volume 4. Imperial College Press, London. 371pp.

van Tienhoven, A.M., Zunckel, M., Emberson, L., Koosailee, A., Otter, L., 2004. Preliminary assessment of risk of ozone impacts to maize (Zea mays) in southern Africa. Environmental Pollution. 140: 220-230.

Vassey, T.L., Sharkey, T.D., 1989. Mild water stress of Phaseolus vulgaris plants leads to reduced starch synthesis and extractable sucrose phosphate synthesis activity. Plant Physiology. 89: 1066-1070.

Villalobos-Ridriquez, E., Shibles, R., 1985. Response of determinate and indeterminate tropical soybean cultivars to water stress. Field Crops Research. 10: 269-281.

Volz, A., Kley, D., 1988. Evaluation of the Montsouris series of Ozone Measurements made in the nineteenth century. Nature. 332: 240-242.

von Caemmerer, S., Farquhar, G.D. 1984. Effects of partial defoliation, changes of irradiance during growth, short-term water stress and growth changes at enhanced p(CO2) on photosynthetic capacity of leaves of Phaseolus vulgaris L. Planta. 160: 320-329.

von Caemmerer, S., Farquhar, G.D., 1981. Some relationships between the biochemistry of photosynthesis and the gas exchange of leaves. Planta. 153: 376-387.

Walker, D.A., Osmond, C.B., 1986. Measurement of photosynthesis in vivo using a leaf disc electrode: Correlations between light dependance of steady state photosynthetic O_2 evolution and chlorophyll a fluorescence transients. Proceedings of the Royal Society of London. Series B, Biological Sciences. 227: 267-280.

Wang, L., He, X., Chen, L. 2008. Effects of elevated ozone on photosynthetic CO_2 exhange and chlorophyll a fluorescence in leaves of Quercus mongolica grown in urban area. Bull Environ Contamination and Toxicol. 82: 478-481.

Wellburn, A. 1994. Air Pollution and Climate Change: The Biological Impact. John Wiley & Sons, New York, 268pp.

Willikens, H., Chamnongpol, S., Davey, M., Schraudner, M., Langebartels, C., Van Montagu, M., Inzé, D., van Camp, W. 1997. Catalase is a sink for H_2O_2 and is indispensable for stress defence in C_3 plants. EMBO Journal. 16: 4806-4816.

Willmer, C., Pantoja, O., 1992. The plasma membrane and tonoplast of guard cell membranes. [In:]. Leshem, Y. eds. Plant membranes: A Biophysical Approach to Structure and Function. Kluwer Academics Press, Dordrecht, The Netherlands. 266pp.

Winner, W.E., 1994. Mechanistic analysis of plant responces to air pollution. Ecological Applications. 4: 651-661.

World Meteorological Organization. 2009. Measurement of reactive gases. Date of access: 24 June 2009.

Yordanov, I., Goltsev, V., Stefanof, D., Chernev, P., Zaharieva, I., Kirova, M., Gecheva, V., Strasser, R.J., 2008. Preservation of photosynthetic electron transport from senescence-induced inactivation in primary leaves after decapitation and defoliation of bean plants. Journal of Plant Physiology. 165: 1954-1963.

Yusuf, M.A., Kumar, D., Rajwanshi, R., Strasser, R.J., Tsimilli-Michael, M., Govindjee. & Sarin, N.B. 2010. Overexpression of γ-tocopherol methyl transferase gene in transgenic Brassica juncea plants alleviates abiotic stress: Physiological and chlorophyll a fluorescence measurements. Biochimica et Biophysica Acta (in press).

Zieslin, N., Ben-Zaker, R., 1991. Peroxidase, phenylalanine ammonia-lyase and lignifications in peduncles of rose flowers. Plant Physiology and Biochemistry. 29: 147-151.